UNIVERSITÀ DEGLI STUDI DI MILANO

PhD in Pharmacological Biomolecular Sciences, Experimental and Clinical
Department of Pharmacological and Biomolecular Sciences

XXXIV Cycle

PhD Thesis:

Identification of pharmacological approaches blocking alpha-synuclein synaptic toxicity

BIO/14

PhD Candidate: Elena Ferrari

Tutor: Prof. Fabrizio Gardoni
PhD coordinator: Prof. Giuseppe Danilo Norata

A.A. 2020/2021

INDEX

ABSTRACT

Misfolding and aggregation of the synaptic protein alpha-synuclein (αsyn) is, at present, considered one of the main drivers of the pathogenesis of Parkinson's disease (PD). PD is a complex neurodegenerative disorder characterized by progressive loss of DAergic neurons in the *substantia nigra pars compacta* (SNpc) and deposition of insoluble proteinaceous inclusions containing αsyn, called Lewy Bodies (LB), in different regions of the nervous system. Toxic species of αsyn were demonstrated to affect multiple cellular pathways, mediating synaptic dysfunction even before a dramatic loss of SNpc neurons has occurred. Besides its neurotoxicity towards the DAergic system, αsyn has been recently reported to affect also the corticostriatal glutamatergic signalling, modulating the synaptic levels and activity of NMDA-type glutamate receptors. However, the precise molecular events underlying αsyn synaptic toxicity are still elusive.

The synaptic retention of NMDARs was recently demonstrated to be strictly correlated to the interaction with the protein Rabphilin-3A (Rph3A). Interestingly, alterations of Rph3A expression and its interaction with NMDARs at the corticostriatal synapse have been described in advanced PD stages. Besides, a direct αsyn/Rph3A interaction, modulated in presence of LB, has been put forward. Starting from these previous findings, this PhD project is aimed at characterizing Rph3A role in the early stages of PD to identify pharmacological approaches able to slow down αsyn-induced synaptic toxicity.

Exploiting different imaging and biochemical approaches, Rph3A was confirmed as a novel αsyn interactor at synaptic sites. In addition, using an *in vivo* mouse model of αsyn-induced PD, we found that oligomers and fibrils (PFF) of αsyn reduced AMPAR and NMDAR subunits at the striatal excitatory synapse, prior to cause significant DAergic neurodegeneration. At the same time point, αsyn-mice showed decreased striatal dendritic spine density and early motor impairments. Interestingly, I also found that αsyn oligomers and PFF selectively reduced striatal Rph3A postsynaptic levels and Rph3A binding to GluN2A subunit of NMDAR, suggesting Rph3A and Rph3A/αsyn complex as possible mediators of the synaptic dysfunction. Based on these hypothesis, modulatory strategies aimed at restoring Rph3A synaptic levels were firstly tested in an *in vitro* model of PFF-induced synaptopathy. In particular, a Rph3A/αsyn uncoupling compound (Compound B), identified through a bioinformatic screening, revealed efficacious in blocking spine loss caused by PFF exposure. In the same experimental model, synaptic defects were also prevented by Rph3A overexpression. Based on these *in vitro* results, these Rph3A-modulatory approaches were then investigated using the αsyn-induced PD mouse model. Notably, chronic intracerebroventricular

treatment with Compound B confirmed its efficacy in blocking αsyn-dependent decrease in striatal spine density. Furthermore, striatal delivery of an AAV overexpressing Rph3A resulted sufficient in preventing the early motor impairments found in αsyn-lesioned mice.

In conclusion, the results of this PhD thesis demonstrate that Rph3A and Rph3A/αsyn complex significantly contribute to the molecular events underlying early dysfunction of the striatal glutamatergic synapse in PD, therefore representing novel and promising pharmacological targets.

RIASSUNTO

Ad oggi, il processo di misfolding e aggregazione della proteina sinaptica alfa-synucleina (αsyn) è considerato tra i principali mediatori della patogenesi della malattia di Parkinson (MP). La MP è una complessa malattia neurodegenerativa caratterizzata dalla morte progressiva dei neuroni dopaminergici (DAergici) della *substantia nigra pars compacta* (SNpc) e accumulo neuronale di inclusioni insolubili di natura proteica contenenti αsyn, denominati Corpi di Lewy (LB), in diverse regioni del sistema nervoso. È stato dimostrato che specie tossiche di αsyn influenzano numerosi processi cellulari, provocando disfunzione sinaptica anche in stadi che precedono una significativa neurodegenerazione nella SNpc. In aggiunta agli effetti neurotossici nei confronti del sistema DAergico, è stato recentemente dimostrato che aggregati di αsyn causano disfunzioni anche della trasmissione glutamatergica corticostriatale; in particolare, sono in grado di modulare i livelli sinaptici e l'attività dei recettori del glutammato di tipo NMDA. Tuttavia, gli specifici eventi molecolari alla base della tossicità sinaptica indotta da αsyn non sono ancora stati chiariti.

Un recente studio ha dimostrato come la localizzazione sinaptica dei recettori NMDA sia strettamente correlata all'interazione con la proteina Rabphilin-3A (Rph3A). Inoltre, evidenze sperimentali hanno dimostrato che in fasi avanzate della MP sono presenti alterazioni dell'espressione di Rph3A e della sua interazione con i recettori NMDA a livello della sinapsi corticostriatale. Infine, è stata ipotizzata un'interazione diretta tra Rph3A e αsyn che sembra essere alterata in presenza di Corpi di Lewy.

Sulla base di queste evidenze, il progetto di Dottorato ha come obiettivo la caratterizzazione del ruolo di Rph3A nelle fasi precoci della MP al fine di identificare approcci farmacologici in grado di rallentare il danno sinaptico provocato da αsyn.

Prima di tutto, l'utilizzo di diverse tecniche sperimentali quali immunofluorescenza, biochimica ed *in silico*, ha permesso di confermare che Rph3A è un partner sinaptico di αsyn. Secondariamente, utilizzando un modello murino di MP indotto da αsyn, è stato dimostrato che oligomeri e fibrille di αsyn, ancora prima di causare significativa degenerazione DAergica, provocano una riduzione dell'espressione delle subunità dei recettori del glutammato di tipo AMPA e NMDA a livello della sinapsi eccitatoria cortico-striatale. Allo stesso time point sperimentale, i topi iniettati con forme tossiche di αsyn mostrano una riduzione della densità di spine dendritiche striatali accompagnata da precoci difetti motori. Inoltre, oligomeri e fibrille di αsyn riducono selettivamente i livelli postsinaptici di Rph3A e la sua interazione con la subunità NMDA di tipo GluN2A, suggerendo che Rph3A e il complesso Rph3A/αsyn possano essere coinvolti nell'insorgenza dei difetti sinaptici. Basandosi su questa ipotesi, strategie sperimentali volte a ripristinare fisiologici livelli sinaptici di

Rph3A sono state prima di tutto testate in un modello neuronale *in vitro* di sinaptopatia indotta da fibrille di αsyn. In particolare, il trattamento con una molecola in grado di competere con l'interazione Rph3A/αsyn (Composto B), identificata tramite uno screening bioinformatico, si è rivelato efficace nel bloccare la perdita di spine dendritiche causata dal trattamento con le fibrille. Nello stesso modello sperimentale, anche l'overespressione della proteina Rph3A è stata in grado di prevenire i difetti sinaptici. Considerando questi risultati *in vitro*, è stata successivamente investigata l'efficacia degli approcci modulatori di Rph3A *in vivo*, utilizzando il modello murino di MdP precedentemente caratterizzato. In particolare, la somministrazione cronica intracerebroventricolare del Composto B si è confermata efficace nel prevenire la perdita di spine dendritiche striatali riscontrata nei topi iniettati con fibrille. Inoltre, l'overespressione striatale di Rph3A tramite iniezione di AAV, è stata sufficiente a prevenire l'insorgenza di precoci disfunzioni motorie.

In conclusione, questi risultati dimostrano che Rph3A e il complesso Rph3A/αsyn contribuiscono in maniera significativa ai meccanismi molecolari che mediano la disfunzione della sinapsi glutamatergica striatale nelle fasi iniziali della MP. Di conseguenza, possono essere considerati come innovativi e promettenti bersagli terapeutici.

INTRODUCTION

1. Parkinson's disease

Since from its first description 200 years ago by James Parkinson in the *Essay of shaking palsy*, Parkinson's disease (PD) perception as a merely movement disorder has significantly evolved over years (Parkinson, 2002). Several non-motor features as cognitive impairments, sleep disorders, autonomic dysfunction, hyposmia and depression emerged as key components of PD clinical manifestations (Chaudhuri and Schapira, 2009). However, clinical features originally described by James Parkinson are still able to recapitulate the cardinal motor presentations of the disorder (Poewe et al., 2017)

PD is a highly complex and slowly progressive neurological disorder representing the second most common neurodegenerative disease. It is estimated to affect 2-3% of the population higher than 65 years old, with differences of prevalence across countries (Dorsey et al., 2007).

The neuropathological hallmarks of PD are the progressive loss of dopaminergic (DA) neurons in the substantia nigra pars compacta (SNpc) and cytoplasmic accumulations of insoluble proteinaceous inclusions called Lewy Body (LB). LBs, of which the main component is the presynaptic protein alpha-synuclein (αsyn), aggregate in specific neuronal types and spread disease through interconnected brain regions (Braak et al., 2003; Spillantini et al., 1997). Indeed, PD is the most frequent disorder among synucleinopathies, neurodegenerative conditions characterized by presence of αsyn inclusions in different neuronal and cell types, including also Lewy-Body dementia, Multiple System Atrophy and Pure Autonomic Failure (PAF) (Galvin et al., 2001). Neurodegeneration of DA neurons in the SN consequently leads to a dramatic decrease of DA levels within the basal ganglia and in particular the striatum. After reaching a significant threshold, striatal DA denervation is responsible for the onset of the typical parkinsonian motor features (Goetz, 2011).

Great progresses have been made in the understanding of neuropathology and molecular pathways involved in disease mechanisms, however clear mechanisms underlying PD etiology are still unknown. The majority of PD cases are sporadic and only the 5-10% of PD have a known genetic cause. It is now clear that PD etiology raises from a complex interplay of genetic risk factors, epigenetic mechanisms, ageing and environmental clues (Klein and Westenberger, 2012).

Though PD is a rare example of a neurodegenerative disorder with manageable clinical symptoms (at least in its first stages), it remains still uncurable and several issues are related to its treatment. Indeed, the gold standard therapy based on pharmacological replacement of dopamine, mainly its precursor levo-DOPA (L-DOPA) and DA-agonists, despite its initial efficacy, does not target non-motor

features and give rise to severe side effects. Besides, L-DOPA complications, treatment resistant motor manifestations and progression of non-motor features ultimately originate a significant disability burden (Kalia and Lang, 2015). Indeed, treatment that blocks disease progression focused on disease-causing molecular mechanisms and research for specific biomarkers able to identify the disorder in its precocious stages represent still open challenges for clinician and research community.

1.1 Epidemiology and risk factors

PD is the second most common neurodegenerative disease after Alzheimer disease, found in 2–3% of the population ≥65 years of age (Alzheimer's Association, 2014; Dorsey et al., 2007). Incidence is estimated to go from 5 to 35 new cases out of 100 000 individuals per year worldwide (Twelves et al., 2003). Before the 5th decade of life, PD is rare but the incidence increases dramatically (5-10 fold) considering population aged between 60 and 90 years (Pringsheim et al., 2014; Van Den Eeden, 2003). Global prevalence is considered around 0.3% and it is estimated to be higher in Europe, North America, and South America with respect to African, Asian, and Arabic countries. It shows a substantial increase to more than 3% considering population of >80 years of age (Pringsheim et al., 2014). The same consideration can be made for incidence that reaches its peak at 80 years of age, suggesting the ageing is the greatest PD risk factor (Van Den Eeden, 2003).

Together with ageing, another established risk factor is gender; numerous studies described a male to female incidence ratio ranging from 1.3 to 2.0 depending on the populations considered and the age. The only exception of an increased female incidence was found by a Japanese study (Baldereschi et al., 2000; Kusumi et al., 1996; Taylor et al., 2007). Sex-specific genetic mechanisms, protective effects of sex hormones, differences in environmental agents exposure could be responsible for this disparity (Poewe et al., 2017)

Mortality of PD patients rises after the first decade from disease onset, when it is doubled with respect to the general population (Pinter et al., 2015). Taking into account the health care improvements and the consequent increased worldwide life expectancy, the number of PD patients is expected to double by 2030 (Dorsey et al., 2007).

1.1.1 Environmental risk factors

The involvement of environmental factors in PD pathogenesis has been extensively investigated in the last four decades, contributing to provide a better understanding of specific molecular disease pathways. The first toxic agent to be associated to PD development was 1-methyl-4-phenyl-1,2,3,6-tetrahydropyridine (MPTP), substance contained in synthetic heroin. Association became clear when MPTP was discovered to cause severe DA-responsive parkinsonism in drug abusers (Langston,

2017). Once crossed the blood-brain-barrier, MPTP selectively damages dopaminergic neurons, due to its 2-step glial conversion into MPP^+. This metabolite is taken up by the DA transporters and, once entered the mitochondria, inhibits complex I of the mitochondrial respiratory chain (Javitch et al 1985, Schober 2004; Nicklas et al 1985). This discovery led to the development of the first experimental model of PD; MPTP-based animal and cellular model are still widely used today in PD research (Gosh et al 2016).

Till then, several works and epidemiological studies have reported the association of a multitude of environmental agents to increased risk of developing PD, although with different levels of consistency. For instance, 11 environmental factors were reported to significantly alter risk for PD according to a recent meta-analysis that considered 30 possible risk factors (Noyce et al., 2012).

Positive association with the disease was described for pesticides exposure, head injury, beta-blocker use, well water drinking, agricultural occupation. Main factors described, instead, as negatively associated with the disease are represented by coffee drinking, tobacco smoke, NSAID and calcium channel blocker use (Noyce et al., 2012).

The contribution of pesticides as rotenone, paraquat, dichlorodiphenyltrichloroethane, dieldrin, and organophosphates was extensively studied and some confirmed by experimental evidence and still used in modelling the disease, as in the case of rotenone (Priyadarshi et al., 2000).

On the whole, the interpretation of epidemiologic findings and impact of environmental insults on PD risk is often complex due to several inconsistency issues.

1.1.2 Genetic risk factors

The first convincing evidence of a genetic contribution in PD etiology came in 1996 with the mapping and identification of the first gene related to inherited PD, revealing the existence of monogenic forms of the disorder (Polymeropoulos, 1997). Presence of a family history makes the distinction between sporadic and familiar PD; even if rare, hereditary forms of the disease caused by known genetic lesions have helped to shed light on altered cellular pathways even of sporadic PD. Indeed, monogenic forms of the disorders represents only the 3-5% of all PD cases and the 30% of hereditary forms, highlighting the intrinsic complexity of PD etiology (Klein and Westenberger, 2012).

Autosomal dominant PD

SNCA encodes for the protein αsyn, the main component of LB, and was the first gene whose alterations were found associated to autosomal dominant PD, having usually a high penetrance. In particular, genetic lesions include duplications or triplications of the entire locus and different missense mutations (A53T, A30P, E46K, H50Q, G51D) (Krüger et al., 1998; Lesage et al., 2013;

Proukakis et al., 2013; Singleton et al., 2013; Zarranz et al., 2004). Multiplications of the gene, leading to increased protein expression, or pathogenic aminoacid substitutions are responsible for an increased tendency of αsyn to aggregate. Moreover, discovery of genetic lesion in *SNCA* allowed the identification of αsyn as a major component of LB inclusions (Spillantini et al., 1997).

Mutation in LRRK2 represents the most common cause of autosomal dominant PD, found in 13% and 1-2% of non-sporadic and sporadic cases, respectively (Berg et al., 2005; Paisán-Ruíz et al., 2004). The gene product, also known as Dardarin, is a large multi-domain protein involved in numerous cellular pathways, including autophagy, protein synthesis, membrane trafficking and neuronal specific function as neurite outgrowth and synaptic vesicle release (Rideout and Stefanis, 2014). More than 80 mutations have been described in *LRRK2*, missense mutation being the most represented. Among them, the most frequent and better characterized is an aminoacid substitution falling on the kinase domain of the protein, G2019S, that accounts for 4% of familiar and 1% of sporadic cases (Healy et al., 2008).

Another gene confirmed as causative of monogenic autosomal dominant PD is *VPS35*, which encodes vacuolar protein sorting 35 retromer complex component, involved in trafficking between endosomes and trans-golgi network (Trinh and Farrer, 2013; Vilariño-Güell et al., 2011).

Autosomal recessive PD

Classic gene mapping approaches discovered three genes whose loss of function mutation cause autosomal recessive PD: *PARK2*, coding the E3 ubiquitin protein ligase (*Parkin*)*, PINK1*, PTEN, induced putative kinase 1, and PARK7, which stands for Parkinson protein 7, mostly known as *DJ-1* (Bonifati, 2003; Kitada et al., 1998; Valente, 2004). Despite being rare in general PD patients, mutations in these genes are reported to cause a great proportion of early onset PD cases; among them, the most common cause of AR PD is *Parkin.*(Bonifati, 2003; Kilarski et al., 2012)

Other genetic risk factors

Several polymorphisms and variants of monogenic PD genes and other unrelated genes (*MAPT*, *GBA, NAT2, INOS2A, GAK, HLA-DRA,* and *APOE*) are recognized as risk factor for the disorder, expanding the complex genetic landscape of PD (Klein and Westenberger, 2012).

In particular, a large multicenter study identified in 2009 heterozygous mutation in GBA, encoding for the lysosomal enzyme β-glucocerebrosidase, as the most common and universally found risk factor for PD. Indeed, heterozygous individuals carrying *GBA* mutations have five times greater risk of developing PD than non-carrier individuals (Sidransky et al., 2009).

1.2 Clinical features and natural history

The motor presentation of PD has been recognized since its first description by James Parkinson, as a substantial component of the disease. The great part of PD clinical presentation is represented by cardinal motor symptoms; bradykinesia, muscular rigidity, rest tremor, postural and gait instability (Gibb and Lees, 1988; Goetz, 2011). These core motor signs tend to be unilateral for all the disease progression. However, motor presentation is highly heterogeneous among individuals and attempts to classify different clinical subtypes have been made. Essentially, based on clinical observations, PD can be classified as tremor dominant, with a slower progression and less overall disability, and non-tremor dominant, characterized instead by prevalence of akinetic-rigid and gait instability phenotypes (Martinez-Martin et al., 2011). However, non-motor features of PD are emerging as a substantial component of its clinical presentation, having an impact of the health related quality of life of patients (Martinez-Martin et al. 2011). They comprise a multitude of manifestations including olfactory dysfunction, cognitive impairment, psychiatric symptoms, mood disorders, autonomic dysfunction, sleep disorders, fatigue and pain (Chaudhuri and Schapira, 2009). Most of them precedes the onset of the motor symptom, in the prodromal phase of PD (Mahlknecht et al., 2015; Postuma et al., 2012). This premotor stage of PD generally starts with impaired olfaction, constipation, sleepiness, mood disorders and rapid eye movement sleep behaviour disorder (RBD). This phase lasts as an average of 12-14 years prior to the occurrence of parkinsonian motor symptoms. Duration of the premotor phase is about 12-14 years as an average before the onset of parkinsonian motor symptoms (Postuma et al., 2012). Underlying this premotor stage are disease mechanisms that involve also other regions of the peripheral nervous system (PNS) and central nervous system (CNS) besides the dopaminergic system. As the disease progress, motor features become apparent and gradually worsen. While initially symptomatic therapy is efficacious in handling symptoms, lately side effects and complications overcome the beneficial effects. Among them, motor and non-motor fluctuations, psychosis and dyskinesia represent one of the most important issue in clinical management of the disease (Hely et al., 2005).

Treatment-resistant symptoms as freezing of gait, postural instability, falls, dysphagia, speech impairment characterize the late phases of disease, together with autonomic dysfunctions (urinary incontinence, postural hypotension) and dementia, highly prevalent after 20 years from PD onset (Hely et al 2008).

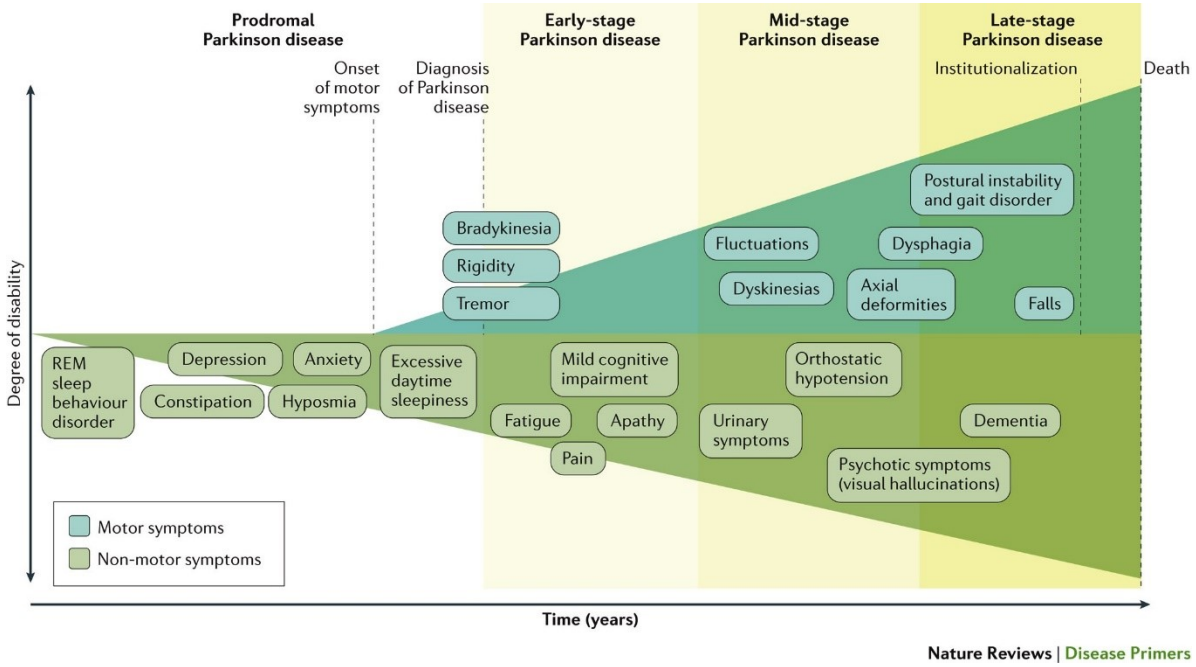

Fig.1. Relationship between clinical symptoms and degree of disability along PD disease progression. (Poewe et al., 2017)

1.3 Diagnosis

Diagnosis of PD is still clinical, based on observations of cardinal motor symptoms. In details, bradykinesia has to be associated with rigidity or rest tremor; further supportive criteria and exclusion criteria are additionally considered for the diagnosis. (Postuma et al., 2015) . However, in the common clinical practice a straightforward diagnosis is still a challenge, with error rate ranging from 15 to 24% in the early disease stages. Clinical misdiagnosis is common with essential tremor, vascular parkinsonism and drug induced parkinsonism (Tolosa et al., 2006). The use of stringent diagnostic clinical criteria, as the UK Parkinson's Disease Society Brain Bank (UKPDSBB) criteria, can only slightly increase the accuracy of diagnosis (Rizzo et al., 2016).

Diagnosis can then be supported by a post-mortem neuropathological examination of a severe neuronal loss in SNpc, mainly in the ventrolateral tier and presence of LB pathology. However, standardization of neuropathological criteria is still mostly needed to improve differential diagnosis with other neurodegenerative conditions (Dickson et al., 2009).

Neuroimaging has become a relevant diagnostic tool in supporting PD diagnosis since the first visualization of dopamine depletion in 1983, thanks to the use of ^{18}F-labelled L-DOPA and PET (Garnett et al., 1983). Brain imaging of structural, functional e molecular changes *in vivo* can be achieved thanks to basic and advanced Magnetic Resonance Imaging (MRI), Single Photon Emission Computed Tomography (SPECT) and Positron Emission Tomography (PET) techniques.

For instance, a tool that has entered clinical routine to make differential diagnosis of PD is 123I-ioflupane single-photon emission CT (SPECT)(Politis, 2014; Stoessl et al., 2014). To this purpose, different MRI techniques able to visualize variations in basal ganglia structures, including structural MRI, can help in distinguishing PD from other parkinsonism (Mahlknecht et al., 2010). Indeed, these methods are effective only in distinguishing PD from other diseases not characterized by presynaptic dopaminergic degeneration. Disorders that include neurodegeneration in SNpc, as multiple system atrophy, corticobasal degeneration, dementia with Lewy bodies, dopamine responsive dystonia, cannot be distinguished from PD with dopamine imaging approaches alone (Mahlknecht et al., 2010). Research efforts are currently aimed at the identification of reliable early diagnostic biomarkers of PD that can reveal the disease in its prodromal phase or even in asymptomatic population. Since its pathogenic role in disease onset and progression, studies have focused in particular on levels of different αsyn species in the cerebrospinal fluid (CSF) and blood. Furthermore, the assessment of CSF concentration of other protein like DJ-1, tau, and β-amyloid, activity of b-glucocerebrosidase are being investigated (Hong et al., 2010). Unfortunately, up to now no biomarkers with good specificities and sensitivities have been found out, neither in CSF nor in blood (Chen-Plotkin, 2014). Particularly helpful would be the correlation of panels of potential biomarkers, instead of a single protein concentration, with disease onset and progression (Shi et al., 2011).

Even if it is not part of the diagnostic routine, in presence of individuals with early onset PD or family history (monogenic form of PD), genetic testing can help the diagnostic process. Issues, thought, are to be considered when approaching genetic testing due to the variable expressivity and reduced penetrance of monogenic PD related genes (Kalia and Lang, 2015; Poewe et al., 2017).

1.4 Pathophysiology

1.4.1 Neuropathology

As mentioned-above, the two main neuropathological hallmarks of PD are the selective degeneration of DA neurons of the SNpc and the presence of cytoplasmic proteinaceous inclusion in the soma (LB) and neurites (Lewy neurites-LN) of surviving neurons (Braak et al., 2003). Neuronal loss is restricted to specific brain areas; initially affects mainly the ventrolateral region of the SNpc that project to the dorsal striatum and become more widespread along disease progression (Damier et al., 1999). The early phases of disease are already characterized by a major loss of DA neurons in this area, thus neurodegeneration is thought to begin in the premotor disease stage, as described by clinicopathological studies (Dickson, 2018; Dijkstra et al., 2014). As the disease progresses, neurodegeneration also impact the locus coeruleus, the nucleus basalis of Meynert, the dorsal motor nucleus of the vagus (DVN), amygdala and hypothalamus (Dickson, 2012)

Widespread deposition of αsyn-positive inclusions is the other key neuropathological sign of the disorder, although not solely found in PD (Iacono et al., 2015). These intracellular proteinaceous aggregates are made up mainly by misfolded, insoluble and phosphorylated forms of αsyn, together with other uncatabolized molecules and lipids (Wakabayashi et al., 2013). αsyn has a high tendency, under certain environmental and cellular conditions (or upon mutations), to aggregate into oligomers, protofibrils and insoluble-amyloid fibrils that finally accumulates into LB. Deposition of LB and LN is not limited to certain areas of the CNS but it can be found in several peripheral nervous system districts (vagus nerve, sympathetic ganglia, cardiac plexus, enteric nervous system, salivary glands, adrenal medulla, cutaneous nerves and sciatic nerve) (Arizona Parkinson's Disease Consortium et al., 2010; Del Tredici et al., 2010; Fumimura et al., 2007; Iwanaga et al., 1999). To note, Lewy pathology has been hypothesized by Braak and colleagues in 2003 to spread in a stereotyped way across interconnected and selectively vulnerable brain areas (Braak et al., 2003). The original theory divides Lewy Pathology progression into 6 different stages, that seems to follow the spatial and temporal PD clinical course.

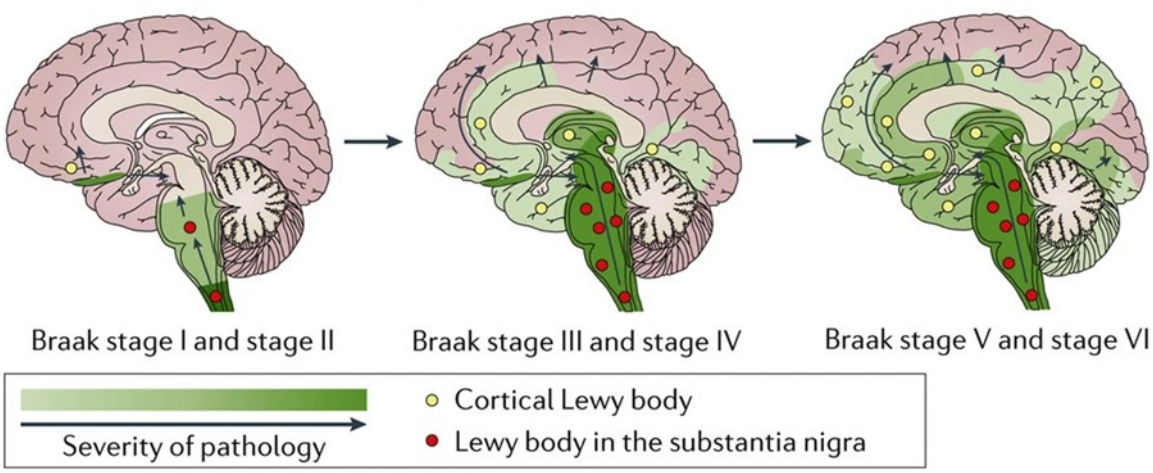

Fig.2. The theorized progression of α-synuclein aggregation in PD firstly proposed by Braak in 2003 (adapted from (Poewe et al., 2017)

Lewy pathology would start from the peripheral nervous system and propagates in a caudo-rostral direction towards the CNS. LB inclusions initially affects monoaminergic and cholinergic neurons of the DVN and olfactory bulbs (Stage I-II), reach then the midbrain and neostriatum (stage III), the basal forebrain and cortical areas (stage IV), ultimately affecting the neocortex (stages V-VI). Onset of premotor symptoms can be ascribed to stage I-II, then, consequent to the depletion of striatal dopamine, stage III could correspond to the typical motor symptoms. Stages IV-VI can be associated instead to non motor symptoms occurring in the advanced phases (Braak et al., 2003; Kalia and Lang, 2015). Related to non-motor symptoms, the specific association between cortical Lewy pathology

and cognitive impairments in PD is strongly supported by various neuropathological studies (Irwin et al., 2012; Kempster et al., 2010; Selikhova et al., 2009).

1.4.2 Molecular pathophysiology

Despite the precise molecular mechanisms underlying PD pathophysiology are still not clarified, multiple cellular pathways have been shown to contribute to neuronal loss. Among them, evidences coming from genetic PD lesions, studies on patient-derived tissues and experimental works highlight as relevant players αsyn proteostasis and degradation, mitochondrial dysfunction, oxidative stress and neuroinflammation. In addition, abnormal levels of toxic forms of αsyn undoubtedly impact on many of these cellular processes, triggering or contributing to the molecular alterations (Michel et al., 2016). In this regard, several works report αsyn to exert neurotoxicity in multiple ways, causing endoplasmic reticulum stress, synaptic dysfunctions, alterations in Golgi transport, calcium deregulations and impairments of cytoskeletal dynamics (Ganguly et al., 2018).

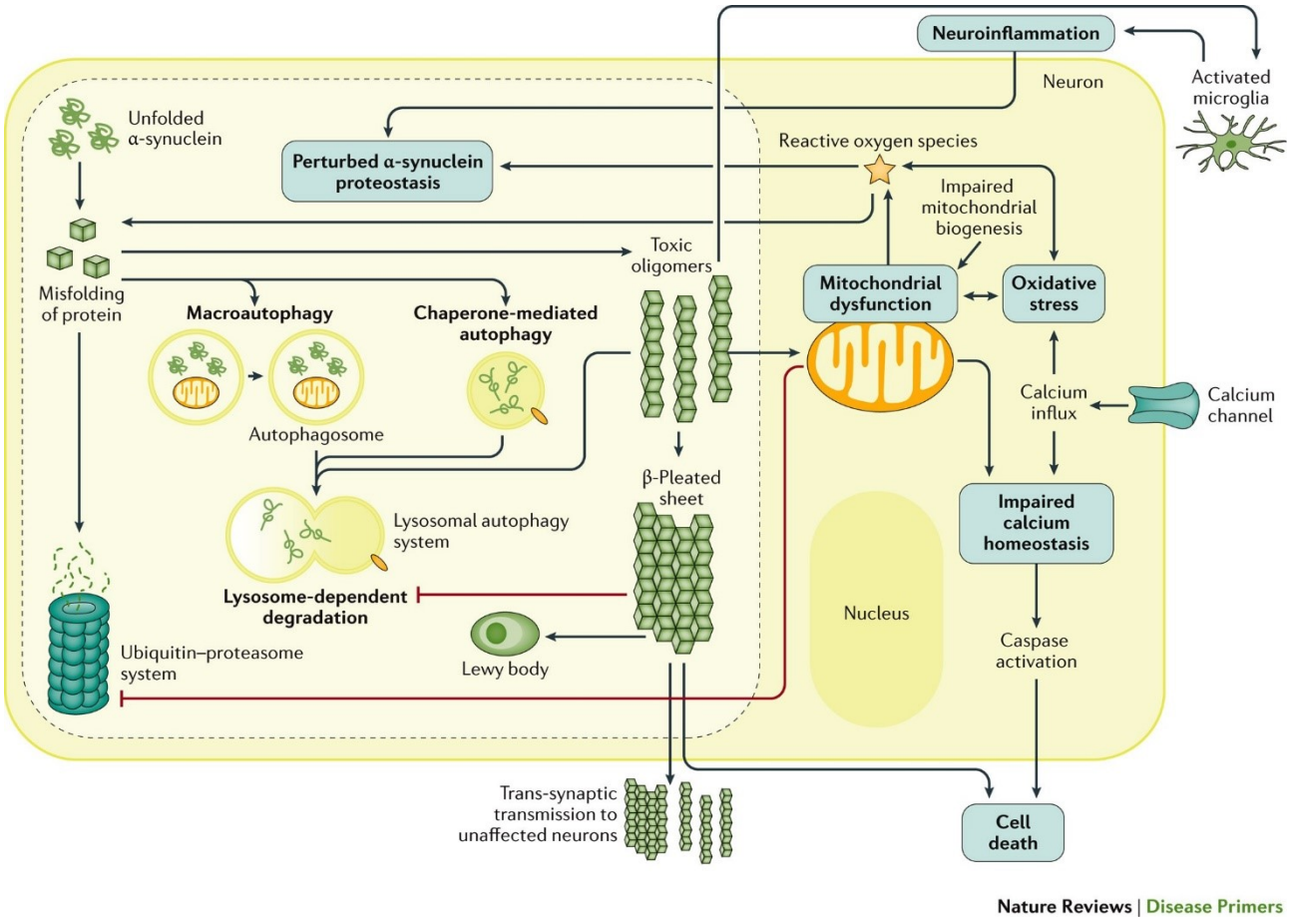

Fig.3 Major molecular pathways involved in PD molecular pathogenesis and their interactions. (Poewe et al., 2017)

Mitochondrial dysfunction

As in many neurodegenerative conditions, impairment of the mitochondrial function is undoubtedly a core element in PD molecular pathogenesis (Schapira, 2007). In the first place, directly supporting this hypothesis, features of PD neuropathology were replicated by experimental models based on use of toxins specifically targeting mitochondrial function (Langston et al., 1984; Przedborski et al., 2004). In addition to this evidence, target genes of the mitochondrial master transcriptional regulator PCG1α were shown to be underrepresented in PD (Schapira, 2007). Interestingly, a detrimental interplay between αsyn and mitochondrial dysfunction has been emerging from recent studies. Aberrant accumulation of the protein within mitochondria can cause impairment of the complex I, whose activity is also reduced in PD-patients derived tissues (Zheng et al., 2010). αsyn oligomers, instead, were described to impact negatively on PCG1α levels. Moreover, genetic forms of PD caused by mutations in genes regulating mitochondrial homeostasis (*LRRK2*, *PINK1*, *PARK2*) further support a key involvement of this organelles (Bose and Beal, 2016; Pickrell and Youle, 2015; Schapira, 2007).

Oxidative stress

Strictly linked to mitochondrial dysfunction, PD is characterized by augmented levels of oxidative stress. This pathogenic feature can be found in patients brain tissues and, moreover, confirmed by hereditary PD forms caused by lesions in antioxidant-related genes, such as *DJ1* (Bonifati, 2003; Dias et al., 2013). Interestingly, various features of nigral dopaminergic neurons make them particularly susceptible to oxidative stress. For instance, the homeostatic maintenance of their long unmyelinated axons with high synaptic density and of the autonomous pace-making activity, based on oscillations of cytosolic calcium, need a significant energy expenditure (Pissadaki and Bolam, 2013; Surmeier et al., 2011). Moreover, high concentrations of dopamine and its metabolites is thought to promote the generation of toxic oxidative species (Lotharius and Brundin, 2002). A detrimental effect of mitochondrial dysfunction and oxidative stress seem to impact also on the proper functionality of the lysosomal-autophagic system, indicating that alterations in different cellular pathways can be strongly interconnected (Dehay et al., 2010).

Neuroinflammation

Another emerging key feature of PD is neuroinflammation, as displayed by various post-mortem, fluid biomarkers and brain imaging studies (Moehle and West, 2015). Several genes expressed by immune cells and participating to immune modulation were associated to the risk of developing PD by GWAS studies (International Parkinson's Disease Genomics Consortium (IPDGC) et al., 2014). Furthermore, a vicious cycle between αsyn aggregation and neuroinflammation have been reported

by several works. For instance, αsyn can activate adaptive and innate immune system and, the other way round, neuroinflammation seems to trigger αsyn aggregation (Gao et al., 2008; Hirsch and Hunot, 2009). Nevertheless, a merely detrimental effect of neuroinflammation in PD onset and progression is presumably not representative of the whole picture. Beneficial effects of microglia and activated immune cells have been reported as well. Moreover, various immunotherapeutic strategies, especially targeting toxic αsyn species, have been tested as potential novel therapeutic approaches (George and Brundin, 2015).

1.4.3 Motor circuit pathophysiology

Besides neurodegeneration, many PD symptoms derive from an aberrant neuronal activity established at the circuit level. In particular, the thalamo-cortical basal ganglia (BG) circuitry is the main site of the neuronal circuit dysfunction in PD pathogenesis.

The BG and related nuclei consist of a system of subcortical nuclei, primarily involved in motor control and other functions such as motor learning, executive functions, reward-related behaviors and emotions. Indeed, forming a complex network of parallel but anatomically segregated loops, BG integrate inputs from different cortical regions to the thalamus and back to the cortex (Alexander et al., 1990, 1986).

Although the classic model of BG motor circuit has been largely revisited and integrated in the last years, it was essential for the current understanding of how dopamine depletion give rise to PD symptoms and reshape the thalamo-cortical BG network (Alexander et al., 1986; DeLong, 1990; Obeso et al., 2000). Cortical areas project to the primary input structure of the BG, the striatum, through glutamatergic synaptic connections with GABAergic spiny projection neurons (SPNs). According to the classic view, SPNs originate two separate pathways towards the globus pallidus pars interna (GPi) and the substantia nigra pars reticulata (SNr), the BG output nuclei. SPNs expressing class 1 DA receptors (D1-SPNs) mediate the *direct pathway* by directly inhibiting the GPi and SNr neurons. A decreased output activity of these structures disinhibits the thalamus that, sending excitatory projections to the cortex, ultimately leads to increased cortical excitation. D2-type SPNs, instead, project to the SNr and GPi through connections with the external region of the globus pallidus (GPe) and the STN, forming the *indirect pathway* (Albin et al., 1989; Deng et al., 2006; Gerfen et al., 1990). STN glutamatergic neurons activate then the GPi and SNr. Therefore, activity of neurons in the indirect pathway inhibits the GPe leading to disinhibition of the STN and excitation of the GPi/SNr, that in turns reduces excitation of cortical neurons. Activity of the BG results from a controlled balance, essential for a proper control of movement, between the opposing direct and indirect pathway. According to this model, the glutamatergic impact on the cortico-striatal inputs is

modulated by DA that, activating firing of D1 SPN neurons and dampening D2 neurons, promotes the direct pathway and inhibits the indirect. In the parkinsonian condition, striatal DA depletion leads to a decreased inhibition of indirect pathway neurons and reduced excitation of the direct pathway neurons. This imbalance eventually leads to increased output activity of the GPi and SNr, with consequent inhibition of thalamic excitatory connections with the cortex. The downstream overinhibition of thalamocortical regions would be at the basis of the cardinal motor symptoms of PD (Albin et al., 1989; Obeso et al., 1997).

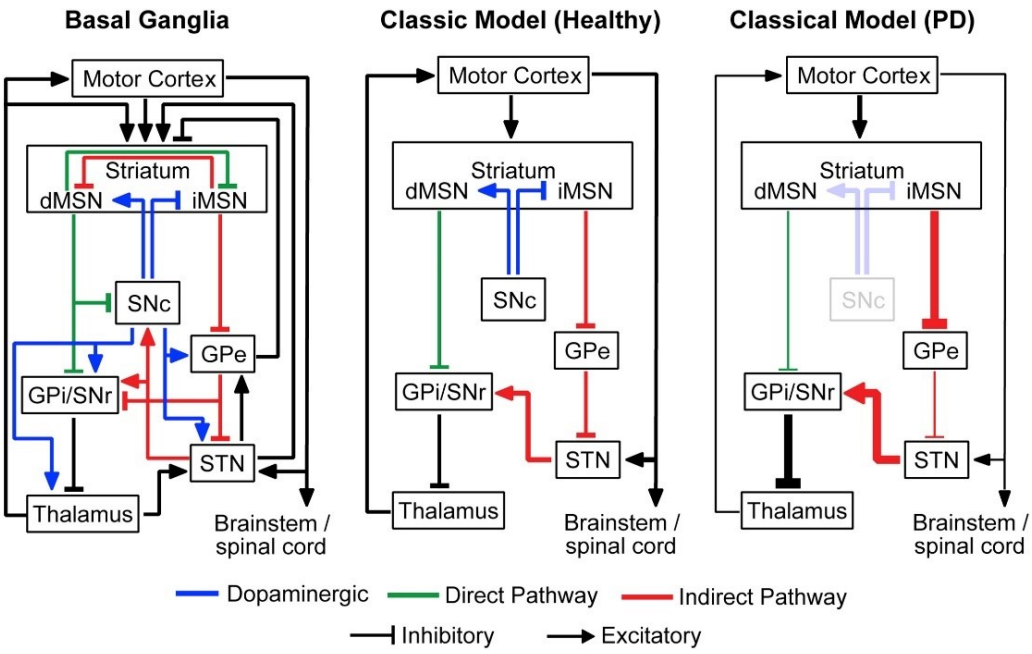

Fig.4. Schematic representation of the classical Basal Ganglia model in healthy and PD conditions. (McGregor and Nelson, 2019)

However, years of extensive research have demonstrated that the model is far more complex than this description. For instance, SPNs cannot be so easily distinguished in D1 or D2 type, since colocalization of D1 and D2 receptors in SPNs has been also reported (Lester et al., 1993). Then, other pathways have been integrated in this circuit, such as a direct connection between cortical motor regions and the STN, the *hyperdirect pathway* (Nambu et al., 2000). Moreover, changes in interconnection between the BG and the cerebellum as well as aberrant neural synchronization may contribute as well to PD pathophysiology (Dirkx et al., 2016).

1.5 Therapy

Currently, PD can be still considered an incurable neurodegenerative disorder. Although relevant steps towards the understanding of its underlying pathophysiology have been made, no disease-modifying drugs able to dampen the neurodegenerative process nor providing neuroprotection are approved and used in clinics so far. Major challenges derive from the high complexity of its pathogenic mechanisms that involves multiple cellular processes and the lack of valid diagnostic biomarkers allowing an early diagnosis. Animal models generally reproduce only features restricted to few pathogenic pathways, thus not being able to fully recapitulate the human disorder. Moreover, besides the dopaminergic systems, other neurotransmitter systems are dysfunctional, even in the early disease stages (AlDakheel et al., 2014). Nonetheless, PD can be managed through pharmacological treatment and, at least for some years, quality of life can be improved. Pharmacological approaches currently used in clinics can be generally distinguished in drugs that acts on dopaminergic or non-dopaminergic targets.

1.5.1 Dopaminergic therapy

Cardinal motor features of PD are strictly dependent on the neurodegeneration of the SNpc neurons and to the consequent deficiency of striatal dopamine. Thus, the aim of the dopaminergic therapy is to replace, acting at different levels, the concentration of the neurotransmitter within the striatum.

L-DOPA. The revolutionary idea of substituting the endogenous dopamine through administration of the aminoacid L-DOPA, direct dopamine precursor, dates back to the1960s (Birkmayer and Hornykiewicz, 1961). Systemic administration of L-DOPA, although with several improvements, is still considered the gold standard of PD treatment after more than 50 years (Olanow et al., 2009). Indeed, it is estimated that almost all PD patients will receive L-DOPA treatment during the clinical course of the disease (LeWitt and Fahn, 2016; PD MED Collaborative Group, 2014). Exogenous DA cannot be administered because of its hydrophilic structure incapable of passing the blood-brain-barrier (BBB); L-DOPA, instead, is able to enter the CNS and be efficiently converted into the active neurotransmitter within the nigrostriatal system (Melamed et al., 1980; Rautio et al., 2008). Delivered systemically, L-DOPA is metabolized at the periphery through different pathways, and primarily by the aromatic L-amino acid decarboxylase (AAAD, DOPA decarboxylase), which drastically diminished its availability at the CNS. Thus, L-DOPA is administered systemically through the oral route in combination with peripheric DOPA decarboxylase inhibitors (Carbidopa) or COMT inhibitors (Entecapone) (Hagan et al., 1997; LeWitt and Fahn, 2016; Nutt, 2000; Nutt et al., 1994).

L-DOPA has a high initial symptomatic efficacy in relieving motor symptoms, however its long-term use is particularly complicated by the onset of debilitating side effects. L-DOPA dependent motor complications include motor fluctuations, dyskinesias and on-off effects of the treatment (Muenter and Tyce, 1971). After 5 years from the beginning of L-DOPA therapy, about 80% of patients are estimated to suffer from drug-induced dyskinesias, whose clinical manifestations are often described as worse than the disease symptoms (Bastide et al., 2015). Core mechanisms underlying the onset of dyskinesias are still not totally understood. Both pre- and post-synaptic modifications concur in their establishment, causing a pulsatile stimulation of striatal DA receptors and consequent maladaptive plasticity mechanisms (Cenci, 2014; Mellone and Gardoni, 2018; Olanow et al., 2006). The unhelpful pharmacokinetic properties of this molecule as its short half-life lead to an intermittent drug delivery. In addition, variations of gastrointestinal absorption also affect the final CNS concentration (Poewe and Antonini, 2015). To overcome these important issues, different approaches have been and are currently being developed, as sustained-release formulations or continuous delivery of the drug (Poewe and Antonini, 2015).

***Dopamine agonists*.** By directly stimulating DA receptors, dopaminomimetics represent the alternative approach to elicit the physiological neuronal responses triggered by dopamine on striatal medium spiny neurons. DA receptors are widely expressed in the CNS and can be divided in two classes, specifically the D1-type and the D2-type, with opposing effect on neuronal activity. Many dopamine receptor agonists currently used in clinics primarily act on the D2 types (Jenner, 1995). The first agonists (ergoline-derivatives) were introduced in therapy in the 1970s and since then have been widely used as PD symptomatic treatments (Connolly and Lang, 2014; Fox et al., 2011). First generation agents have a limited use for safety issues, in particular their ability to cause severe side effects due to their action on the 5-hydroxytryptamine (5HT) receptor (Hubble, 2002). Currently, the most used DA agonists (all non-ergoline derivatives) include Pramipexole, Ropinirole, Rotigotine and Apomorphine and are approved both as monotherapy or combined with L-DOPA in late disease phases (Alonso Cánovas et al., 2014). In this regard, they have some advantages with respect to L-DOPA such as a longer half-life and a better pharmacokinetics profile that allow to be administered once a day. Generally, patients treated with dopaminomimetics have a significant decreased risk of developing motor fluctuations and dyskinesias, possibly due to a less-pulsatile stimulation of the DA receptors. On the other side, issues are represented by a decreased efficacy in reducing motor symptoms with respect to L-DOPA and significant increased risk of drowsiness and psychiatric side effects (Fox et al., 2011; Jankovic and Poewe, 2012). Development of hallucinations and impulse control disorder, in particular, are possibly due to an overstimulation of D3 receptors preferentially

expressed in the ventral striatum, with consequent imbalances of the brain reward systems (Voon et al., 2011).

Monoamine oxidase type B (MAO-B) inhibitors. Together with the presynaptic reuptake by the dopamine transporter DAT, the enzymatic activity of MAO-B in glial cells participate to DA clearance from the synaptic cleft (Schapira, 2011). Therefore, MAO-B inhibition allows to prevent dopamine degradation and to increase synaptic dopamine concentration. Selective and irreversible MAO-B inhibitors as selegiline or rasagiline, initially combined with L-DOPA, have now been demonstrated to have efficacy as monotherapy too (Schapira, 2011). Recently approved, the reversible inhibitor safinamide combines its dopaminergic action with the blockade of voltage-dependent Na^+ and Ca^{2+} channels and inhibition of glutamate release (Fox et al., 2011).

Catechol-O-methyltransferase (COMT) inhibitors. Due to formulations of L-DOPA containing DOPA-decarboxylase inhibitors, its peripheral metabolism shifts to a different pathway and in particular to the orto-methylation performed by COMT. Therefore, co-administration with COMT inhibitors is the treatment of choice in those patients experiencing wearing-off motor fluctuations, to further enhance half-life and bioavailability of L-DOPA (Müller, 2015).

1.5.2 Non dopaminergic agents

Despite the undoubtedly symptomatic efficacy of dopaminergic therapy in ameliorating PD motor impairments, imbalances in other neurotransmitters system participate to PD pathogenesis along the different disease stages. Therefore, other pharmacological targets need to be considered in clinics to address non-motor PD features and treatment-dependent side effects. Those symptoms comprise consequences of L-DOPA treatment as motor fluctuations, dyskinesias and L-DOPA resistant motor symptoms (freezing of gait, postural instability and falls, treatment-resistant tremor, impairment in speech and swallowing). The only approved agent to manage L-DOPA induced dyskinesia is amantadine, *N*-methyl-d-aspartate receptor (NMDA-R) antagonist (Connolly and Lang, 2014; Perez-Lloret and Rascol, 2018). Non-dopaminergic therapy can also be used to ameliorate other non-motor issues of PD, and in particular cognitive impairment, depression, autonomic disturbances. Cholinesterase inhibitors can be prescribed to PD patients with dementia helping in managing cognitive dysfunction (Connolly and Fox, 2014; Seppi et al., 2011). Clozapine, however its precise mechanisms of action in PD is still poorly understood, is the most efficacious antipsychotic agent used in PD since other atypical neuroleptics, by presumably blocking D2-type receptors, have a deleterious effect (Seppi et al., 2011). Especially in advanced disease stages, autonomic dysfunctions can significantly worsen patients' quality of life. The mineralcorticoid fludocortisone, adrenergic agents and the noradrenergic precursor droxidopa are administered to address orthostatic

hypotension. Antimuscarinics are prescribed to manage urinary incontinence while pro-kinetics drugs can improve constipation (Perez-Lloret et al., 2013).

Deep brain stimulation (DBS). Beyond pharmacological therapy, DBS is based on the high frequency electrical stimulation of the subthalamic nucleus, able to mimic the effect of a lesion. The evidence of the antiparkinsonian effect of a STN lesion came in 1993 and currently DBS is a clinically approved therapy for dyskinesia and motor fluctuations in advanced stages PD (Fox et al., 2011). Criteria for DBS therapy is idiopathic PD with excellent response to L-DOPA and long-term drug induced motor complications. Exclusion criteria comprise psychiatric symptoms as major depression, dementia and acute psychosis (Bronstein et al., 2011). However, DBS is complex treatment mainly due to high expertise level for the correct placing of the brain electrode, postoperative clinical course and balancing drug therapy with the neurostimulation (Bronstein et al., 2011). Moreover, intracranial bleedings, device infections and misplacements are the most relevant adverse events together with development of psychiatric sequelae of (Voges et al., 2007; Volkmann et al., 2010).

αsyn immunotherapy. The rationale for targeting αsyn aggregates through immunotherapeutic approaches reside in the ability of the protein, even of the oligomeric species, to spread trans-synaptically in a prion-like manner (Antonini et al., 2020; Valera and Masliah, 2013). Data on animal models highlight the disease-modifying potential of reducing aggregated αsyn species and its neuronal propagation (Brundin et al., 2017; Games et al., 2013). Several monoclonal antibodies against αsyn are being evaluated in clinical trials. For instance, two large double-blind phase two trials of passive immunotherapy in early PD are currently ongoing, and one of them seemed to show effects of clinical efficacy after 52 weeks treatment (Chatterjee and Kordower, 2019; Jankovic and Poewe, 2012). However, passive immunotherapy has the issue of requiring monthly intravenous infusions. Interestingly, also strategies based on vaccination with specific active immunotherapy are under study, allowing to bypass this disadvantage. The aim of this approach is to self-induce an immune response against a specific protein. In this regard, PD01A, a specific active immunotherapy addressed to oligomeric αsyn, has showed safety and tolerability in a recent phase 1 study in PD patients (Volc et al., 2020).

Innovative strategies. Moreover, among innovative therapeutic strategies cell replacement therapy represent a promising option. Transplantation of DA neurons or progenitors generated from pluripotent stem cells, usually embryonic stem cell (ESCs) and human induced pluripotent stem cells (hiPSC) is currently evaluated by different pre-clinical and clinical trials (Barker et al., 2017; Garitaonandia et al., 2016; Wang et al., 2018). Gene therapy delivered through AAV vectors is another approach that is being investigated for PD treatment. In particular, genetic targets identified

till now can be classified in i. non disease modifying, mainly aimed at expression of DAergic or GABAergic enzymes ii. disease modifying, based on overexpression of neuroprotective growth factors or on the repairing of specific gene mutations (Axelsen and Woldbye, 2018).

1.6 PD models

1.6.1 *In vitro* models

The establishment of reliable *in vitro* experimental models to investigate the early events of PD pathogenesis represents a key issue in the field. However, to mimic and reproduce *in vitro* the complex neuronal circuitry involved in PD-associated degeneration of DAergic neurons still remains a highly challenging issue. *In vitro* PD models used in the last 25 years of research range from cell lines, primary rat or mice neuronal cultures to the more recent use of human induced pluripotent stem cells (hiPSCs) and, finally, the development of 3D midbrain organoids (Ferrari et al., 2020).

Cell lines. The pathological hallmarks of PD can be reproduced in culture either genetically, through the overexpression or silencing of PD-related genes (*SNCA*, *Parkin*, *PINK1*, *LRKK2*, *GBA*), or chemically, through the use of neurotoxins (such as 6-OHDA, MPP^+, rotenone). Allowing to investigate the different molecular pathways altered in PD pathophysiology, genetic models are able to reproduce a condition that is more similar to the *in vivo* one. Overall, cell lines have been used mainly for evaluating apoptosis, mitochondrial and gene dysfunction, oxidative stress, screening of potential drugs and their relative neuroprotective properties. The most frequently adopted include SH-SY5Y, PC12, LUMHES, N2a, N27, MN9D cell lines. However, the use of these models is limited by relevant disadvantages such as further differentiation steps to reproduce physiology and morphology of DAergic neurons and issues related to their oncogenic origin (Lopes et al., 2017).

Primary DAergic cultures. Primary DAergic neurons, whose culturing method has been optimized in recent studies, have been widely used for evaluation of cell survival after treatment with neurotoxic compound possibly involved in PD pathogenesis or putative neuroprotective agents (Lopes et al., 2017; Weinert et al., 2015). The setting up of reliable cell cultures of DAergic neurons provide a very useful *in vitro* model for the study of the molecular and cellular mechanisms involved in the neurodegeneration and for the understanding of the causes of selective neuronal vulnerability for this disorder (Studer, 1997) Furthermore, development of PD-related transgenic mice has brought back a more extensive use of primary DAergic neurons prepared from these animal models (Lin et al., 2012; Ramonet et al., 2011).

Primary striatal neuronal cultures. At dendritic spines of striatal SPNs, DAergic terminals from the SNpc converge with glutamatergic terminals from the cerebral cortex. The degeneration of the nigrostriatal DAergic pathway in PD leads to significant morphological and functional changes in the striatal neuronal circuitry, including modifications of the corticostriatal glutamatergic synaptic architecture (Calabresi et al., 2007). To investigate these mechanisms *in vitro*, striatal neurons have to be co-cultured with cortical neurons to acquire a correct physiological network activity and development of dendritic spines (Burguière et al., 2013; Segal et al., 2003). Nevertheless, co-cultures of cortical and striatal neurons, although spontaneously active, are almost absent of cholinergic interneurons and develop connections from striatal cells to cortical cells that are not present *in vivo*.

Human induced pluripotent stem cells. The introduction of human induced pluripotent stem cells (iPSCs) technology, discovered by Takahashi and Yamanaka in 2006, revolutionized the modelling of human diseases, especially neurodegenerative disorders and thus, PD as well (Takahashi and Yamanaka, 2006). The possibility to reprogram fully differentiated cells from patients to the stemness and then redirecting them towards the desired cell type brought a great power to biomedical research. iPSCs give the opportunity to have disease-relevant neuronal subtypes that retain the specific genetic background of the patient. Consequently, depending on their origin, iPSCs-derived neurons allow to investigate molecular alterations either of genetic or sporadic PD forms and assess the impact of novel risk variants (Ferrari et al., 2020).

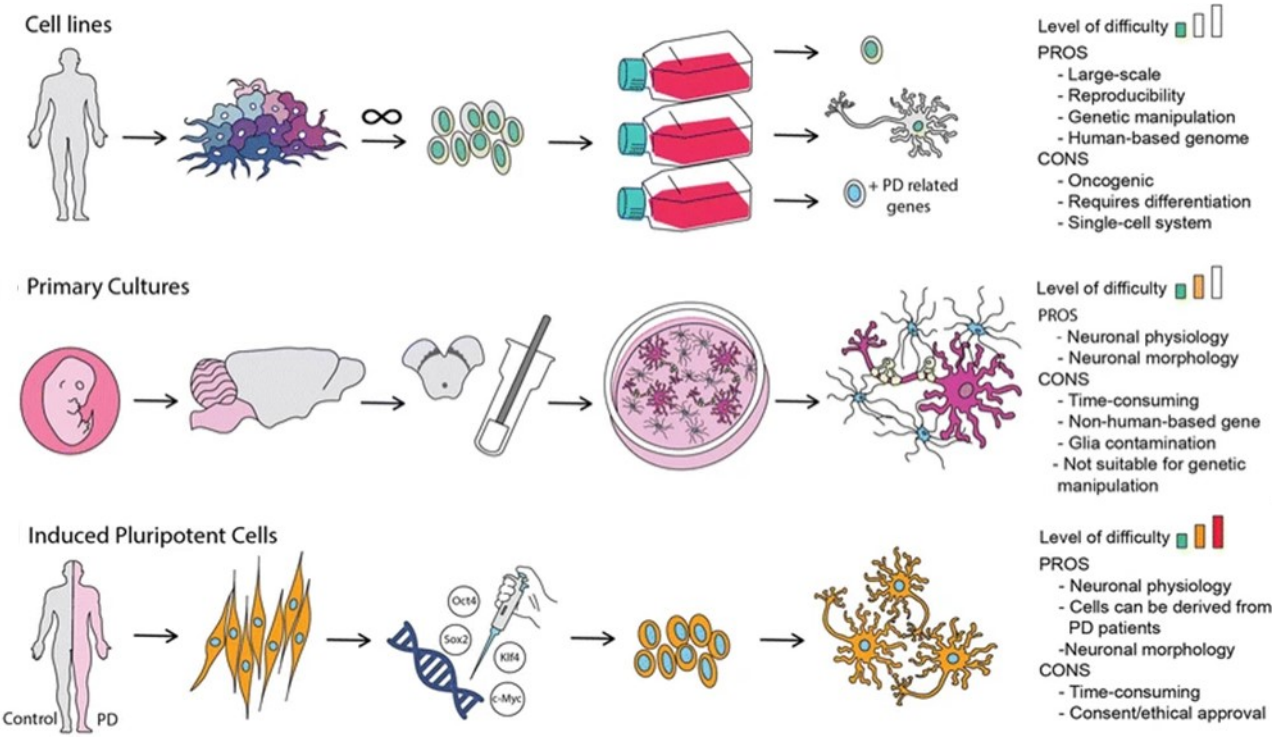

Fig.5. Schematic representation of the most used PD *in vitro* model, highlighting advantages and issues of each approach. Adapted from (Lopes et al., 2017)

1.6.2 Neurotoxin-based *in vivo* models

Discovery of structural analogues of DA able to exert selective neurotoxicity towards DAergic neurons lead to the development of experimental *in vivo* models of sporadic PD, which are still widely used today in research. In particular, the most commonly employed toxic compounds to generate animal PD models are 6-hydroxydopamine (6-OHDA) and MPTP.

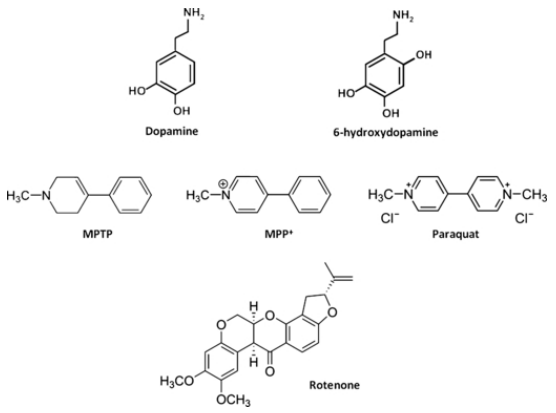

Fig.6. Structures of DA and major DAergic toxins used in experimental PD models (Blandini and Armentero, 2012)**.**

6-OHDA experimental models

6-OHDA was the first toxin used to generate an animal model of PD (Ungerstedt et al., 1974). Due to its incapability to cross the BBB, 6-OHDA has to be delivered through intracerebral injection. Once in the CNS, it is taken up through DAT inducing mitochondrial toxicity and ROS production that finally lead to neurodegeneration of DAergic neurons within the nigrostriatal system (Glinka and Youdim, 1995). 6-OHDA rodent models, most commonly rats, are based on stereotaxic injection of the toxin directly into the SNpc, in medial forebrain bundle (MFB) or striatum. The unilateral lesion of the MFB causes ipsilateral neuronal loss and fiber degeneration in striatum and SNpc (Park et al., 2018). This model have been and is still used to study PD motor behavioral deficit related to the nigrostriatal system degeneration (Blandini et al., 2008; Deumens et al., 2002). Striatal injection of the toxin is generally chosen for the study of early PD stages, since it induces a partial DAergic cell loss with mild progressive motor impairments. The targeting of the MFB, instead, generally causes a massive neurodegeneration that results in severe motor symptoms, efficiently mimicking late disease stages (Carta et al., 2010; Francardo et al., 2011; Winkler et al., 2002). Moreover, 6-OHDA models are extensively used to investigate the effects of treatment-induced motor complications and, in particular, the molecular mechanisms leading to the onset of L-DOPA-induced dyskinesias (LIDs) (Aristieta et al., 2012; Tronci and Francardo, 2018). However, this model lack one of the essential key neuropathological feature of PD, since αsyn does not deposit into LB.

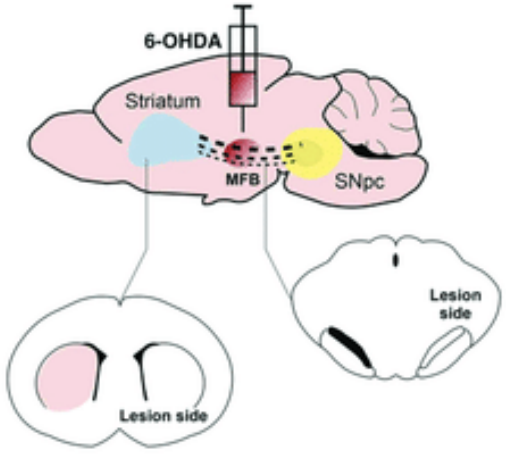

Fig.7. Schematic representation of 6-OHDA unilateral lesion of the MFB showing injection site and side of the lesion. Adapted from (Mendes-Pinheiro et al., 2019)

MPTP-based model

The brain-penetrant compound 1-methyl-4-phenyl-1,2,3,6-tetrahydropyridine (MPTP) undergoes metabolic transformation into the dopaminergic neurotoxin 1-methyl-4-phenylpyridinium ion (MPP^+) by MAO-B enzymes in glial cells (Chiba et al., 1984; Schinelli et al., 1988). Transported into

neurons by DAT, MPP^+ localize within the mitochondria and inhibits a key step of the electron transport chain, impairing complex I activity and inducing ROS production (Burns et al., 1985; Ramsay et al., 1991). Firstly discovered in the 80s among contaminants of synthetic heroin, MPTP administration can be considered a classic PD model, widely used to reproduce parkinsonism in various species (Langston, 2017; Meredith and Rademacher, 2011). Due to several advantages, MPTP-based mice models are the most commonly used, primarily to investigate the molecular mechanisms underlying DAergic neurodegeneration and to test potential neuroprotective agents (Meredith and Rademacher, 2011). Rats, instead, show significant resistance towards MPTP toxicity due to high activity of MAO-B in cerebral microvessels. Indeed, MPP^+ hardly manages to cross the BBB and MPTP has to be directly injected into the striatum or SNpc to induce toxicity in this species (Di Matteo et al., 2006; Galpern, 1996). In mice, parkinsonism is usually achieved by intraperitoneal administration of the toxin: different injection dosages (acute, subacute and chronic) and timings allow to reproduce different stages and severity of the disease. Repeated chronic injections are useful to study disease progression and motor impairments (Hwang et al., 2016; Xu et al., 2017). Although able to replicate different aspects of PD phenotype, the usual lack of neuronal deposition of LB-like inclusions represents the main drawback of this model (Schober, 2004; Shimoji et al., 2005).

The non-human primate MPTP model

The MTPT-treated monkey remains still today the mainstay for the study of possible pharmacological interventions in PD, due to their anatomic, genetic and physiologic proximity to humans. Considering the close similarity between the human and monkey brain organization and in particular of the striatal regions, non-human primates have definitely more developed fine motor skills with respect to rodents, constituting a great advantage for modelling and studying PD-related motor impairments (Gnanalingham et al., 1995). The validated MPTP-treated monkey phenocopies multiple parkinsonian dysfunctions and, most importantly, the response to therapy, making it essential to preclinical studies of potential neuroprotective compounds and drug candidates (Emborg, 2007; Jenner et al., 2000; Stephenson et al., 2005).

2. Role of αsyn in PD

2.1 Structure and functions

Firstly discovered in 1988, αsyn, encoded by *SNCA* gene, is a small, soluble intracellular protein containing 140 residues (15 kDa) belonging to the synuclein superfamily, that also comprises β and γ synuclein (Maroteaux et al., 1988). It is widely expressed in neurons and is mainly enriched at presynaptic terminals, though it localizes also in mitochondria, endoplasmic reticulum, and, at a lower extent, in nuclei. (Guardia-Laguarta et al., 2015; Maroteaux et al., 1988; Yuan and Zhao, 2013). However, its expression is not brain-restricted, as it can be found in red blood cells and at a lesser degree in other tissues, thus suggesting different physiological functions (Baltic et al., 2004; Nakai et al., 2007).

Structure

Structurally, αsyn can be divided into three main domains with distinct physico-chemical properties, given by the different aminoacidic composition. The N-terminal region is characterized by seven 11-mer repeats with a KTKGEV consensus sequence (residues 1–95) (Bussell and Eliezer, 2003). Similarly to apolipoproteins structure, this domain forms an amphipathic α-helix which confer to the protein the ability to bind negatively charged lipid membranes (Bussell, 2005; Davidson et al., 1998). Aminoacids from 60 to 90 constitute the NAC (Non-amyloid β component) domain, thought to favour αsyn aggregation and lipid sensing (George et al., 1995; Xu et al., 2016). Interestingly, all the identified *SNCA* PD missense mutations fall within the N-terminal region of the protein, indicating the crucial role of lipid-binding. αsyn C-terminus aa (96-140) is highly acidic and mainly unstructured, and it is targeted by post-translational modifications at various sites, including phosphorylation at Ser129, nitration at Tyr125, Tyr133 and Tyr136, possibly promoting toxic species formation (Burai et al., 2015; Fujiwara et al., 2002; Souza et al., 2000). The C-terminus was shown to interact with proteins and ions, to modulate membrane binding and protects from aggregation of the protein (Hoyer et al., 2004; Nielsen et al., 2001; Oueslati et al., 2010).

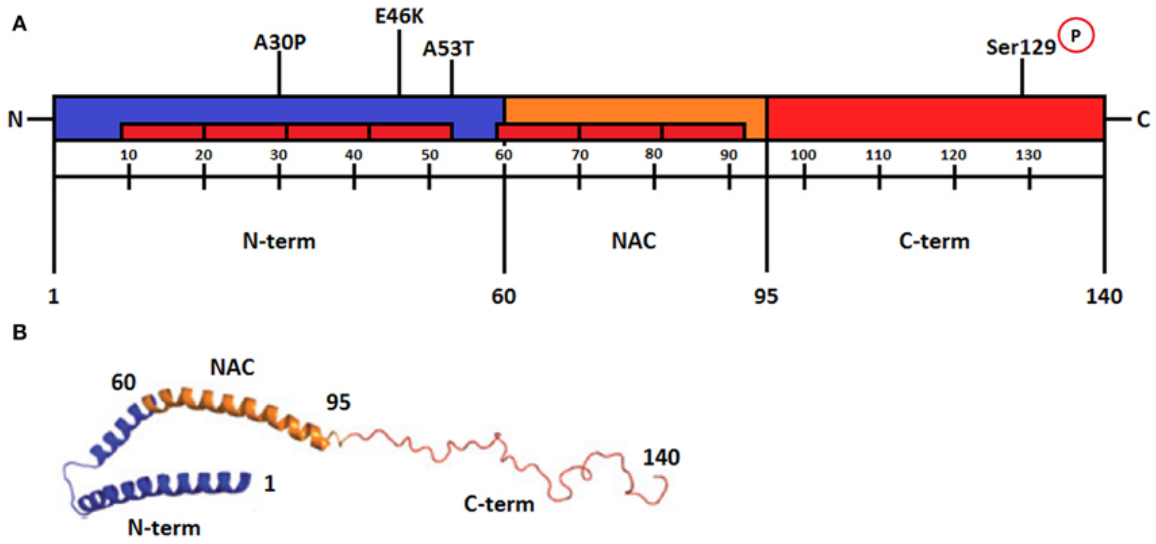

Fig.8. Schematic representation of the a) secondary structure of the protein αsyn and b) micelle-bound αsynuclein (Adapted from Gallegos et al., 2015)

αsyn can be mainly referred to as a natively unfolded protein, whose structure changes depending on its localization, interactions and membrane binding (Burré et al., 2013; Kim, 1997; Weinreb et al., 1996). Therefore, relationship of the protein with membranes is fundamental for its cellular functions and physio-pathological role in the disease. αsyn exists in the cell as a dynamic pool of monomers, tetramers, multimers in an equilibrium between a soluble and a membrane bound state (Bartels et al., 2011; Burre et al., 2010). αsyn interaction with negatively charged membrane lipids modulate its α-helical conformation that in turns influence the bending and curvature of the membrane itself. Moreover, lipid interaction is thought to impact on its aggregation ability (Jo et al., 2000; Middleton and Rhoades, 2010; Ulmer et al., 2005).

Functions

Although it is a protein associated to synaptic vesicles, αsyn seems not to be involved in synaptic development, since it is one of the last proteins to appear at synaptic terminals. Yet, an important role in neuronal function can be assumed, since it is expressed in many neuronal types both in the CNS and PNS (Burré et al., 2018; Withers et al., 1997). A multitude of synaptic functions have been attributed to αsyn, despite its role in neurons is still not fully understood. The intrinsically unfolded nature of the protein, its tendency to aggregate and possible compensatory effect by the β- and γ synuclein make the study of its physiologic functions particularly challenging (Burré, 2015). Data from a triple knock-out mice for all the synuclein members suggest pre-synaptic alterations, including a reduced size of the synaptic terminal (Greten-Harrison et al., 2010). Indeed, it is thought to play a major role in the regulation of synaptic function and release of neurotransmitters, behaving like a hub of interaction at the presynaptic terminal (Burré, 2015; Longhena et al., 2019). This last aspect

together with its high affinity and interaction to curved lipidic membranes strongly support its function in regulation of synaptic activity, plasticity, maintenance and cycle of synaptic-vesicle pool, dopamine metabolism and release.

Although specific functions remains elusive, αsyn colocalizes and interact with synaptic vesicles, phospholipids and synaptobrevin-2, the G-protein Rab3a, and acts as a chaperone for the SNARE-complex assembly (Burre et al., 2010, p. 201; Chen et al., 2013; Diao et al., 2013; Maroteaux et al., 1988). Moreover, it contributes in maintaining the overall size of recycling vesicle pool, keeping their mobility stable and inhibiting their docking to plasma membrane, as reported by *in vitro* studies (Longhena et al., 2019). In addition, αsyn has been reported to foster the clustering of synaptic vesicle and to cooperatively modulate with synapsin-3 synaptic function in dopaminergic neurons (Wang et al., 2014; Zaltieri et al., 2015). Given the selective vulnerability of DA neurons in PD pathogenesis, a supposed role of the protein in monoamine homeostasis seemed reasonable. Indeed, αsyn was demonstrated to interact with the vesicular monoamines transporter 2 (VMAT2), the dopamine transporter (DAT) and to modulate tyrosine hydroxylase (TH), rate-limiting enzyme of DA synthesis, activity (Butler et al., 2015; Guo et al., 2008; Perez et al., 2002; Swant et al., 2011). Overall data on synaptic functions of the protein suggest a role in intense and regulated neuronal activity rather than participating to basal neurotransmission (Burré, 2015).

Moreover, due to its biochemical features, αsyn behaves also as a molecular chaperone, a function mainly supported by the high level of structural and functional homology that shares with 14-3-3 protein family with known chaperone activity (Ostrerova et al., 1999).

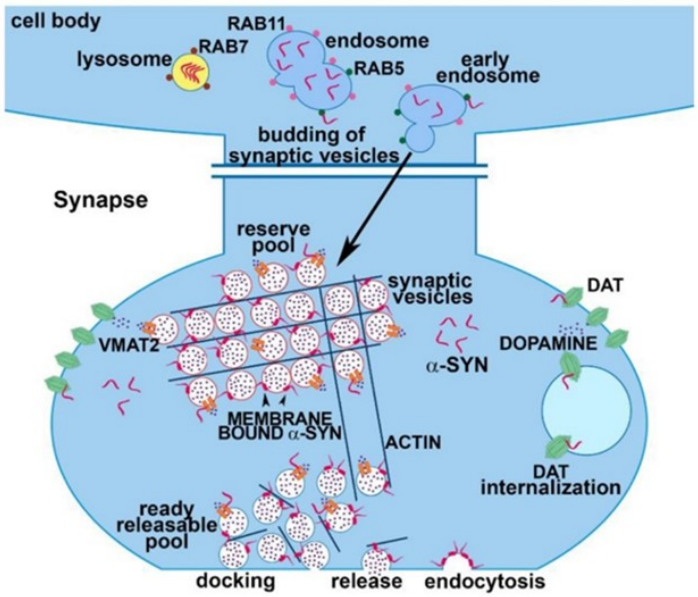

Fig.9. The image is representative of the role of αsyn and its interactome at the synapse. (adapted from (Longhena et al., 2019)

2.2 Toxic αsyn conformations

Due to its peculiar structure and the presence of the hydrophobic NAC region, αsyn has a high tendency to shift its conformation into β-sheet rich structures prone to aggregate into oligomers and insoluble amyloid fibrils. They ultimately deposit in LB inclusions, reaching lengths in the order of 5-10 nm (Spillantini et al., 1998). Nonetheless, these largest insoluble fibrils seem not represent the primary toxic species. Short fibrils and oligomers are currently considered the toxic forms causing neurotoxicity and driving molecular mechanisms of the disease (Alam et al., 2019)

2.2.1 Oligomers

The characterization of the αsyn oligomers role in cellular damage and amyloid formation has been quite challenging, because of their transient nature and high conformational variability. Oligomers can be described as a *continuum of species* going from low-molecular weight prefibrillar oligomers to larger aggregates that are on-pathway to amyloid formation (Pieri et al., 2016). From recent studies oligomeric species are emerging as having a leading role in causing neurotoxicity, especially small and soluble species (S. W. Chen et al., 2015; Chiti and Dobson, 2006; Winner et al., 2011). Indeed, the possibility of kinetically trap oligomers brought new insights into their biophysical properties and their impact in PD pathogenesis with respect to that of fibrillar species (S. W. Chen et al., 2015; Cremades et al., 2012; Froula et al., 2019). Chen and co-workers identified 2 main types of oligomers, built up on average by 18 and 29 monomers. AFM studies helped to confirm their properties: they approximately have a length of 50 nm and differently from synuclein fibrils, they have a very low percentage of β-sheet structures in an antiparallel disposition (Celej et al., 2012) and are not able to drive the conversion of monomeric synuclein/seeding competent. Subsequently, other groups described features of various oligomeric species. Interestingly, different protocols of generation or isolation allowed the identification of oligomer types comparable for their biophysical and toxic properties; in particular, a subtype that can be correlated to the one isolated by Chen, was confirmed to be able to exert cytotoxicity and disrupt lipid bilayers. (Fusco et al., 2017; Iljina et al., 2016)

2.2.2 Fibrils

The process of αsyn amyloid fibril formation is not totally understood yet. However, an alteration in the dynamic pool of structurally diverse αsyn forms and defects in proteostasis mechanisms are probably relevant players in the process (Brehme et al., 2014; Morimoto, 2011). A better comprehension of their structure have been provided mainly with NMR studies and more recently thanks to advancement in cryo-EM technology (Bousset et al., 2013a; Heise et al., 2005; Tuttle et al., 2016; Verasdonck et al., 2016). To note, independent groups by use of different techniques, obtained highly comparable structures. The protein in its β-sheet rich conformation was described at an atomic

resolution; it adopts a Greek key topology with each subunit making hydrogen bonding with the adjacent ones. The hydrophobic β-sheet core of the structure corresponds to aminoacids 42-102 while the N-terminus (1-41) and C-terminus (103-121) are largely unstructured, acquiring a random coil conformation (Guerrero-Ferreira et al., 2018; Li et al., 2018; Tuttle et al., 2016).

Interestingly, recent works postulate the existence of different strains of amyloid fibrils, capable of provoking distinct disease phenotype (Melki, 2015). *In vitro*, varying the buffer and salt conditions it is possible to obtain diverse αsyn species as classic fibrils or ribbons, which define flat and twisted structures. Upon *in vivo* injection in rodents, ribbons seem to produce αsyn inclusions especially in oligodendrocytes, typical neuropathological sign of the synucleinopathy Multiple System Atrophy (MSA). Fibrils instead are reported to cause mainly PD-like features with loss of dopaminergic nigral neurons and motor impairment (Bousset et al., 2013a; Peelaerts et al., 2015).

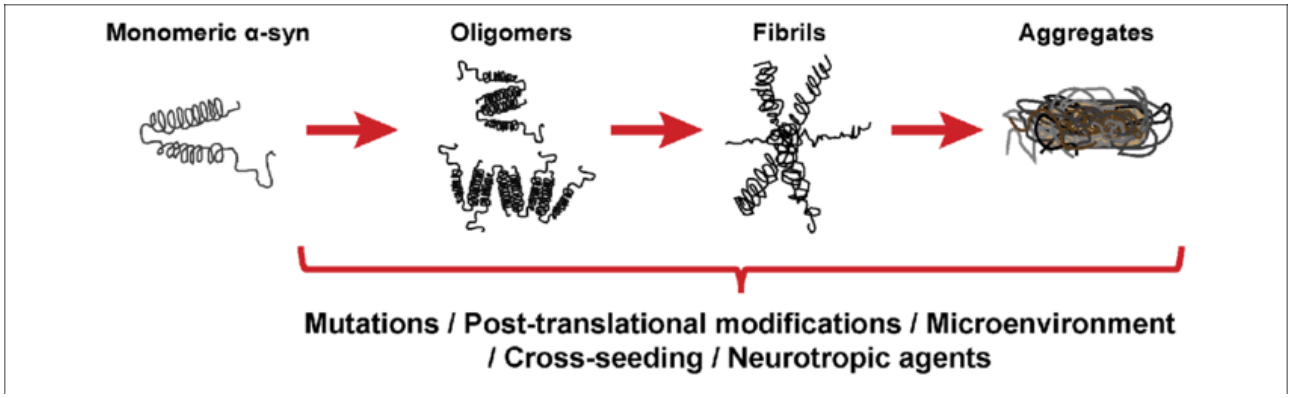

Fig.10. Schematic representation of the hypothetical aggregation process of monomeric α-syn (Heras-Garvin and Stefanova, 2020)

Prion-like propagation of α-synuclein

A recently developed theory assigns a major contribution to the propagation of LB pathology along PD stages to the prion-like behaviour of αsyn. The prion-like hypothesis was firstly supported in 2008 by two reports that found LBs in grafted mesenchymal midbrain neurons transplanted in PD patients striatum in a therapeutic attempt over ten years after the transplantation (Kordower et al., 2011; Li et al., 2008). Indeed, aggregates of misfolded αsyn spread intra-axonally neuron to neuron, following the stereotyped progression of LB through interconnected brain regions. Once aggregates are taken up by an healthy neurons, misfolded αsyn would act as *seeds* able to self-propagate by triggering the aberrant aggregation of the native soluble protein. (Angot et al., 2010; Brundin et al., 2010). Transfer of misfolded αsyn is hypothesized to occur through several mechanisms, not totally elucidated yet, comprising: exo-endocytosis, exosome release, axonal transport, trans-synapsis and tunnelling nanotubes (Vargas et al., 2019). This cell-to-cell propagation gradually involves different neuronal types in multiple brain regions over years following the initial trigger, mirroring the disease course.

Braak and coworkers proposed a dual-hit hypothesis for PD origin and spreading; initial αsyn seeds would form in the gut and in the olfactory bulb, thanks to an unknown neurotropic pathogen, and subsequently transmitted to the CNS via sympathetic fibres of the vagus nerve (Hawkes et al., 2009, 2007). Increasing line of evidences supports the gut origin of PD, including *in vivo* works on rodent animal model in which systemic inoculation of αsyn fibrils propagate neuropathology towards the CNS (Challis et al., 2020; Kuan et al., 2019). Moreover, in PD patients LB were found in plexa of the enteric nervous system in the foregut (Braak et al., 2006).

In this process, the deterioration of degradative system able to maintain cellular αsyn homeostasis plays a fundamental role (Chu and Kordower, 2007). Multiple experimental evidences claim that impairments of ubiquitin–proteasome system and the lysosomal autophagy system (LAS) could favour αsyn accumulation and, the other way round, accumulated αsyn could further inhibit these systems (Chu et al., 2009; Emmanouilidou et al., 2010; Steele et al., 2013). Ageing, the greatest risk factor for PD development, or genetic lesions (for instance, *GBA* and specific *LRRK2* mutations) are the main responsible for diminished αsyn proteolysis in the disorder (Fernandes et al., 2016; Rocha et al., 2015; Volpicelli-Daley et al., 2011).

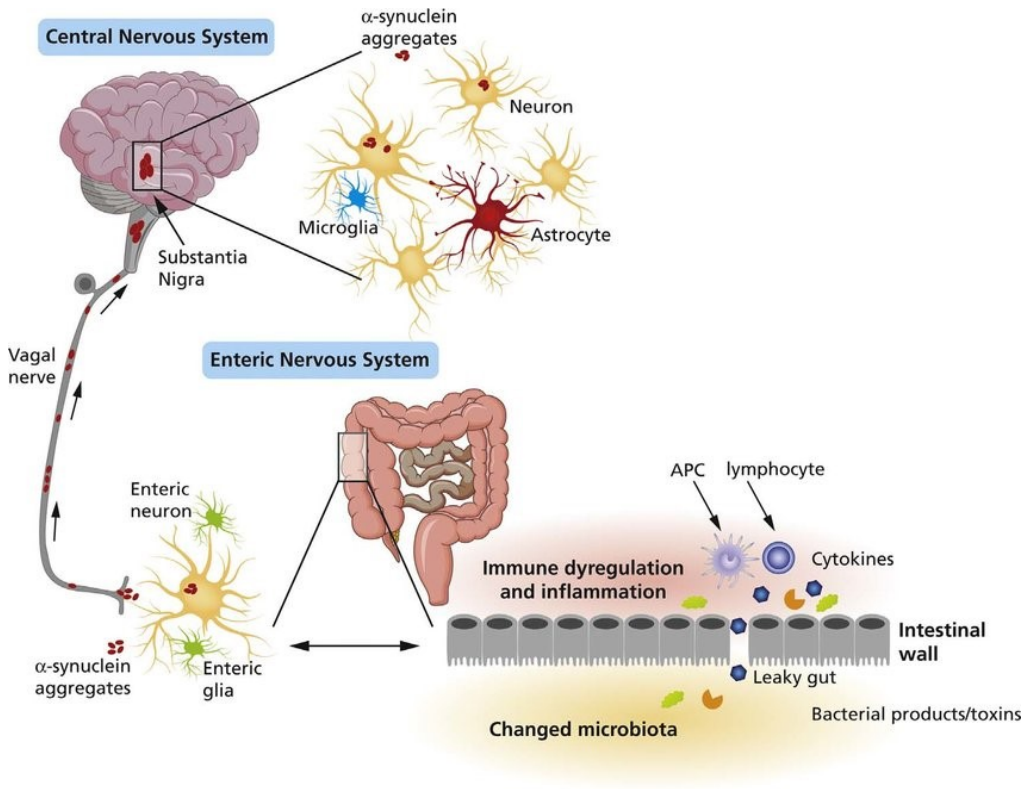

Fig11. **A schematic representation of the hypothesis of αsyn pathology spreading from the ENS towards the brain**. Environmental factors as microorganisms, including the gut microbiota, and toxins might start a pathological process within enteric nerve cell plexus, causing inflammation and oxidative stress, thus initiating protein aberrant accumulation. (Perez-Pardo et al., 2017)

2.3 αsyn-based experimental PD models

Classical toxin-based PD and transgenic experimental models fail to properly recapitulate human neuropathology, especially regarding LB deposition and spreading. Given the emerging importance of αsyn in PD pathophysiology, experimental models based on αsyn prion-like properties has now become an essential tool to unravel the relationship between αsyn aggregation and neurodegeneration of vulnerable neurons. In general, experimental models based on αsyn display a slowly-progressive disease course that mirrors in a more physiological way human pathology. In recent years, a multitude of different *in vivo* models have been characterized; they are mainly based on i. overexpression of αsyn by recombinant adeno-associated viral vectors (rAAV) and ii. αsyn pre-formed fibrils (PFF) inoculation.

2.3.1 rAAV-mediated overexpression of αsyn

The use of rAAV for the delivery and overexpression of proteins is an efficient system to model PD thanks to several characteristics. Both dividing and non-dividing cells as neurons can be transduced by rAAV, crucial feature to neurodegenerative disease modelling, providing a long-lasting transgene expression in several brain regions, without provoking an immune reaction (Pignataro et al., 2018). Smaller than lentivirus, rAAV can be injected in minimal volume reaching a high titer and efficient tissue spreading, effectively transducing neuronal cells with almost zero risk of mutagenesis because of their inability to integrate into the host genome (Albert et al., 2017).

rAAV can be exploited to drive the overexpression of wild-type or mutant forms of αsyn associated to familiar PD, mainly A53T or A30P *SNCA* mutations, in the striatum or the SNpc of rodents. The most significant findings obtained on these models are progressive neurodegeneration in the SN, degeneration of DA striatal fibers and decreased striatal dopamine concentration (Ip et al., 2017; Koprich et al., 2011, 2010; Lu et al., 2015; Oliveras-Salvá et al., 2013). From all these works, what is clearly emerging is the variability in the extents of nigrostriatal defects reported. Differences in the parkinsonian phenotypes are mostly due to different rAAV serotypes and titer used, promoters, sites of injection, time course followed in the study and the choice of wild-type or mutated αsyn. In these models, presence of aggregated and phosphorylated αsyn has been reported. However, the αsyn-positive inclusions do not resemble the structure of LBs found in human pathology and they can be distinguished as well from the aggregate displayed by rodent PFF-based models. In most of the studies they appear as small and punctate structures, nuclearly localized. To note, these structures, although reported by some studies to be proteinase-k resistant, seemed not to be able to spread from neuron to neuron (Gómez-Benito et al., 2020; Ip et al., 2017; Koprich et al., 2010; Lu et al., 2015).

Variable motor deficits are described by some works to appear after several weeks from rAAV injection, concomitant to significant DA neuron loss (Decressac et al., 2012, 2011; Gombash et al., 2013; Ip et al., 2017; Koprich et al., 2011; Oliveras-Salvá et al., 2013). Generally, the capability of generating progressive nigrostriatal degeneration together with appearance of precocious synaptic defects still make rAAV based models a valuable tool in modelling PD.

2.3.2 Injection of αsyn PFFs

The establishment of animal models (rodents and non-human primates) based on the systemic or intracerebral inoculation of exogenous αsyn species came in more recent years. The injected material can be constituted either by αsyn PFFs or other toxic species generated *in vitro* or LB-containing extracts from PD brains (patients or transgenic mice) (Luk et al., 2012b, 2012a). Regarding PFFs injection, the general procedure involves a first step of amyloid fibrils generation starting from the monomeric protein through *in vitro* protocols. Subsequently, fibrils are broken via a sonication procedures and are finally injected into the selected site (Polinski et al., 2018).

In particular, seminal studies by Luk and coworkers demonstrated that inoculation of either mice brain extracts containing pathogenic αsyn or synthetic PFFs could accelerate inclusions formation and propagation through the CNS of transgenic A53T αsyn mice (Luk et al., 2012b, 2009). Subsequently, another study from the same group showed the ability of exogenous PFFs to induce and spread pathology in wild-type mice as well (Luk et al., 2012a). These findings contributed, in a first instance, to a further validation of the prion-like behavior of αsyn and then to a significant diffusion of PFF-based experimental model in PD research field.

Various transmissible models of PD have been generated over the years and among them PFFs-based are the most exploited. The exogenous protein can be inoculated intracerebrally either in the dorsal striatum (the most widely adopted model), being then retrogradely transported to the SNpc via DA striatal fibers, or, less frequently, directly into the SNpc (Luk et al., 2012a; Masuda-Suzukake et al., 2014). The deposition of LB-like inclusions at the site of injections and their subsequent propagation through predictable interconnected networks have been deeply validated. Interestingly, unilateral lesions allowed to deeply map the pattern of inclusions even between the two hemispheres (Luk et al., 2012a; Patterson et al., 2019; Paumier et al., 2015). The aggregates found in these animals closely resemble human neuropathology: they colocalizes with LB markers (pSyn, p62, ubiquitin), are thioflavin-S positive and resistant to proteinase-K (Chu et al., 2019; Luk et al., 2012a; Paumier et al., 2015; Wakabayashi et al., 2013). Notably, the time dependent spatial progression of neuropathology is usually mirrored by the progressive degeneration of DA striatal fibers and SNpc neurons (Luk et al., 2012a; Patterson et al., 2019; Paumier et al., 2015).

As can be guessed from the wide heterogeneity these models, data on the extent and timing of neurodegeneration, pattern of disease progression and appearance of motor impairments exhibit a great variability. The type and concentration of PFFs injected, the site of inoculation and the strain of animal model can undoubtedly influence the resulting phenotype (Peelaerts et al., 2015; Polinski et al., 2018).

PFF-models are particularly valuable to obtain a late onset and slowly-progressive disease, which allow the study of the initial phase of synucleinopathies. This same feature could also represent its main drawback, since several months are needed to reach a severe neuronal loss and motor symptoms. Furthermore, to study the most recent theory of a peripheral origin of PD, specifically from the gastrointestinal tract and the olfactory bulb, PFF-models generated by a systemic injection are also being characterized. Overall, recent studies showed that inoculation of PFFs in the muscular layers of the duodenal wall or in the olfactory bulb resulted in aggregation of αsyn, gastrointestinal defects and, in some cases neuropathology progression to the CNS with consequent DA degeneration and onset of motor symptoms (Challis et al., 2020; Kim et al., 2019; Rey et al., 2016).

Even these models are characterized by relevant levels of variability, however they are a useful tool to investigate the molecular mechanisms underlying prodromal stage of PD and its transmission towards the CNS.

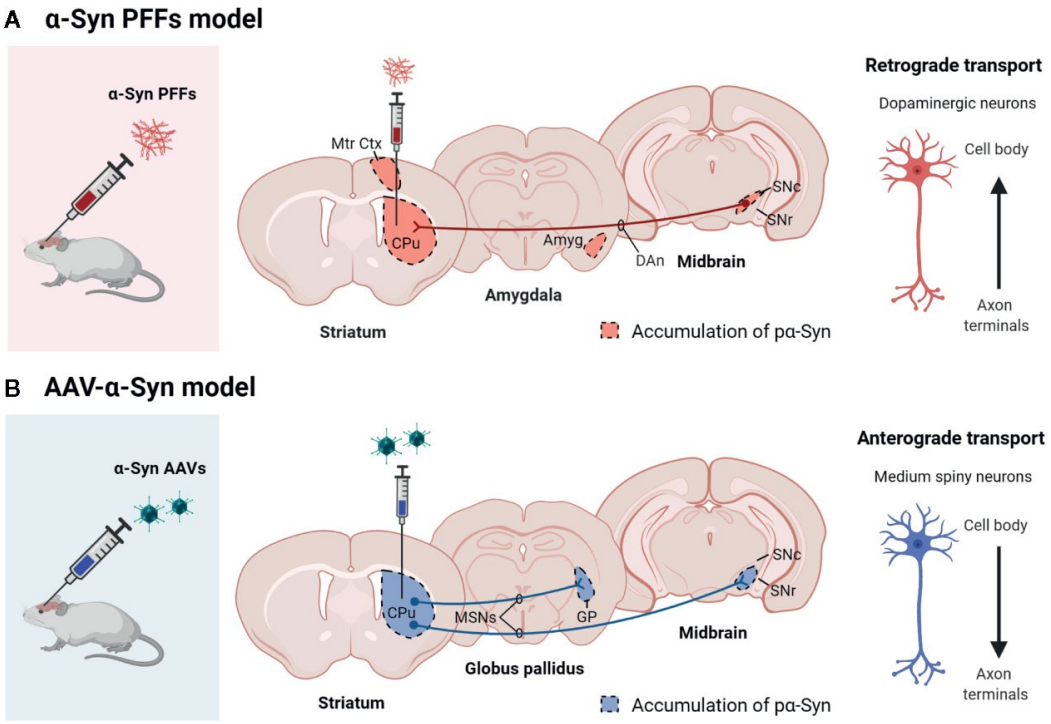

Fig.12. Schematic model showing the propagation pattern of α-Syn in PFFs and AAV models. The colored areas represent the brain areas where we find pα-Syn expression after (A) α-Syn PFFs inoculation or (B) AAV-α-Syn administration. (Gómez-Benito et al., 2020)

3. Glutamatergic neurotransmission

The non-essential aminoacid L-glutamate is the primary excitatory neurotransmitter used in the CNS, taking part in several fundamental functions as learning, memory and synaptic plasticity. Glutamatergic neurotransmission in the brain is finely regulated; aberrant glutamate signaling can mediate excitotoxic pathways as in several neurological disorders (Obrenovitch et al., 2000).

The glutamatergic synapse is essentially composed by a pre- and a post-synaptic compartment with different specialized functions and molecular organizations. At the pre-synaptic site, glutamate is most commonly synthetized from glutamine released by glial cells through the action of the enzyme glutaminase. Glutamate is subsequently embedded in vesicles via the VGLUT transporter and docked at the active zone of the presynaptic compartment, ready to be released. As soon as an action potential reaches the presynaptic neurons, glutamate is released in the synaptic cleft and, by binding to pre- and post-synaptic glutamate receptors (GluRs), raises downstream signalling responses. The neurotransmitter is eventually taken up by astrocytes, converted in glutamine and transferred back to the presynaptic sites.

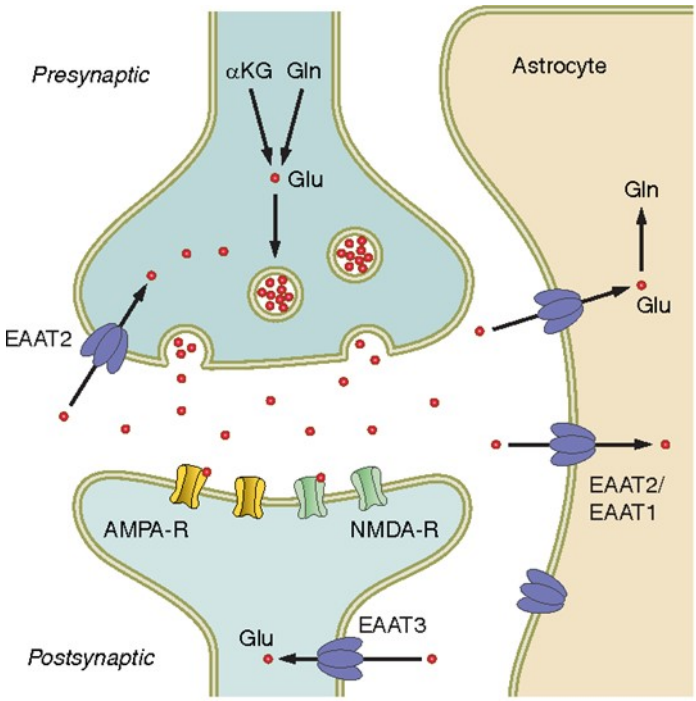

Fig.13. Schematic diagram of a glutamatergic synapse showing synthesis of glutamate from glutamine or from -ketoglutarate. After glutamate is released into the synapse, it is removed by glutamate transporters on the pre- and postsynaptic membranes and also glial cells. EAAC1 (EAAT3) is located on the postsynaptic membrane, whilst GLAST (EAAT1) and GLT1 (EAAT2) are located on glial cell membranes (Vandenberg and Ryan, 2013).

3.1 Glutamate receptors

GluRs comprise both ligand-gated ionotropic (iGluRs) and G-protein coupled metabotropic (mGluRs) receptors (Hansen et al., 2018; Traynelis et al., 2010). mGluRs, distinguished in 3 classes depending on their specific functions, are mainly involved in modulatory activity of the synaptic response triggered by the activation of iGluRs, both at the pre- and at the post-synaptic compartment.

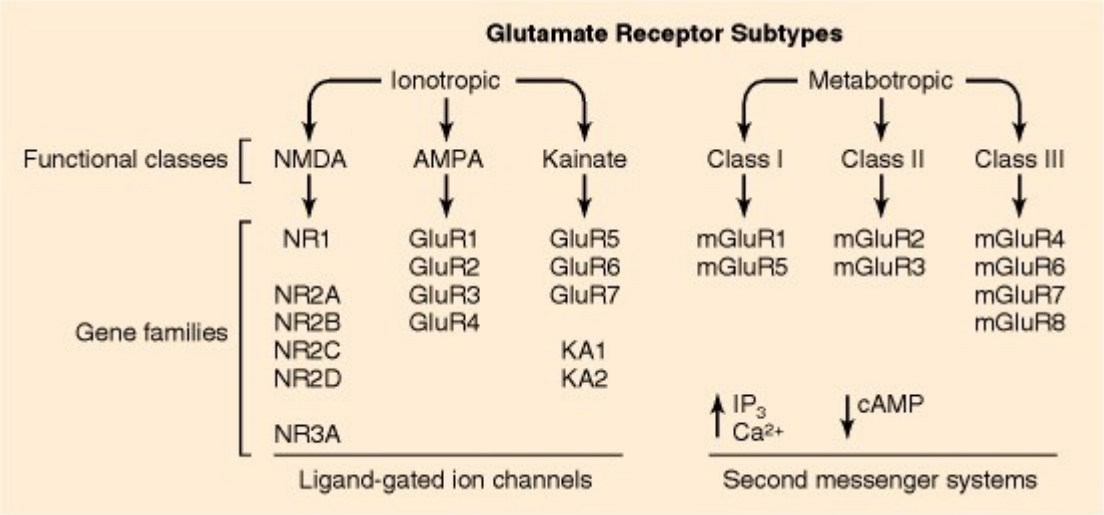

Fig.14. Functional and molecular classification of glutamate receptors. (Adapted from Basic Neurochemistry: Molecular, Cellular and Medical Aspects. 6th edition. Raymond Dingledine and Chris J McBain.)

Once activated, cation permeable iGluRs mediate depolarization of the postsynaptic plasma membrane, driving excitatory post-synaptic currents (EPSCs). Three distinct functional classes of iGluRs can be distinguished: the α- amino-3-hydroxy-5-methyl-4-isoxasolepropionic acid receptors (AMPARs), kainate receptors (KARs), and NMDA receptors (NMDARs) (Traynelis et al., 2010).

3.1.1 AMPARs

Activation of AMPARs by glutamate binding results in fast excitatory currents at the glutamatergic synapse, thanks to their Na^+ permeability. Structurally, they are mainly heterotetramers composed by different combination of GluA1-4 subunits; receptor properties such as channel opening time, ion-permeability and trafficking are strictly dependent on their subunit composition and interaction with scaffolding proteins. Therefore, heteromerization can be considered a significant source of functional diversity(Seeburg and Hartner, 2003). In contrast to NMDARs, AMPARs binds to glutamate at resting membrane potential leading to consequent current flow (Traynelis et al., 2010). This feature is fundamental to allow subsequent NMDARs activation by relieving the voltage-dependent Mg^{2+} block of the channel (Bliss and Collingridge, 1993; Huganir and Nicoll, 2013; Newpher and Ehlers,

2008; Opazo and Choquet, 2011; Shepherd and Huganir, 2007). Moreover, their synaptic localization, number, post-translational modifications and interactions are rapidly modulated by synaptic plasticity events (Huganir and Nicoll, 2013; Newpher and Ehlers, 2008; Opazo and Choquet, 2011; Shepherd and Huganir, 2007). To note, AMPARs lacking the GluA2 subunits are Ca^{2+}-permeable, thus mediating specific events of synaptic plasticity (Cull-Candy et al., 2006; Liu and Zukin, 2007).

3.1.2 NMDARs

Among iGluRs, NMDARs display unique properties underlying their key role in physiological synaptic plasticity events, and on the other side, in several pathological processes as well. These peculiar features include the voltage-dependent channel block by extracellular Mg^{2+}, an high Ca^{2+} permeability and the binding of two co-agonist (glutamate and glicine or D-serine) to allow channel opening (Traynelis et al., 2010). Their ability to mediate influx of Ca^{2+}, a second messenger that elicits molecular and biochemical changes in the postsynaptic neurons, is the primary reason for their involvement in synaptic plasticity but also in excitotoxic neuronal death (Paoletti et al., 2013). Indeed, besides functions in plasticity and learning and memory they are involved in pathophysiology of many CNS disorders (Hansen et al., 2018; Paoletti et al., 2013).

NMDARs structure

NMDARs are heterotetrameric receptors made up by combination of two or three different subunits among GluN1, GluN2 (A-B-C-D) and GluN3 (A-B) subtypes, encoded by different genes. Most commonly, they are composed by two obligatory subunits GluN1 and two GluN2 of identical or different types; GluN3-containing NMDARs, instead, have been described as ternary tetrameric complexes where GluN3 is assembled together with GluN1 and GluN2 subunits (Dingledine et al., 1999).

Each different subunit shows a significant homology and shares the same modular architecture formed by four different domains: two large extracellular regions including the N-terminal domain (NTD), responsible for assembly and allosteric modulation of the channel, and the agonist-binding domain (ABD), four transmembrane domains (TMDs) that form the ion channel and an intracellular carboxy-terminal domain (CTD). The ABD of GluN1 subunit binds to glycine or D-serine while GluN2 binds to glutamate (Johnson and Ascher, 1987). Thanks to the presence of asparagine residues on the M2 loop, the TMDs mediate the Mg^{2+} interaction. The CTD, the least conserved region among the different subunits, is extremely important for the synaptic trafficking, anchoring and signaling of the NMDARs. Their heterogeneity is mainly responsible for the functional diversity of NMDARs, allowing subunit-specific modifications, modulation and interactions (Martel et al., 2012; Paoletti et al., 2013).

Upon glutamate binding to iGluRs, a conformational change in the receptor structure allows the opening of the channel and the flow of ions (gating) (Hansen et al., 2018). As already mentioned, in order to let the channel pore open, a depolarization of the postsynaptic membrane concomitant to the presynaptic glutamate release is needed to relieve the Mg^{2+} block (Traynelis et al., 2010). Generally, this depolarization is achieved through an initial activation of AMPARs and the consequent influx of sodium ions. Glutamate and the co-agonist glycine or serine will bound to the specific sites on the extracellular receptor region, allow the conformational shift and finally lead to Ca^{2+} flowing into the postsynaptic compartment. This significant increase in calcium ions concentration in the dendritic spine ultimately produce short- and long-term synaptic strength modifications (Hansen et al., 2018; Paoletti et al., 2013). Importantly, diverse pools of cellular receptors lead to different responses; in particular, synaptic NMDARs (localized at the post-synaptic density-PSD) are strictly linked to the induction of pro-survival and plasticity events, while extrasynaptic NMDARs mainly mediate detrimental effects, leading also to excitotoxicity and neuronal death (Bell and Hardingham, 2011; Hardingham and Bading, 2010; Lin et al., 2012).

Neuronal development is characterized by a change in composition of synaptic NMDARs, since GluN2A starts to be incorporated in synaptic NMDARs in mature stages while GluN2B subunits are more prevalent in early neuronal phases (Sheng et al., 1994; Tovar and Westbrook, 1999). Surface mobility of NMDARs has been demonstrated to significantly contribute to shape synaptic NMDARs composition. Besides trafficking through intra and intracellular pool of receptors, synaptic NMDARs can be replaced by extrasynaptic ones through lateral diffusion (Groc et al., 2006; Tovar and Westbrook, 2002). In mature neurons GluN2A was shown to be enriched at synaptic sites, constituting a relatively stable pool of receptors. GluN2B-containing NMDARs, instead, are reported to be more mobile and to preferentially localize at pery- and extra- synaptic sites (Groc et al., 2006). The spatial and temporal regulation of NMDARs' subunit composition is dependent also on the region of the nervous system. Early neonatal stages are characterized by predominant expression of GluN2B-2D and GluN3A-3B subunits while in adult stages GluN2A-N2C become more abundant (Akazawa et al., 1994; Monyer et al., 1994; Sheng et al., 1994). Although in hippocampus, neocortex and striatum, GluN2A-2B are the most diffuse regulatory subunits, their ratio is in favor of 2B subunits in the striatum, while the opposite situation occurs in hippocampus and neocortex (Gardoni and Bellone, 2015; Paoletti et al., 2013).

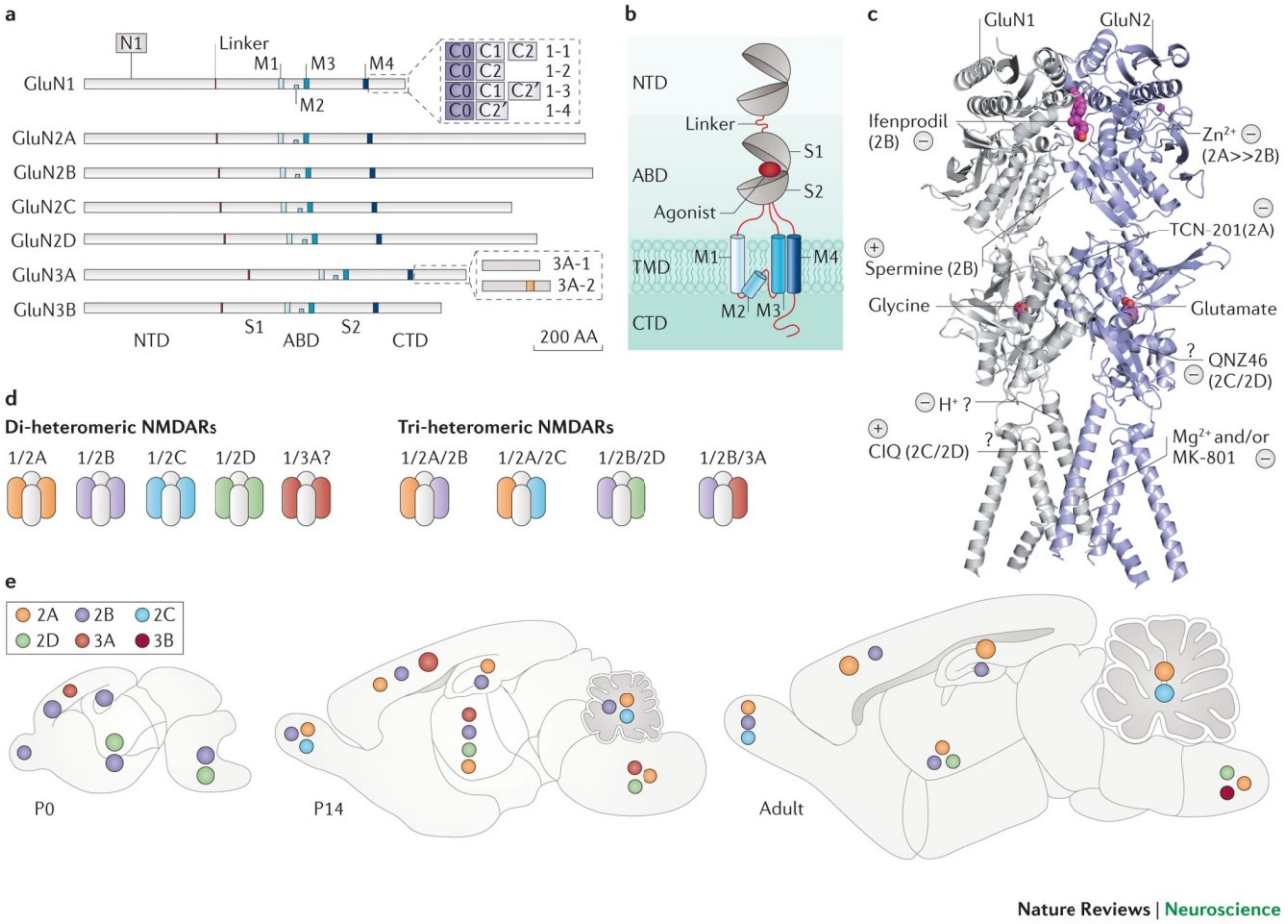

Fig.15. All NMDAR subunits share a modular architecture. Structure of NMDARs highlighting multiple binding sites for small molecules acting as allosteric modulators. A sample of various populations of diheteromeric and tri-heteromeric NMDARs in the CNS and developmental profile of GluN subunits in mouse brain. (Paoletti et al., 2013).

3.2 Dendritic spines as mediators of the excitatory neurotransmission

Dendritic spines, the small protrusions along neuronal dendrites, represent the site in which most of the excitatory synapses of the mammalian brain localize. Linked to the dendritic shaft through a narrow neck, spines display a wide heterogeneity of sizes, shapes and densities among the different neuronal types and brain areas and even within the same neuron. Based on their morphology, they can be distinguished in different subtypes (Harris, 1999; Peters and Kaiserman-Abramof, 1970):

- Mushroom shaped spines, the most stable, containing the largest excitatory synapses and characterized by a large bulbous head and a thin neck,
- Thin spines, less stable and frequently subjected to morphological changes, with smaller excitatory synapses and absence of the large head.
- Stubby spines, short structures lacking a neck, are considered immature structures since they are prevalently expressed in the early-postnatal development (Harris, 1999).

Dendritic spines function as signalling units and represent highly dynamic structures that undergoes shape and size changes, forming and disappearing along neuronal activity modifications and plasticity events (Hering and Sheng, 2001). On the pathologic sides, important alterations in spine morphology or density occur in multiple psychiatric and neurological disorders, including PD, significantly contributing to their pathophysiology (Deutch et al., 2007; Penzes et al., 2011; Picconi et al., 2005; Villalba and Smith, 2010; Zaja-Milatovic et al., 2005).

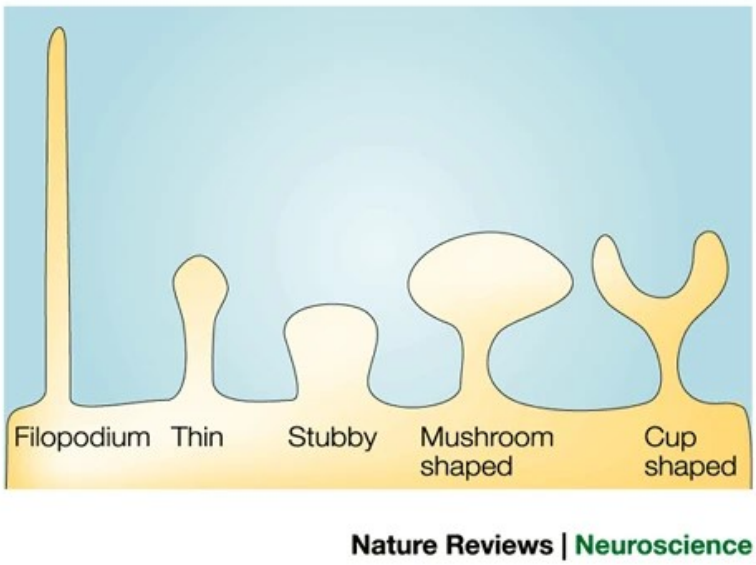

Fig.16. Morphological classification of dendritic spines. (Hering and Sheng, 2001)

Mature spines usually contain a single synapse (associated to excitatory inputs) on their head, in which a thick protein rich PSD is close to the active zone of a presynaptic terminal. (Sorra and Harris, 2000). The PSD characterizes excitatory (type 1) synapses and can be defined as a finely tuned architecture of proteins forming a scaffold in which glutamate receptor are anchored (Sheng and Hoogenraad, 2009).

Synaptic plasticity. One of the most fascinating features of the mammalian brain is the ability to change the function of neural circuits in response to an experience. Synaptic plasticity, defined as *the activity-dependent modification of the strength or efficacy of synaptic transmission at preexisting synapses,* is key to learning and memory functions and neural development. Several plasticity phenomena have been recognized, involving pre- and post-synaptic events, comprising short and long term processes (Citri and Malenka, 2008). Multiple neuronal biological processes, as synaptic vesicle release, synaptic components modifications, receptors trafficking and stimulus-induced changes in gene expression are necessary to establish the different forms of plasticity. Among long term mechanisms at excitatory synapses, NMDAR-dependent long-term potentiation (LTP) or long-term

depression (LTD) are two important forms of bidirectional synaptic plasticity. LTP and LTD lead to long lasting synaptic strengthening and weakening, respectively, mainly through the activity-dependent modification in the number of postsynaptic glutamate receptors (Sheng, 2002). They are called NMDA-dependent since they are triggered by NMDAR activation and postsynaptic increase in the intracellular calcium within dendritic spines; however, this influx, probably depending on the threshold reached, give rise to opposite results (Citri and Malenka, 2008; Sheng, 2002). Very briefly, the ultimate consequence of cellular signaling pathways of LTP and LTD observed in experimental conditions are reflected on spine structures and density. Indeed, LTP finally results in a rapid enlargement of spine heads, rapid formation of new spines followed by their stabilization (Kopec, 2006) Lang et al., 2004; Park et al.,2006; Lin et al., 2004; Nägerl et al., 2004;). LTD, instead, lead to a significant reduction in dendritic spines size, a fast shrinkage of spine head and decreased spine density (Nägerl et al., 2004; Zhou et al., 2004).

3.3 Role of Rabphilin3A (Rph3A) in glutamatergic signalling

Rph3A is a 78 kDa protein of 694 aminoacids, encoded by *RPH3A* gene, primarily expressed in membranes of neurons and neuroendocrine cells, but also in other secretory cell types (Rastaldi et al., 2003; Q. Yuan et al., 2017), firstly identified in brain as a putative Rab3A effector protein. Rab proteins are low molecular weight GTPases involved in vesicular trafficking and specific endo-exocytosis pathways (Pylypenko et al., 2018). Subsequently, Rph3A detection in synaptic vesicle and granules of chromaffin cells reinforced its possible role in vesicle trafficking and exocytosis (Chung et al., 1995; Mizoguchi et al., 1994).

3.3.1 Protein structure

The structure of the protein can be subdivided into distinct domains, namely an NTD and a C-terminal domain comprising two tandem C2-like domains (C2A and C2B). The NTD of Rph3A, thanks to a cysteine-rich zinc-finger domain, is mainly involved in interaction with the small GTPases Rab3, Rab27 and α-actinin (Chung et al., 1995; Fukuda, 2003; Kato et al., 1996; McKiernan et al., 1996). A linker of 200 aminoacids connect the NTD to the tandem C2-like domains, common structural protein motifs involved in Ca^{2+}-dependent phospholipid binding, that allow Rph3A to behave as a Ca^{2+} sensor in membrane interactions (Corbalan-Garcia and Gómez-Fernández, 2014; Montaville et al., 2008). Interestingly, upon deletion of one or both C2-domain, the Ca^{2+} dependent exocytosis is suppressed (Shirataki et al., 1993).

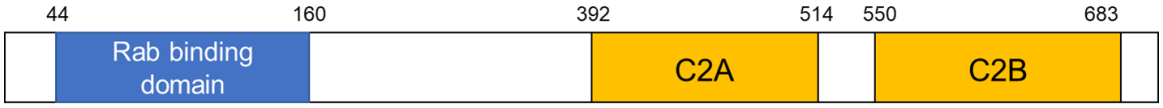

Fig.17. Schematic representation of the Rph3A protein domains

3.3.2 Presynaptic Rph3A function

Rph3A is reported to bind to Rab3A, prevalently when the protein is in a GTP-bound state. Deletion of Rab3A, interestingly, leads to a diminished Rph3A expression (Geppert and Südhof, 1998; Li et al., 1994; Schluter, 2004). Rab3A and Rph3A have been reported to act together in the docking process of vesicles at the membrane, thereby promoting release. Moreover, Rph3A has been shown to participate in the recycling of synaptic vesicles and to directly interact with SNAP25, a member of the SNAREs proteins which constitute the core machinery for synaptic vesicle exocytosis (Deák et al., 2006a; Tsuboi and Fukuda, 2005). Rph3A activity in various steps of the synaptic vesicles cycling has been reported in different cell-type such as adrenal chromaffin cells, PC12 cell-line and neurons (Chung et al., 1995; Deák et al., 2006a; Komuro et al., 1996). Furthermore, the crystal structure of the Rph3A-SNAP25 complex revealed a putative membrane-binding mode of the C2 domains in cooperation with SNAP25 and PIP_2/Ca^{2+}, promoting membrane bending and regulation of vesicles fusion (Ferrer-Orta et al., 2017). A recent work also reported an inhibitory activity of Rph3A towards the spontaneous release in hippocampal networks (Bourgeois-Jaarsma et al., 2021a). However, data of Rph3A KO mice did not reveal apparent electrophysiological, behavioural or morphological alterations (Schlüter et al., 1999). An explanation of this discrepancy can reside in the redundancy of Rab-effectors, and consequently, in the establishment of compensatory mechanisms.

Although multiple lines of evidence suggest a key role of Rph3A in Ca^{2+}-dependent vesicle release, its precise function is still poorly understood and it seems to act at various steps of the neurotransmitter release.

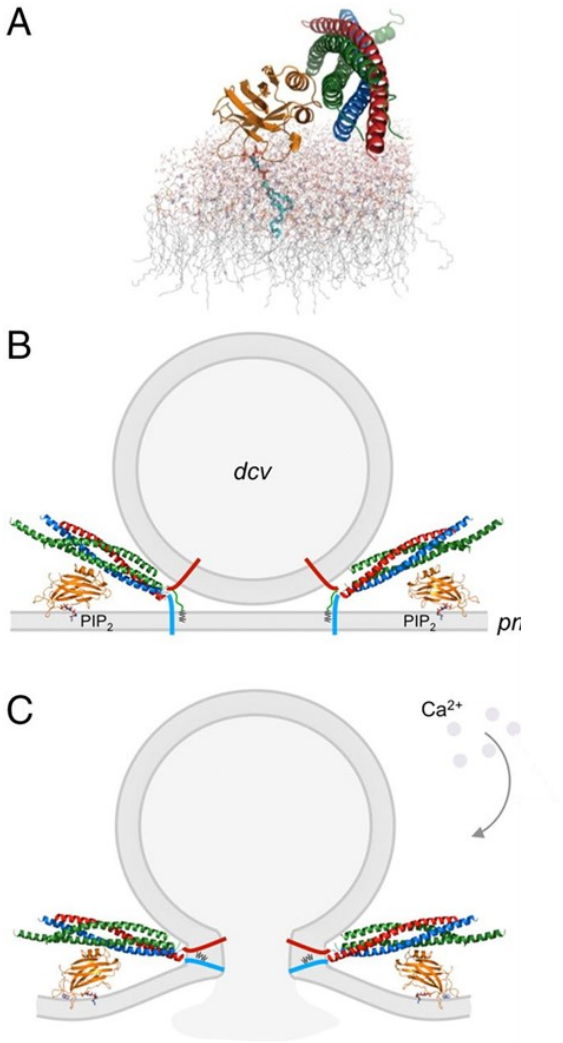

Fig.18. Binding model of Rph3A-C2B and SNAREs at the plasma membrane. Cartoon representations of two symmetric Rph3A C2B (orange)–SNAP25–STX1A–VAMP2 complexes docked to the plasma membrane by PIP2, SNAP25 palmitoylation (black line), and the STX1A transmembrane helix (blue line), before (B) and after (C) Ca2+ binding. (Adapted from (Ferrer-Orta et al., 2017)

3.3.3 Postsynaptic Rph3A function

Although Rph3A has been initially described as a presynaptic protein, in 2015 a work from our lab demonstrated its postsynaptic localization and function (Stanic et al., 2015). Through a two-yeast hybrid assay using the C-terminal fragment of GluN2A, Rph3A was discovered to localize at the post-synaptic compartment as a novel binding partner of the GluN2A subunit of NMDARs. Colocalization experiments in rat hippocampal primary neurons and Electron Microscopy data confirmed the presence of Rph3A at the PSD of dendritic spines (Stanic et al., 2015). In particular, Rph3A interaction with NMDARs is specific to the GluN2A subunit and involves its N-terminal domain. Rph3A was discovered to form a ternary complex also with the scaffolding protein PSD95 (a member of the MAGUK scaffolding protein family), promoting stability and retention at synaptic

sites of NMDARs. This findings is in agreement with previous reports of Rph3A interaction with other proteins showing a postsynaptic localization such as CASK, another MAGUK member, and Myosin-Va (Brozzi et al., 2012). Disruption of GluN2A/PSD-95/Rph3A ternary complex, either by Rph3A silencing or through uncoupling peptides, led to a decreased post-synaptic localization of GluN2A-NMDARs, due to an increased internalization. (Stanic et al., 2015)

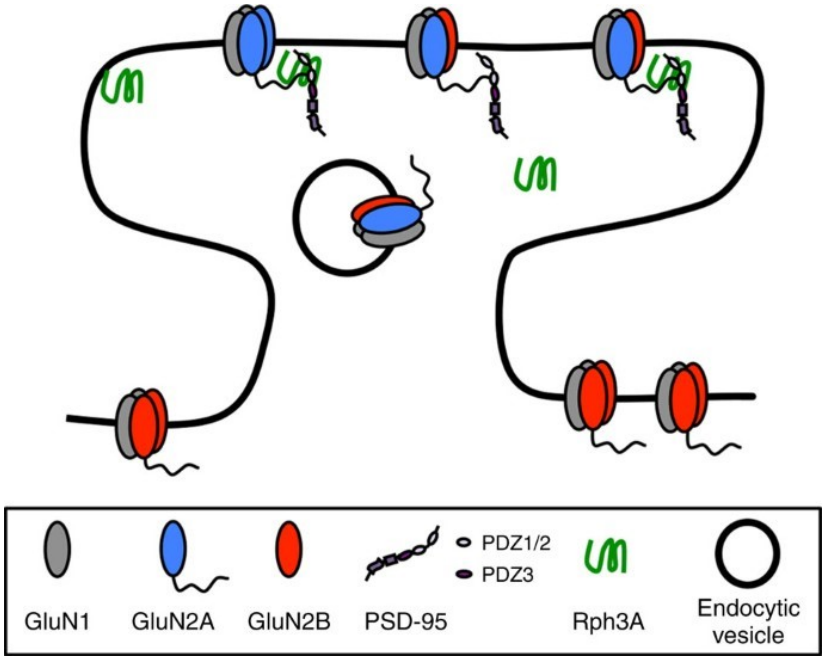

Fig.19 Schematic representation of GluN2A/Rph3A/PSD-95 ternary complex at the PSD.

Pre-embedding immunohistochemistry data showed that about half of the dendritic spines in CA1 region of rat hippocampus display Rph3A. To note, Rph3A+ spines feature an increased spine head area and size of the PSD, possible defining a pool of more potentiated synapses. Furthermore, Rph3A seems to have a fundamental role also in synaptic plasticity mechanisms, as long-term potentiation (LTP). Indeed, interfering with Rph3A/NMDARs complex prevented LTP induction and the *in vivo* acquisition of spatial memories (Franchini et al., 2019).

3.4 Alteration of the glutamatergic signalling in PD

Along PD progression and pharmacological treatment, glutamatergic signalling from the cortex to the striatum undergoes to a significant modulation. Alterations in structure and activity of the dendritic spines of spiny projection neurons (SPNs), representing the majority of striatal neurons, have a significant role in mediating these pathophysiological changes. Indeed, DAergic terminal from the SNpc and the glutamatergic input from the cortex converge onto SPNs dendritic spines and

integrate to allow a proper motor behaviour. Striatal DA depletion, due to degeneration of the nigrostriatal pathway in PD, leads to changes in subcellular localization and activity of striatal postsynaptic glutamate receptors, eventually causing loss of striatal plasticity (Calabresi et al., 2007; Gardoni and Di Luca, 2015; Mellone and Gardoni, 2013).

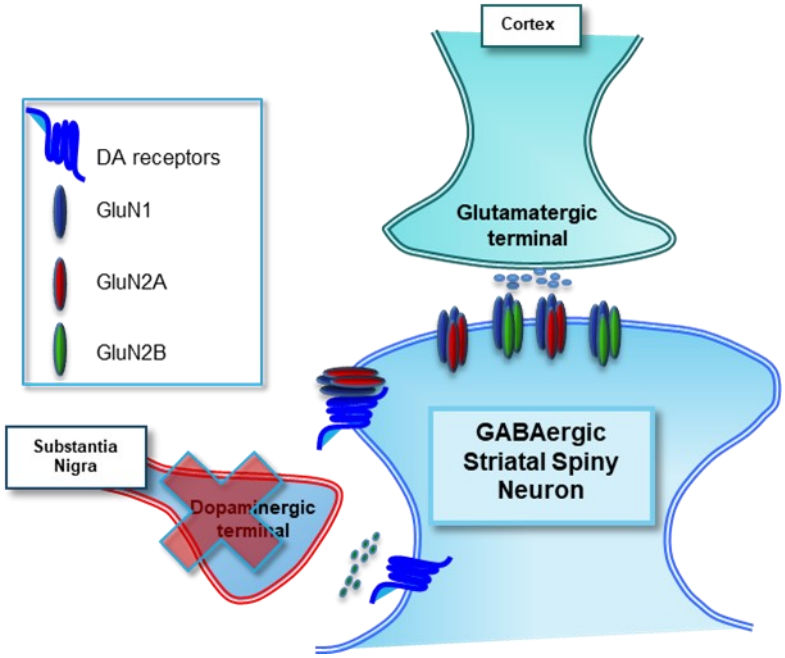

Fig.20. Schematic representation of the cortical glutamatergic and DAergic terminal converging on dendritic spine of the striatal SPNs in PD.

Multiple studies mainly on 6-OHDA rodent and primate PD models indicate that different extent of DA denervation cause specific NMDARs alterations (Paille et al., 2010). GluN2B is the prevalent regulatory NMDARs subunit of striatal SPNs, where the majority of NMDARs are made up by GluN2A-GluN2B subunits (Dunah and Standaert, 2001). A decreased GluN1/GluN2B-NMDARs expression in the striatal membrane was detected by early works both in 6-OHDA-lesioned rats and MPTP-treated macaques (Dunah et al., 2000; Gardoni, 2006; Hallett et al., 2005). A partial nigrostriatal lesion in a parkinsonian rat model, instead, was reported to cause augmented expression of GluN2A, but not GluN2B, regulatory subunit (Paille et al., 2010). The crucial role of scaffolding proteins in glutamate receptors postsynaptic localization is further demonstrated by decrease in PD experimental model of proteins belonging to the MAGUK family (Nash et al., 2005).

Aberrant functioning, localization and subunit compositions of NMDARs is not only a feature of PD, but also participate to the pathophysiological mechanisms of L-DOPA-induced dyskinesia (LID) (Mellone and Gardoni, 2013; Sgambato-Faure and Cenci, 2012).

For instance, chronic L-DOPA treatment in dyskinetic 6-OHDA-lesioned rats causes a redistribution of GuN2B subunit to the extra-synaptic membrane and increase of GluN2A synaptic levels at dendritic spines of SPNs (Gardoni, 2006). Interestingly, interfering with GluN2A/PSD95 interaction to prevent the aberrant GluN2A/N2B ratio demonstrated to be sufficient to reduce onset and severity of dyskinetic behaviors in rat and monkey experimental PD models (Gardoni et al., 2012; Mellone et al., 2015).

3.4.1 Rph3A in pathophysiology of L-DOPA-induced dyskinesia

Given its role in NMDARs synaptic retention, Rph3A was demonstrated to play a role in glutamatergic alterations driven by dopamine depletion in PD and LIDs. For the first time, a work from our group investigated the expression of Rph3A at the striatal PSD and its interaction with GluN2A (Stanic et al., 2017). In particular, both its postsynaptic expression and GluN2A interaction resulted increased in dyskinetic parkinsonian rats. Interestingly, in these animals interfering with Rph3A/GluN2A striatal interaction revealed to be effective in reducing the abnormal motor behaviours. On the whole, these data confirmed a critical role of Rph3A/GluN2A complex also in pathological conditions, suggesting it as a novel pharmacological target to counteract the aberrant NMDARs activity (Stanic et al., 2017).

3.4.2 Role of αsyn in PD glutamatergic alterations

In the context of PD pathophysiology, aberrant levels and forms of αsyn exert neurotoxicity through multiple mechanisms, affecting homeostatic cell pathways and synaptic functions. In particular, recent experimental evidences using both *in vivo* and *in vitro* models report an early impact of αsyn on the glutamatergic neurotransmission. Indeed, several works report a modulation of the synaptic levels, composition and activity of NMDARs. For instance, αsyn oligomers were shown to block LTP induction in rat hippocampal slices through NMDARs activation, while on hippocampal neurons increased cellular αsyn caused GluN1 internalization, with a consequent reduction in NMDARs' currents (Y. Chen et al., 2015; Diogenes et al., 2012). Moreover, an *in vivo* study investigated the early effects of αsyn overexpression on striatal dopamine levels and striatal cholinergic interneurons. Indeed, in this neuronal subset the αsyn modulation of GluN2D-containing NMDARs provoked a block of LTP induction, that also reflected in early memory and motor alterations of the parkinsonian animals (Tozzi et al., 2016). Furthermore, a work in collaboration with our lab subsequently demonstrated that oligomeric forms of αsyn, as wells, affect synaptic transmission and cortico-striatal plasticity. In particular, at the level of SPNs in both of the direct and indirect pathway, αsyn reduced NMDARs currents and impaired the induction of LTP, selectively reducing the postsynaptic localization of GluN2A subunit. In line with this finding, the *in vivo* striatal injection of toxic forms

of the protein caused visuo-spatial alterations that are strictly dependent on NMDARs activation. (Durante et al., 2019). A recently published study involving the contribution of our laboratory contributed to the understanding of detrimental αsyn effects on the nigrostriatal circuitry, focusing in particular on the role of DA (Tozzi et al., 2021). Using the striatal PFF-rat model, they demonstrated a decreased release of striatal DA even before overt SNpc neuronal loss. Animals showed specific behavioral alterations accompanied by time-dependent electrophysiological impairments of DA SNpc neurons, already detectable in absence of significant αsyn deposition. Interestingly, also striatal LTP, strictly dependent on NMDARs activity, and LTD were impaired; to note, a subchronic treatment with L-DOPA resulted sufficient to restore both forms of plasticity (Tozzi et al., 2021). Overall, these recent findings highlight a complex and significant role of αsyn in disrupting activity of different neuronal types through specific pathologic mechanisms, even before a dramatic striatal dopamine depletion.

Moreover, deposition of αsyn in LB has been reported to affect Rph3A physiological synaptic interactions. A study in 2004 on tissue from patients with diffuse LB disease (LBD) detected in the entorhinal cortex an interaction between αsyn and Rph3A in control cases (Dalfó et al., 2004). In presence of LB however, this interaction was lost; moreover, in LBD patients even Rph3A binding to is synaptic partner Rab3A was impaired. This study hypothesized and showed for the first time a direct interaction between Rph3A and αsyn and how this binding is affected by αsyn pathology. At the presynaptic levels, an aberrant modulation of the interplay between this three protein could possibly lead to impairment in synaptic vesicle release (Dalfó et al., 2004)

AIM

Alpha-synuclein (αsyn) is a small soluble protein mainly involved in synaptic functions, neurotransmitter release and regulation of synaptic vesicle pools (Burré, 2015). Upon specific cellular conditions or mutations of its coding gene, αsyn tends to aggregate into oligomers and higher order amyloid fibrils, that can finally deposits into inclusions called Lewy Bodies (LB) (Polymeropoulos, 1997; Spillantini et al., 1998). At present, aggregated species of αsyn are considered the main driver of sporadic and familiar PD pathogenesis, promoting αsyn spreading across interconnected brain regions (Braak et al., 2003; Gallegos et al., 2015; Spillantini et al., 1998). Together with loss of DAergic neurons in the SNpc, LB constitute the main pathological hallmark of PD.

αsyn aggregates mediate neurotoxicity through multiple cellular pathways; however, the precise mechanisms by which αsyn oligomers and fibrils cause synaptic disfunction in the early phases of PD are still mostly unclear.

Besides degeneration of the DAergic system, PD progression is characterized by a pathogenic modulation of the glutamatergic cortico-striatal signalling (Gardoni and Di Luca, 2015). Interestingly, αsyn was described to modulate also NMDARs synaptic levels and activity at the excitatory synapse (S. W. Chen et al., 2015; Diogenes et al., 2012; Navarria et al., 2015; Tozzi et al., 2016). Indeed, recently published works show that, already in PD early stages, pathogenic αsyn is able to affect the striatal glutamatergic synapse, causing dysfunction of NMDARs and loss of striatal synaptic plasticity (Durante et al., 2019; Tozzi et al., 2021).

Our lab described that the synaptic retention of NMDARs is strictly correlated to the interaction with Rph3A (Stanic et al., 2015; Franchini et al., 2019). Interestingly, Rph3A expression at the corticostriatal synapse and its interaction with NMDARs are altered in advanced PD stages (Mellone et al., 2015; Stanic et al., 2017). Moreover, a direct αsyn/Rph3A interaction, modulated in presence of LB, has been put forward (Dalfó et al., 2004). Nonetheless, the specific molecular events underlying this molecular interplay are still poorly understood.

Based on these premises, the main aims of my PhD work are:

i. Validating and characterizing αsyn/Rph3A interaction
ii. studying the role of Rph3A and αsyn/Rph3A complex in αsyn-induced models of PD
iii. identification of pharmacological approaches blocking αsyn synaptic toxicity

MATERIAL AND METHODS

1. Generation and characterization of αsyn aggregates

1.1. αsyn pre-formed-fibrils (PFFs) generation

αsyn PFFs were generated *in vitro* starting from recombinant αsyn monomeric protein (Human α-synuclein protein to generate PFFs, Proteos) using an already validated protocol, with some modifications (Polinski et al., 2018). In particular, monomeric protein solution (10 mg/ml) was thawed on ice and then centrifuged at 13,000xg for 10 min at 4°C to discard any protein that may have pelleted. The supernatant was retained and protein concentration measured though Bradford assay.

The solution was then diluted in PBS to a concentration of 5 mg/ml and was incubated in benchtop tubes for 7 days at 37 °C at constant shaking (1000 rpm) using an Eppendorf Thermomixer. At the end of the procedure, amyloid fibrils formation was always checked by Transmission Electron Microscopy (TEM), as described below. The fibrils (PFFs) were then diluted to a final concentration of 2 mg/ml, aliquoted and stored at -80°C. Immediately before their experimental use, PFFs aliquots were thawed at room temperature (RT) and sonicated for a total of 60 pulses (2s ON/1s OFF) in an ultrasonic bath sonicator (Bransonic M2800H-E).

1.2 αsyn oligomers (OLIGO) generation

αsyn oligomers were produced through a recently reported oligomerization protocol with some modifications (Durante et al., 2019). Recombinant αsyn monomeric protein (Human α-synuclein protein to generate PFFs, Proteos) was thawed on ice, centrifuged at 13,000xg for 10 min at 4°C and supernatant retained. After measurement of protein concentration, the solution was diluted to the final concentration of 2 mg/ml in PBS and bubbled with a 95%O_2–5%CO_2 gas mixture for 1h at RT. The oligomers were aliquoted and stored at -80 °C. As for PFF generation, presence of oligomeric species in the solution was checked by TEM.

1.3 TEM validation of OLIGO and PFF preparation

The samples of αsyn-PFF and oligomers were examined by negative staining protocol with a TEM Talos L120C (Thermo Fischer, USA) operating at 120 kV and digital images were acquired using a

CETA-MTM 4k x 4k camera (Thermo Fischer, USA). TEM analyses were performed at the Unitech NOLIMITS imaging facility of the University of Milan.

2. Animals

All procedures involving animals were approved by the Italian Ministry of Health (permits 1200/2020-PR and 330/2018 PR) and local Animal Use Committee and were conducted in accordance with the Guide for the Care and Use of Laboratory Animals of the National Institutes of Health and the European Community Council Directives 2010/63/EU. Distinct cohorts of C57BL/6J animals aged 2 months old were used for each experimental approach (behavior, spine morphology, biochemistry). Animals were housed two to four per cage in a climate-controlled facility (22 ± 2 °C), with ad libitum access to food and water throughout, and with a 12 h light–dark cycle (19:00–07:00 schedule). Experiments were run during the light phase (within 10:00–17:00). All mice were handled on alternate days during the week preceding the first behavioral testing.

2.1 Stereotaxic surgeries

2.1.1 In vivo injection of PFF, OLIGO and AAV

C57BL/6J male mice were anesthetized with a mix of isoflurane (2%) and oxygen (1.5%) by inhalation and mounted into a stereotaxic frame (Ugo Basile) linked to a digital micromanipulator. A small incision was made to expose the skull and bilateral holes were made using a drill above the targeted injection sites. Brain coordinates, taken relative to Bregma, of bilateral injection in the dorsal striatum were chosen as previously described (Luk et al., 2012a): anterior–posterior (AP), +0.2 mm; medial–lateral (ML): ±2 mm; and dorsal–ventral (DV): −2.6 mm. 2.5 µl of PFFs (5 µg), OLIGO (5 µg) and PBS were infused through a 10 µl Hamilton syringe using a microinjection pump at flow rate 0.25 µl/min; at the end of the injection, needle was left in place for further 4 minutes to allow the solution to flow out entirely.

To achieve Rph3A overexpression, 35 days after the lesion, mice were injected with a solution of Adeno-associated virus serotype 9 (AAV9) containing the plasmid construct hSyn-RFP-Rph3A-WPRE (titer: $5.2x10^{14}$**)** or the control hSyn-RFP-WPRE (titer: $3x10^{13}$). 2 µl of virus solution were infused bilaterally using the same brain coordinates described above for the dorsal striatum. After the recovery from the surgical procedures, mice received carprofen (5 mg/kg) in drinking water for three consecutive days.

2.1.2 Cannula implant for intracerebroventricular injections

65 days after the inoculation of PFF, OLIGO or PBS, implant of a guide cannula in the lateral cerebral ventricle was achieved through stereotaxic surgery. In particular, after the incision, skin was removed and a small craniotomy was performed unilaterally to allow placing of the guide cannula. Brain coordinates for cerebral lateral ventricle were chosen as following, in accordance with the mouse brain atlas: +0.2 mm; medial–lateral (ML): ±1 mm; and dorsal–ventral (DV): −1.5 mm (to allow the final DV injection coordinate to be -2.5 mm). Contralateral to the cannula insertion, a small screw was placed to ensure grip of the implant. Once the skull was totally dry, dental cement (zinc phosphate cement powder, Dentsply) was applied with a liquid consistency around the screw and the cannula to secure it in place. Cement was allowed to completely harden and the stereotaxic arm removed, leaving just the guide cannula in place. A dummy cannula was then placed on top of the internal cannula to avoid any entry of external material.

2.2 Compound B chronic administration in the lateral cerebral ventricle

Starting from 70 dpi, mice received every 3 days intracerebroventricular administrations of 3 µl of Compound B (1mM) dissolved in 5% DMSO-95% saline. An injector connected to a microinjection pump was used to infuse the solution at a constant rate of 2 µl/min. Injection of the vehicle only was used for control animals.

2.3 Behavioral tests

2.3.1 Rotarod

To assess motor learning and coordination, mice were tested on the Rotarod apparatus (Ugo Basile). Each mouse was given a training session (3 trials/day of 300s) for 3 days prior to perform the tests to familiarize with the instrument. For the accelerating rotarod, each mouse was placed on the rotarod with speed increasing from 20 rpm to 40 rpm in 300 sec. 1h later, animals were tested in constant speed conditions at 30 rpm for 300s. For each test, the latency to fall off the rod in a maximum of 300s was recorded for each mouse; the mean of three consecutive trials was used in the analysis.

2.3.2 Open Field

To assess general locomotor activity and anxiety-like behaviors, mice were tested in the open field task for 10 minutes. Mice were individually placed in center of the arena (44x44cm) and a video-tracking software (ANY-maze, Ugo Basile) was used to record and analyze animal movements.

Distance travelled, time spent at the centre and corner of the arena was automatically calculated by the ANY-maze software.

2.3.3 Grip Strength test

Forelimb muscle strength was tested by a grip strength test using the grip strength meter (Ugo Basile). Animals were kept from the tail, approached longitudinally to the bar and allowed to grasp it. Mice were gently pulled away from the bar while the peak force (g) applied by the animal was recorded. Each mouse was tested in five consecutive trials. After each trial the animal was let rest for 1 min; the mean of the five values was considered for the analysis.

2.4 *Ex-vivo* DiI-labeling for spine morphology

For confocal imaging of dendritic spines, neurons were labelled with DiI dye (Invitrogen), a fluorescent lipophilic carbocyanine dye. It diffuses along the neuronal membrane labeling finely dendritic arborization and spine structures in brain slices prefixed with 1.5% PFA (Kim et al., 2007)). DiI labeling procedure was performed as previously described (Kim et al., 2007)). In short, DiI solid crystals were applied using a thin needle by lightly touching the region of interest on both sides of 3 mm brain piece comprising the striatum, prepared after cardiac perfusion with 1.5% PFA in PB 0.1 M. Dil dye was left to diffuse for 1 day in the dark at room temperature, then slices were post-fixed with 4% PFA in PB 0.1 M for 45 min at 4ºC. The first slice containing the DiI crystals were discarded and 100 μm striatal slices were then obtained using a vibratome and collected in PBS. Slices were then mounted on Superfrost glass slides (Thermo Fisher) with Fluoroshield (Sigma) for confocal imaging. Fluorescence images were acquired by using Zeiss Confocal LSM510 system with a sequential acquisition setting at 1024x1024 pixels resolution at 555 nm channel. For each image between 20 and 60 sections of 0.5 μm were acquired and an appropriate z-projection was obtained.

3. Cell cultures

3.1 Primary hippocampal neuronal cultures

Primary hippocampal neuronal cultures were prepared from embryonic day 18-19 (E18-E19) Sprague-Dawley rat hippocampi (Charles River, Milan, Italy). The day before the dissection, plates were coated with Poli-L-Lysine (PLL, Sigma) solution (1 mg/ml in Borate buffer) and incubated overnight at 37°C in a humidified incubator. The day of the dissection, plates were washed three times with sterile water, then plating medium (DMEM+glutamax (Invitrogen) additioned 10% Horse Serum (Euroclone) and 1% Pen/Strep (Invitrogen)) was added. For culture preparation, pregnant rat was anesthetized with a mix of isoflurane (2%) and oxygen (1.5%) and sacrificed and then E18-19

embryos were removed, placed in a 100 mm glass Petri dish filled with ice-cold HBSS (Hanks' balanced salt solution, Sigma). Embryos were sacrificed by decapitation and the brains removed. Under a dissecting microscope, hippocampi were isolated and transferred in 15 ml plastic tube filled with ice-cold HBSS. Under a biological hood, HBSS was removed from the tube using a glass Pasteur pipette and hippocampi washed four times with cold HBSS. Then, a solution of HBSS supplemented with trypsin was used to dissociate the tissue; tube was then incubated at 37°C for 13 minutes in a water-bath. Subsequently, the tissue was allowed to precipitate at the bottom of the tube. The supernatant was carefully removed and hippocampi washed with plating media for five times to neutralize the remaining enzyme. After the washes, the tissue was dissociated through a micropipette till a homogenous solution was obtained. Cells were counted using a Burker chamber and plated at the appropriated density (20,000 and 90,000 cells/cm^2 for imaging and biochemical analyses, respectively) in plating medium. 16 hours after plating, the medium was replaced with Neurobasal medium with 2% B27 supplement (Gibco), 1% Glutamax (Invitrogen) and 1% Pen/Strep (Invitrogen).

3.2 Neuronal transfection

Neurons were transfected between *DIV7* and *DIV10* using calcium-phosphate coprecipitation method with 1-4 µg plasmid DNA. The insoluble calcium-phosphate co-precipitate with the DNA and via endocytosis are then internalized by the cells. 1h before transfection, cell culture medium was temporary removed and replaced with pre-warmed 37°C Minimal Essential Medium (MEM; Gibco). Plates were then left in the incubator again at 37°C. 30 minutes before transfection, transfection solution A and B are prepared, mixed according to the following protocol, and incubated 25 minutes before to be added to cell cultures. In particular, solution A consists of 80µL of HBS 2x while solution B is composed of plasmid DNA, sterile water and 10 µl of 2,5 M CaCl2 to a final volume of 80µL. The solutions were mixed by pouring drop by drop solution B into solution A on a gently mixing. After the 25 minutes incubation, the solution consisting in 80 µl of DNA precipitates were poured on cell cultures, which were then left in a 37°C incubator for 8-15 minutes. After having assessed the presence of visible Calcium-Phosphate precipitates, cells were washed twice with MEM in order to remove all precipitates and left in the incubator for 15 minutes at 37°C. Afterwards. if visible precipitates were still present, cells were subjected to another wash as previously described. Otherwise, MEM was removed and replaced with the original neurobasal medium collected at the beginning of transfection procedure.

3.3 Treatments

3.3.1 In vitro PFFs treatment of hippocampal primary neurons

Before administration to cells, αsyn PFFs aliquots were thawed at RT, diluted in PBS to the final concentration of 0.1 µg/µl and sonicated for a total of 60 pulses (2s ON/1s OFF) in an ultrasonic bath sonicator (Bransonic M2800H-E). At *DIV7-9*, PFFs were added in a single administration to the neuronal culture medium at the concentration of 1 or 2 µg/ml and left for 7 days. As control condition, neurons were treated with the vehicle of PFFs preparation (PBS).

3.3.2 In vitro administration of Compound B to hippocampal primary neurons

Subsequently to PFFs treatment at *DIV9*, at *DIV12* Compound B was added directly to the culture medium. In particular, the molecule was resuspended in DMSO at a concentration of 10 mM and added to the neurons in a single administration to reach the final concentration of 10 µM; treatment was then left till the end of PFF-treatment (4 days).

3.3.3 Treatment of acute cortico-striatal slices with Asinex compounds

To obtain acute corticostratial slices, adult Sprague-Dawley were anesthetized with a mix of isoflurane (2%) and oxygen (1.5%) and decapitated. The brain was rapidly removed from the skull and immersed in cold Kreb's solution containing (in mM): NaCl 126, KCl 2.5, $MgCl_2$ 1.2, $CaCl_2$ 2.4, NaH_2PO_4 1.2, $NaHCO_3$ 24, glucose 10, saturated with 95 % O_2–5% CO_2 (pH 7.4). Coronal slices (250 µm thick) containing striatum and cortex were cut using a vibratome (Vibratome 1000 plus, IMEB). Slices were maintained in Kreb's solution at RT for 30 min prior to the treatment administration. Then, resting Kreb's solution was replaced with one containing 10 µM of each compound or vehicle (DMSO), as control condition. At the end of the treatment, free-floating slices were washed with fresh Kreb's solution and striata were quickly isolated and stored at -80 °C for subsequent analyses.

3.4 Immunocytochemistry (ICC)

For colocalization and morphological studies, hippocampal neurons were fixed at DIV14 for 15 min at RT in 4% PFA plus 4% sucrose in Dulbecco's Phosphate Buffered Saline (PBS; Sigma-Aldrich). Coverslips were then washed with PBS, permeabilized with 0,1% triton X-100 in PBS for 15 min at room temperature and blocked for 30 minutes at room temperature with 5% Bovine Serum Albumin (BSA) in PBS. Cells were then incubated with primary antibodies in 3% BSA-PBS overnight at 4ºC in a humid chamber. After washes with PBS, the cells were incubated with the fluorophore-conjugated secondary antibodies in 3% BSA-PBS for 1h at room temperature in a humid chamber

protected from light. The incubation was followed by washes with PBS and mounting on glass slides using Fluoroshield mounting medium (Sigma-Aldrich).

3.5 Proximity ligation assay (PLA)

Primary hippocampal neurons were fixed at DIV14 with 4% PFA + 4% sucrose for 15 minutes at RT in PBS. Coverslips were then washed 3 times with PBS and permeabilized with Triton-X-100 0,1% in PBS for 15 minutes and later blocked with 5% BSA in PBS for 30 minutes at room temperature. Coverslips were then incubated in a dark humid chamber overnight at 4°C with primary antibodies in 5% BSA in PBS, washed 3 times with PBS and then incubated with secondary antibodies conjugated with oligonucleotides (PLA probe MINUS and PLA probe PLUS) for 1 h at 37°C in a dark humid chamber. Coverslips were then washed 3 times with PBS and incubated with the ligation solution (Olink bioscience) supplemented with ligase (25 mU/µL) for 30 min at 37ºC in a dark humid chamber and washed with Wash Buffer A (NaCl 0.15 M, Tris 0.01 M, 0.05 % tween 20, pH 7.4; Olink Bioscence). The amplification solution (containing nucleotides and fluorescently labeled oligonucleotides; Olink bioscence) supplemented with polymerase (0.125 U/µL) was added to each sample and incubated for 100 min at 37 ºC in humid dark chamber. Coverslips were then washed 3 times with decreasing concentration of Wash Buffer B (NaCl 0.1 M, Tris 0.2 M, pH 7.5; Olink bioscience).

Images were acquired through Zeiss LSM 510, Nikon A1 Ti2 system or Zeiss LSM 900 with sequential setting at 1024x1024 pixels resolution. For all images the signals for each image were kept within the linear range and settings were consistent between different experimental conditions.

4. Biochemistry

4.1 Subcellular fractionation and Triton insoluble fraction (TIF) preparation

Striata were homogenized with a hand-held Teflon-glass potter at 4 °C in ice-cold buffer (pH 7.4) containing 0.32 M sucrose, 1 mM Hepes, 1 mM MgCl2, 1 mM NaHCO3 and 0.1 phenylmethanesulfonylfluoride supplemented with Complete™ Protease Inhibitor Cocktail Tablets (Roche Diagnostics) and phosSTOP™ Phosphatase Inhibitor (Roche Diagnostics). An aliquot of the homogenate was frozen at −20 °C, while the rest of the sample was centrifugated at 1000 g for 5 min at 4 °C to remove nuclear contamination and white matter. For the purification of Triton-insoluble postsynaptic fraction (TIF), highly enriched in postsynaptic densities proteins (Gardoni et al., 2001), the supernatant was collected and spun at 13,000 g for 15 min at 4 °C. The resulting pellet (P2-crude

membrane fraction) was resuspended in Triton-KCl buffer (1% Triton™ X-100 and 150 mM KCl) and, after 15 min incubation on ice, it was spun at 100 000 g for 1 h at 4 °C. The pellet (TIF) was resuspended in 20 mM HEPES buffer supplemented with Complete™ Protease Inhibitor Cocktail tablets and stored at −20 °C. TIF and homogenates samples for immunoblotting analysis were denatured with Laemmli buffer and subsequent heating (10 min, 98 °C).

4.2 Co-ImmunoPrecipitation assays (Co-IP)

Homogenate/P2 aliquots containing respectively 150-50µg of proteins were incubated overnight at 4°C with primary antibody in RIA buffer containing 50 mM Tris HCl (pH 7.2), 150 mM NaCl, 1% NP-40, 0,2% sodium dodecyl sulphate (SDS), 0,5% deoxycholic acid. A control No-IgG sample was prepared in same conditions without the antibody. The Protein A/G-sepharose beads (Sigma-Aldrich) were washed three times in PBS-T (0.1% Tween-20 in PBS), resuspended in RIA buffer, added to each sample and incubated for 2 h on a wheel at RT. Beads were precipitated by quick centrifugation and washed three times in RIA buffer supplemented with SDS 0,1% and boiled for 10 minutes in Laemmli buffer. Beads were magnetized and supernatant loaded in a proper acrylamide gel for SDS-PAGE and interacting proteins revealed by immunoblotting. For the input lane a 10-20% of homogenate/P2 samples were used.

4.3 Western blotting

The protein content of TIF and homogenate samples was quantified by Bradford assay, all samples were standardized at a concentration of 1 mg/ml and denatured both chemically with Laemmli buffer and thermally (98°C, 10 minutes). TIF and total homogenates proteins were separated on SDS-PAGE followed by western blotting analysis. 10−15 µg of proteins were separated on 6-12% acrylamide/bisacrylamide gel and transferred on nitrocellulose membrane (Bio-Rad). The membranes were then incubated for 1 h at room temperature in blocking solution (I-block, Tris-Buffered saline (TBS) 1X, 20 % Tween-20) on a shaker and then incubated with the specific primary antibody in blocking solution overnight at 4 C°. The following day, after three washes with TBS and tween 20 (TBS + Tween20 0.1 %; TBSt), they were incubated with corresponding Horseradish Peroxidase (HRP)-conjugated secondary antibody in blocking solution for 1 h at room temperature. After washing with TBSt, membranes were developed using electrochemiluminescence (ECL) reagents (Biorad). Finally, membranes were scanned using a Chemidoc (Biorad Universal Hood III) with Image Lab software (Biorad). Bands were quantified by means of computer-assisted imaging (Image Lab, Biorad). Protein levels were expressed as relative optical density (OD) measurements normalized on level of an housekeeping protein.

5. Molecular modelling

5.1 Ligands

The initial ligand databases were supplied by Asinex (Asinex Glod & Platinum Collection, Asinex BioDesign, http://www.asinex.com/) and correspond to a lead-like structural library of commercial 2D compounds, providing diverse and cost-effective coverage of drug-like chemical space. Most of the included compounds are characterized by a high degree of drug-likeness, in accordance with Lipinski's rule of 5.

5.2 *In silico* ADME prediction

The ADME profile of the investigated compounds was predicted through the Schrödinger QikProp tool (Small-Molecule Drug Discovery Suite 2015–1, Schrödinger, LLC, New York, NY), which uses an algorithm based on the correlation between experimentally determined properties and Monte Carlo statistical mechanics simulations of organic solutes in a periodic box of explicit water molecules.
In parallel, ADME was predicted also through a combination of quantitative structure-activity relationship (QSAR) models, as implemented in the ACD/Percepta ADME Suite predictions (ACD/Labs, Toronto, Canada).

5.3 *In silico* molecular docking simulations using MOE

Molecular docking of all the investigated compounds has been carried out on an homology model of human Rph3A, that included two calcium ions and an IP_3 molecule, built starting from 2CM5, 5LOB, 5LOW and 5LO8 rat crystallographic structures (obtained from RCSB PDB), using the Amber12:EHT force field. The protein was prepared through the Structure Preparation program of the Molecular Operating Environment (MOE) Prepare module [https://www.chemcomp.com/MOE-Mocular_Operating_Environment.htm], to check and correct structures for subsequent computational analysis. The database containing all the investigated compounds were energy minimized by the Energy Minimize program with default parameters of the MOE Compute module, to produce a single low-energy conformation for each putative ligand.
The *in silico* screening was carried out with the MOE Dock program contained in the Compute module, following an already described workflow (Eberini et al., 2011). The full Rph3A model structure was set as receptor and the binding site was defined from Ser618 toLys663.
For each ligand conformations were generated by sampling their rotatable bonds. The selected placement methodology was Triangle Matcher, in which the poses are generated by superposing triplets of ligand atoms and triplets of receptor site points. The receptor site points are alpha spheres

centers that represent locations of tight packing. The generated poses were scored according to the London dG scoring, which estimates the free energy of binding of the ligand from a given pose. The top-scoring 30 poses were passed to a refinement step based on molecular mechanics and then rescored according to the GBVI/WSA dG, a forcefield-based scoring function that estimates the free energy of binding of the ligand from a given pose. All receptor atoms were held fixed during the refinement. During molecular docking procedures, the MMFF94x force field was used both for protein and ligands.

5.4 In silico molecular docking simulations using Schrödinger

Molecular docking was carried out via Glide in its standard (SP) and extra precision (XP) mode (Friesner et al., 2004). Before the docking procedures, Rph3A model was prepared and energy-minimized via the BioLuminate Protein Preparation Wizard with the OPLS3e force field (Harder et al., 2016). The same force field was applied in all the molecular docking procedures. The binding free energy of all the complexes produced by molecular docking pipeline was evaluated via Glide XP Score, that is an empirical scoring function that approximates the ligand binding free energy, to separate putative ligands from non-ligands.

6. Antibodies

6.1 Primary antibodies. Rabbit anti α-Synuclein (D37A6) (WB 1:1000, Cell Signaling #4179); mouse anti Synuclein (WB 1:1000, ICC 1:200, BD #610 787); anti polyclonal Rph3A (WB 1:2000; ICC 1:300, Protein Tech #11396-1-AP); rabbit anti-Rabphilin3A (WB 1:1000, Synaptic System #118003).

Mouse anti-Tubulin (WB 1:30000; #T9026, Sigma), rabbit anti-GluN2A (WB 1:1000 #M264, Sigma); rabbit Anti-GluN2B (WB 1:1000, #718600, Invitrogen); Anti GluN2D mouse mAb (WB: 1:1000 #MAB5578 Millipore); Anti mouse GluN1 (WB 1:1000, #320500, Thermofisher) .

Rabbit anti GluA1 (WB 1:1000 #13185, Cell Signaling), rabbit monoclonal anti-phosphoSer845-GluA1 (WB 1:1000 #04-1073, Merck-Millipore); mouse anti GluA2 (WB 1:1000 #75-002 Neuromab), mouse anti GluA3 (WB 1:1000 #MAB5416 Millipore).

Rabbit Anti tyrosine hydroxylase (WB 1:10000 #AB152 Millipore); mouse anti Neurofilament-L (WB 1:1000 #2835); mouse anti Neurofilament M (WB 1:1000 #2838 Cell Signaling).

Anti-phosphoT202/Y204-MAPK 44/42 Cell Signaling #9101; anti-ERK 44/42 Cell Signaling #9102; monoclonal anti-PSD-95 (WB 1:1000, #K28/43) Neuromab; anti-tGFP ICC 1:300 #AB513, Evrogen.

6.2 Secondary HRP-linked antibodies*:* goat anti-rabbit (1:10,000 #172-1019, Biorad); goat anti-mouse, (WB 1:10,000 #172-1011, Biorad).

6.3 Secondary antibodies for imaging experiments: goat anti-rabbit-Alexa555 (A-21429; Life Technologies), Alexa-fluor 488 (A-11039) goat anti-chicken, goat anti-mouse-Alexa555 (A-21422), 4',6'-diamidino-2-phenylindole (DAPI, 1:50,000 in PBS, Thermo Fischer Scientific), goat anti-rabbit-Alexa-488 (A-11034).

7. Statistical analysis

Western Blot quantification was performed using the software ImageLab (BioRad Laboratories). Protein levels were expressed as relative optical density (OD) normalized on tubulin or actin levels as housekeeping proteins. Images acquired with confocal microscope were analyzed with the use of Fiji / Image J software. Statistical analysis was performed with GraphPad Prism7 software and data were presented as mean ± SEM (standard error of the mean). The tests used to assess data significance are indicated in the figure legends. In particular, the following tests, as appropriate, were used: two-tailed unpaired Student's *t* test, Mann–Whitney test or one-way ANOVA. Numbers of neurons and mice used are reported in the figure legends. For the confocal images analyses at least 10 neurons coming from three different experiments were analyzed.

RESULTS

1. Characterization of the physiological interaction between Rph3A and αsyn

1.1 In vitro assessment of Rph3A/αsyn binding

Rph3A is a pre and postsynaptic protein with different functions in the synaptic compartment. In particular, at the pre-synapse it takes part in the process of release of neurotransmitter vesicles (Bourgeois-Jaarsma et al., 2021b; Deák et al., 2006b; Handley and Burgoyne, 2008). At the same neuronal compartment, αsyn is known to behave like a hub of interaction (Longhena et al., 2019), participating as well in pre-synaptic organization and release of vesicles (Burre et al., 2010; Burré et al., 2014; Diao et al., 2013).

On the pathologic side, it has been shown that small oligomers of αsyn are able to affect the postsynaptic localization of GluN2A containing-NMDARs (Durante et al., 2019). Since Rph3A is fundamental to maintain these receptors at postsynaptic sites (Stanic et al., 2015) and a direct αsyn/Rph3A interaction (Dalfó et al., 2004) has been put forward, a strict interplay between the two proteins can be hypothesized.

Based on these considerations, I decided to confirm and characterize αsyn/Rph3A interaction by means of diverse *in vitro* approaches, in a physiological experimental setting. Starting from imaging experiments, I performed colocalization analysis of the endogenous αsyn and Rph3A on primary cultures of rat hippocampal neurons at *DIV14, (DIV-days in vitro)*. Hippocampal neuronal cultures develop functional synapses and show extensive axonal and dendritic arborizations, thus allowing studies of subcellular localization of proteins (Kaech and Banker, 2006). To analyse the distribution of the two proteins along dendrites, I took advantage of Structured Illumination Microscopy technique (SIM), a super-resolved type of confocal microscopy that allows to reach a xy resolution of about 100-110 nm. As shown by the representative images in Fig.21, colocalization of Rph3A and αsyn was detected in several spots along neurons labelled with MAP2 (white), a validated marker of the dendritic compartment. The overlap of the two signals indicates that the two proteins belong to the same molecular complex, thus suggesting a possible direct protein-protein interaction.

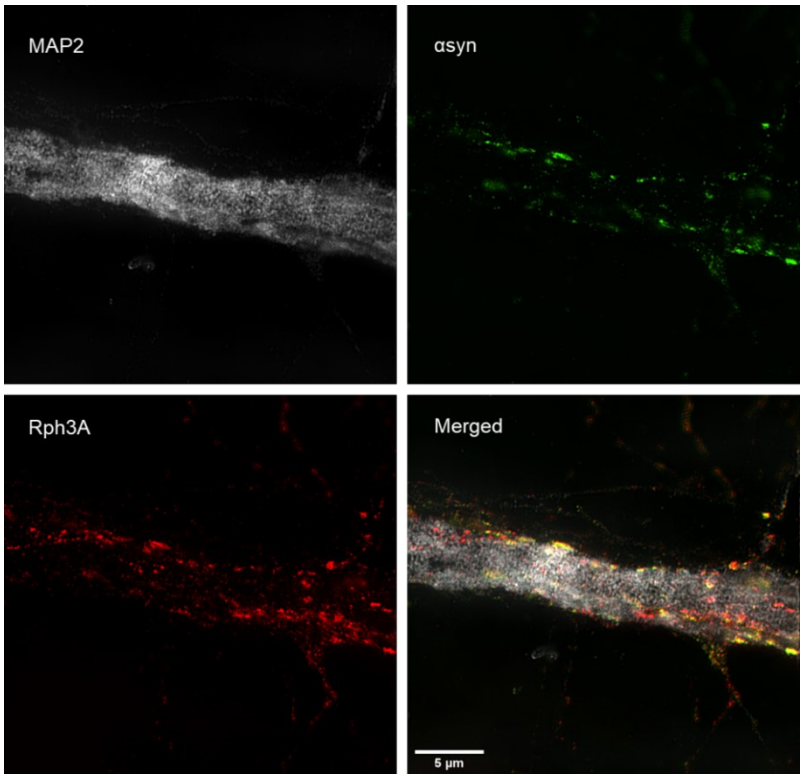

Fig.21. Rph3A colocalizes with αsyn at the dendritic compartment.
Representative Structured Illumination Microscopy (SIM) image of αsyn (green) and Rph3A (red) along MAP2-positive dendrites (white) in DIV14 rat hippocampal neurons. Scale bar: 5µm

To further characterize the clustering of the two proteins, proximity ligation assay (PLA) was performed. This immunocytochemistry technique allows the study of protein-protein interactions by detecting the proximity of proteins. When the two proteins are found closer than 40 nM, a fluorescent spot is produced, allowing to visualize the direct interaction. In line with colocalization results, as shown in Fig.22, a large number of PLA signals (red dots) were detected along dendrites of MAP2-labelled neurons (Fig.22a). PLA clusters were not only present along neurites but also in the proximity of dendritic spines of GFP-transfected neurons (Fig.22b), proving that the interaction occurs at the level of synaptic compartment.

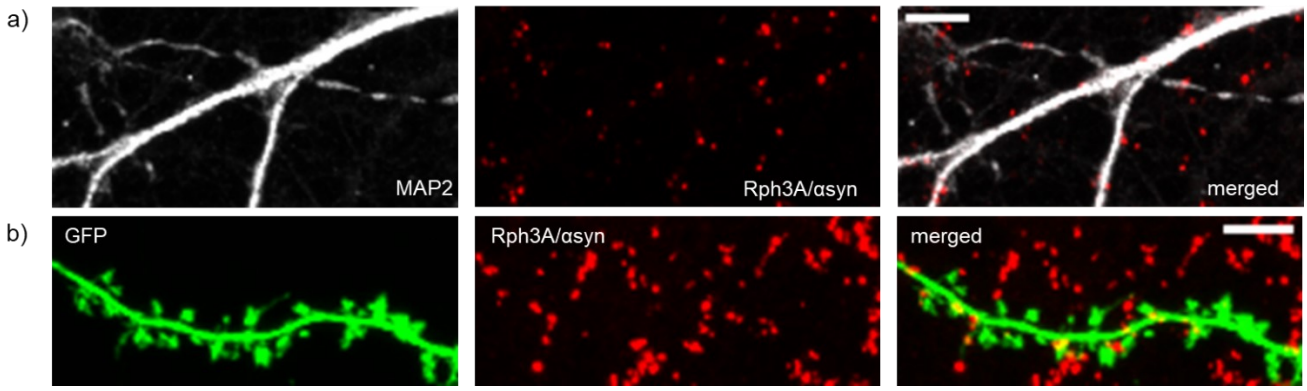

Fig.22. In situ detection of proximity ligation assay (PLA) between αsyn and Rph3A (red) along) a) MAP2-positive dendrites (white) of *DIV14* primary hippocampal neurons b) GFP-transfected neurons (green). Scale bar: 5 µm

Finally, a biochemical approach was used to confirm imaging results. Specifically, co-immunoprecipitation experiments were conducted on total homogenate of primary hippocampal neurons (*DIV14*) and, considered αsyn and Rph3A interplay with membranes (Fusco et al., 2016; Oishi et al., 1996), on the crude membrane fraction (P2) of rat brain. As shown in Fig. 23, αsyn can be detected by western blot (WB) analysis in Rph3A-immunoprecipitates and, on the other way around, Rph3A co-immunoprecipitates with αsyn. Co-immunoprecipitation experiments were conducted using both sepharose-protein A beads (Fig. 23a,b) and confirmed with magnetic beads conjugated with protein A (Fig.23c).

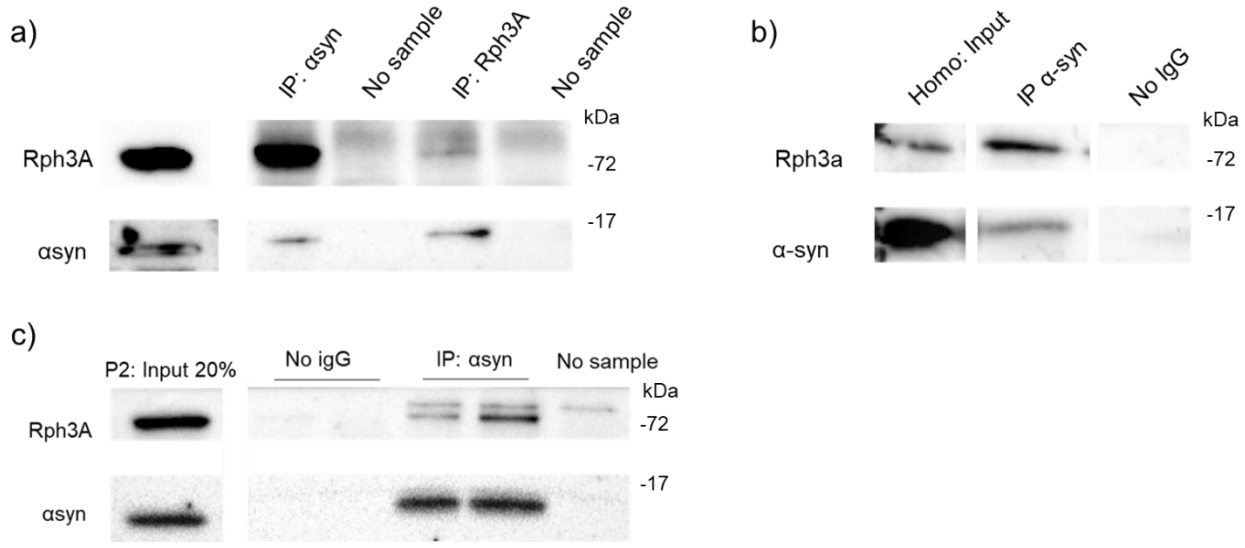

Fig.23. Rph3A/αsyn complex detection in rat brain and hippocampal primary neurons.
Co-immunoprecipitation analysis of αsyn and Rph3A in a) P2 of adult rat brain and b) homogenate of primary hippocampal neurons performed with protein A sepharose beads then confirmed with protein A magnetic beads on c) P2 of adult rat brain.

1.2 *In silico* characterization of Rph3A/αsyn binding mode

In silico structural analysis was employed to characterize the binding mode of the two proteins. To identify the surface of Rph3A that was likely to interact with αsyn, I firstly examined published structural biochemical and biophysical studies of both proteins. As already described in the Introduction Section, Rph3A functional domains consist of a N-term Rab3A-binding domain and a C-term made up by 2 tandem C2-like domains (Yamaguchi et al., 1993). These common structural motifs able to interact with Ca^{2+} and lipids are shared by many proteins involved in vesicle exocytosis (Martens, 2010). Interestingly, Rph3A C2 tandem domains have important roles both at the pre and postsynaptic terminal. By binding to 2 Ca^{2+} ions and 1 IP_3 molecule, each C2 domain (C2A and C2B) dramatically increases Rph3A/GluN2A binding (Stanic et al., 2015). Moreover, it has been demonstrated that interaction of the C2B domain with phosphoinositide molecules (PIP_2) contributes to membrane bending during the vesicle fusion process (Ferrer-Orta et al., 2017). This work, through NMR studies, deeply analyzed the already reported interaction between SNAREs member SNAP25 and the C2B of Rph3A by describing the molecular recognition mechanisms of the binding, represented in Fig.24 (Deák et al., 2006b; Ferrer-Orta et al., 2017).

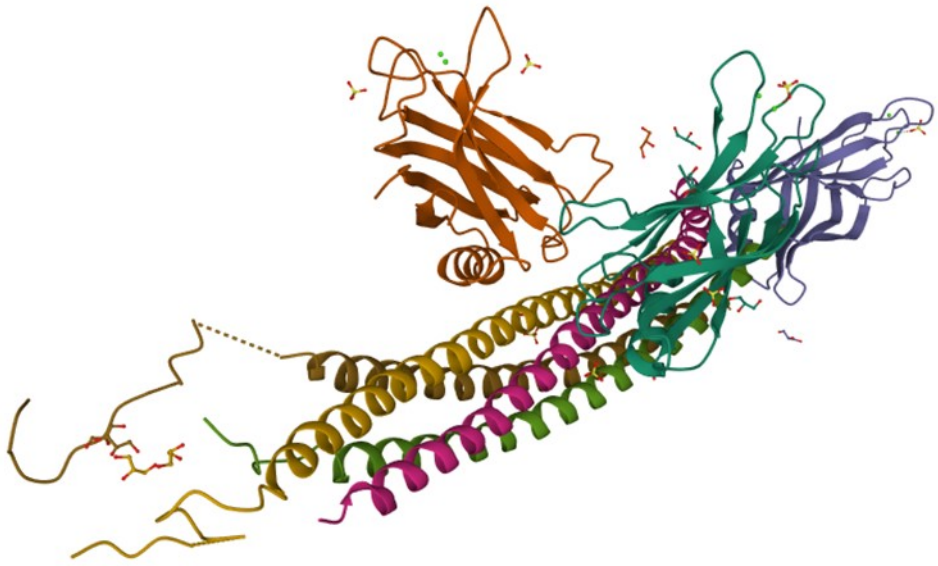

Fig.24 Rph3A interaction with SNAP25 is mediated by the C2B domain. PDB ID: 5LOB 10.2210/pdb5LOB/pdb; Structure of the Ca2+-bound Rabphilin3A C2B- SNAP25 complex (C2 space group)

Similarly, the homologous Rph3A proteins Synaptotagmin-1 and-3, involved in Ca^{2+}-triggered exocytosis of synaptic vesicles, are known to interact with SNAREs proteins through their C2-like domains, although through a different molecular mechanism (Ferrer-Orta et al., 2017; Zhou et al.,

2015). Furthermore, the conserved coiled structure of SNAREs is similar to the NMR structure of the non-fibrillary monomeric structure of αsyn (Fig. 25b) when bound to micelles (PDB: 1XQ8).

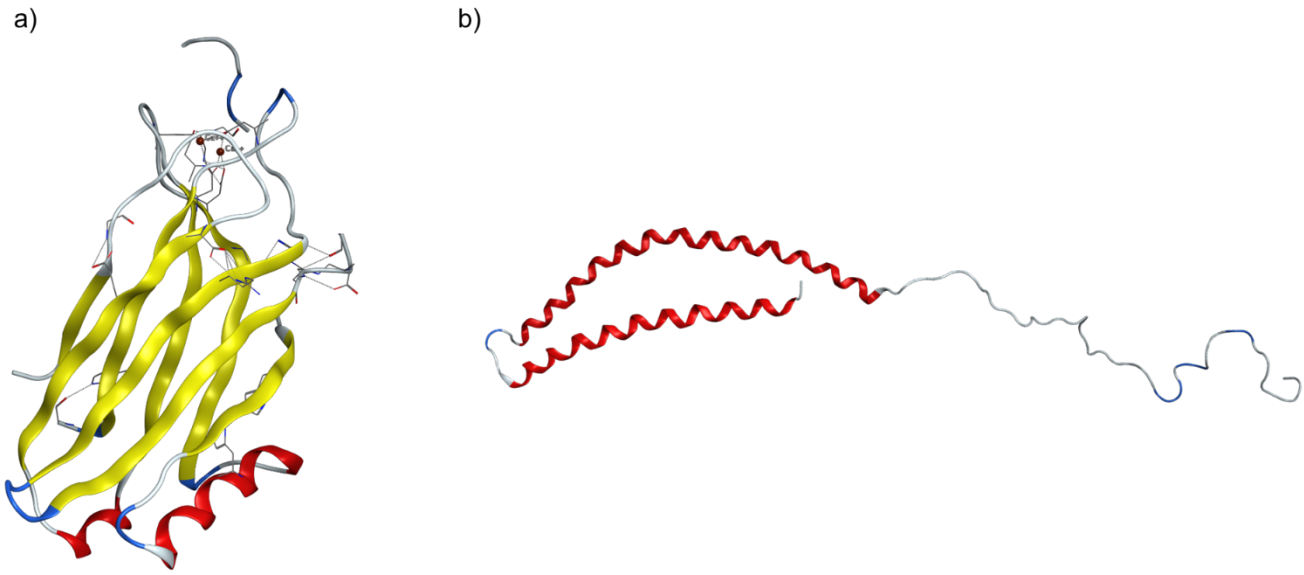

Fig.25. a) PDB ID: 2CM5; crystal structure of the C2B domain of Rph3A b)PDB ID: 1XQ8; Human micelle-bound alpha-synuclein (10.2210/pdb1XQ8/pdb)

These literature findings, the αsyn functional similarity to the SNAREs proteins and their key role in the pre-synaptic compartment, suggest that αsyn could compete to the SNAP25 binding site on the Rph3A C2B domain (Fig.25a).

Starting from these observations, I focused in the structural studies mainly on the C2B Rph3A domain. Protein sequence, structure and surface charges were analyzed starting from the available crystallographic and NMR data of the rat Rph3A. The use of rodent structures was made possible by the high similarity between rat and human Rph3A protein sequence. As shown by Fig.26, protein sequence alignment of human Rph3A (Q9Y2J0) and rat Rph3A (P47709) obtained by BLASTp tool (https://www.uniprot.org/uniprot/) found a 85% sequence identity. To note, protein sequences corresponding to the sole C2B domain of the two species perfectly match (aa 550-683).

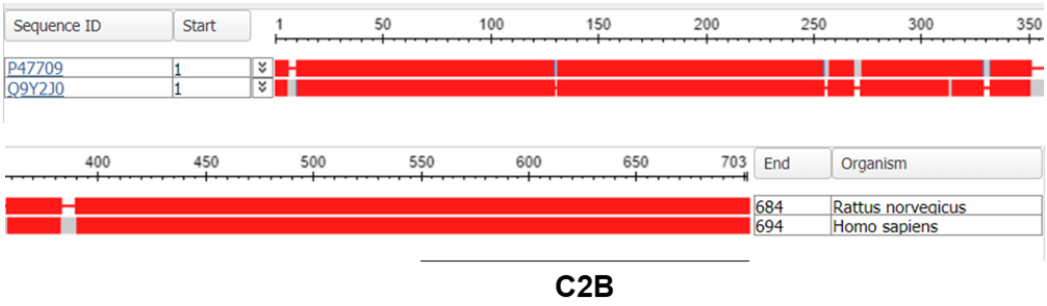

Fig.26. Rph3A human and rat protein sequence share a 85% of identity. BLASTp alignment of human (Q9Y2J0) and rat (P47709) Rph3A protein sequence. Red bars highlight regions of 100% sequence identity.

This 100% sequence identity allowed to easily build a homology model of the human domain taking as a template structure the crystallized C2B rat structure. In particular, using MOE software, PDB structures corresponding to rat Rph3A 2CM5, 5LOB, 5LOW and 5LO8 were aligned and the best structure in terms of sequence coverage and co-crystalized ligands was kept. Ca^{2+} ions, included in 2CM5 structure, and PIP2, co-crystalized in PDB 5LO8, were both added to the model.

To identify a preferential binding surface for the contact with αsyn, protein patches analyses done on our model were compared to C2B-SNAP25 binding surfaces described by the paper by Ferrer-Orta and colleagues (Ferrer-Orta et al., 2017). Fig.27 shows the Rph3A C2B model with the hydrophobic patch (green surface) selected to be the putative motifs involved in αsyn interaction. These two alpha helices comprising AA from Ser618 to Lys663 and distinguishing Rph3A C2B domain from C2A and Synaptotagmins C2, were chosen as the potential aminoacidic stretches able to bind αsyn (Ubach et al., 1999).

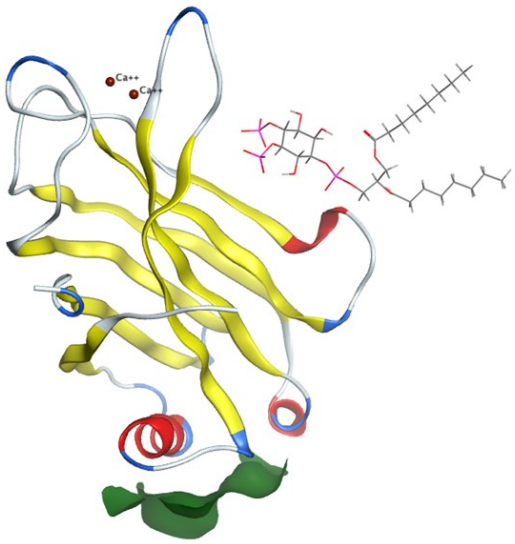

Fig.27. Human C2B Rph3A model built with MOE with the selected hydrophobic patch (green surface) comprising the 2 alpha helical motifs on the bottom of the C2-like domain.

2. Bioinformatic screening of Rph3A:αsyn uncoupling compounds

Having assessed through various experimental approaches the interaction between Rph3A and αsyn, bioinformatic analyses and literature examination allowed to hypothesize the putative Rph3A surface involved in the binding. In order to validate this hypothesis, I moved to the identification of compounds able to uncouple the two proteins. Besides providing a proof of concept of the assumption, modulating Rph3A/αsyn binding could also help in elucidating the role of this protein complex in PD.

2.1 Identification of the putative Rph3A residues mediating αsyn binding

An already available homology model of the human Rph3A-C2B domain was used to perform an *in silico* screening of libraries of commercially available compounds capable of binding to the target Rph3A region. As already described in Results section 1, Rph3A domain mediating SNAP25 interaction (Ferrer-Orta et al., 2017), and hypothesized to contribute to αsyn binding as well, is located within the C2B bottom surface. In particular, this aminoacidic stretch, comprising residues from Ser618 to Lys663, forms two αhelical regions, depicted in yellow in Fig.28. The complete aminoacid sequence of this C2B region is reported in Fig.29c. Residues thought to be critical for the studied interaction (Fig.29a-b) are reported in yellow in Fig.29c, specifically: Ser618, Lys622, Lys623, Lys651, Lys663. This polybasic stretch of aminoacids confers to this region of Rph3A a positive charge, a feature that will be considered as a fundamental constrain for the subsequent compound screening.

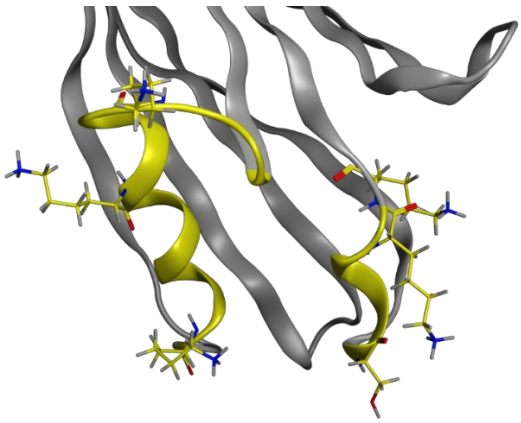

Fig.28. Structure of the C2B-bottom surface of Rph3A indicating the two target αhelices hypothesized to bind αsyn.

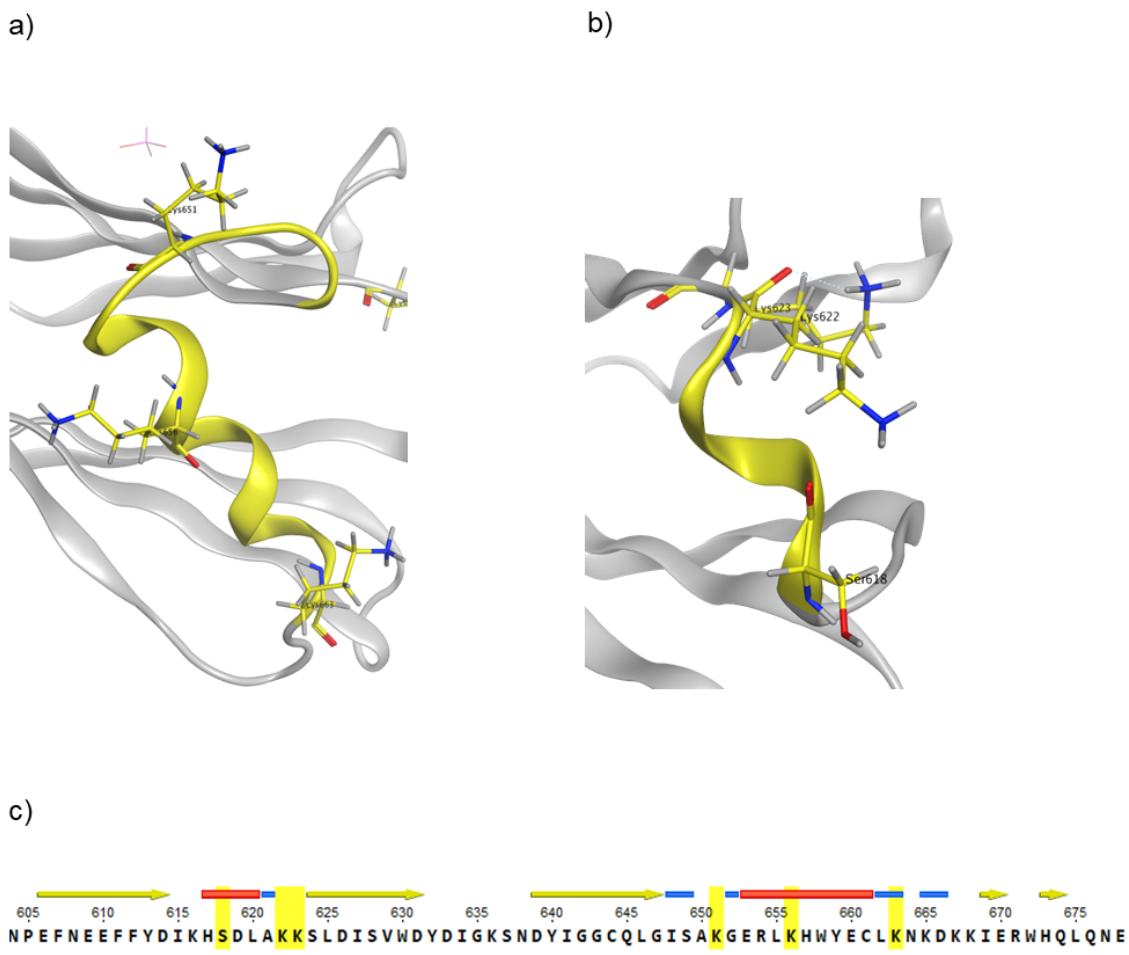

Fig.29. Structure of the C2B bottom surface of Rph3A showing lateral chain of a) Lys651, Lys656, Lys663 and b) Ser618, Lys622, Lys23
b) Protein sequence of Rph3A-C2B region comprising the 2 bottom α-helical regions (red segment). Yellow arrows indicate β-sheet organized regions

2.2 *In silico* screening of libraries of commercial compounds

2.2.1 Sorting based on chemical and ADME properties

Compounds to be evaluated as able to bind the target Rph3A region and, consequently, to interfere with Rph3A/αsyn complex, were chosen from the libraries:

-*Asinex BioDesign*, containing molecules with key structural features of known pharmacologically relevant natural products incorporated on feasible medicinal chemistry scaffold;

.*Asinex Gold & Platinum*, in which the majority of compounds have a high degree of drug-likeness (http://www.asinex.com).

As first step, I analysed drug-like properties to sort out from the libraries the less pharmacologically relevant molecules. To do so, we used the QikProp module of the Schrodinger software, that allows

an accurate prediction of the pharmacokinetic properties of batches of organic molecules. Among the calculated descriptors, number of violations of the Lipinski's rule of five (MW < 500, QPlogPo/w < 5, donorHB ≤ 5, accptHB ≤ 10) and Jorgensen's rule of three (QPlogS > -5.7, QP PCaco > 22 nm/s, # Primary Metabolites < 7) were evaluated and compounds exceeding 4 and 3, respectively, number of violations were excluded.

In parallel, considering structural and chemical properties of the target Rph3A surface and, more specifically, its basic nature, molecules were filtered retaining those bearing negative charges. To do so, we analyzed charge-related descriptors exploiting the QikProp tool and the relative module on MOE (Molecular Operating Environment) software. The most important parameters considered were the Total charge (FCharge, defined as the sum of formal charges) and the number of acidic atoms (a_acid) displayed by the molecules. The compounds exceeding this selection constituted the final library, including 15454 molecules, that was used for the protein-ligand docking studies.

2.2.2 Protein-ligand docking studies

An initial protein-peptide docking was performed using the Glide (Grid-based Ligand Docking with Energetics) module of Schrodinger software. As a constraint (ligand-receptor interaction requirement), a grid of the receptor which contained the bottom α-helical region of Rph3A was generated. The docking protocol was defined to exclude Rph3A volume not containing the selected region. Standard protocol (SP) of ligand docking was used to initially screen the large set of molecules. From the results of the docking procedures, the 7 top scoring molecules were selected and subsequently subjected to a more accurate docking protocol using the extra precision mode of Glide (XP). Ligands showing the 24 best docking poses were analyzed focusing on energy and affinity of the binding, allowing to select three final ligands.

A protein-ligand docking protocol of the same library of acidic compounds were performed also using MOE software. To sort the output docking poses, protein-ligand interaction fingerprints (PLIF) were calculated. Ligands interacting at least with one of the Lys623, Lys651, Lys656, Lys663 were used to create a final database. Specifically, the database included:

- 19 compounds representing the top scoring ligands among the compounds able to interact with Lys663
- 6 compounds able to interact with both Lys663 and Lys623
- 5 compounds interacting with Lys651 and Lys663

A library (22 molecules) including the 19 selected compounds from MOE docking results and the 3 top scoring ligands obtained by Glide XP docking were analyzed to predict their molecular properties (physicochemical, ADME and toxicity) using the ACD/Percepta Software, in order to select

candidate compounds able to be studied in an *in vitro* system. Moreover, for each compound the CNS score (ability to permeate the BBB), logP and Lipinski rules violations were recalculated. Four compounds with different physicochemical properties were selected considering the predicted properties and docking results, as reported in Fig.30. These 4 selected molecules were then tested *ex-vivo* for their ability to modulate Rph3A/αsyn binding.

Molecule	FCharge	a_acid	Docking score	CNS score	LogP	Lipinski violations
Compound A	-4	3	-6.0509	-2.85 (penetrant)	optimal	0
Compound B	-4	8	-3.8411	-7.53 (non penetrant)	very lipophilic	4
Compound C	-2	4	-4.9705	-6.87 (non penetrant)	optimal	0
Compound D	-1	3	-5.6598	-3.30 (weak penetrant)	optimal	0

Fig.30. Table reporting formal charge (FCharge), number of acidic group (a_acid), the docking score and main ADME properties of the 4 selected candidate ASINEX compounds. Physico-chemical properties were predicted using ACD percepta software.

2.3 *Ex vivo* testing of the candidate Rph3A/αsyn uncoupling compounds

I subsequently evaluated the ability of the four candidate compounds to impair Rph3A/αsyn interaction by using a biochemical approach. In particular, acute rat corticostriatal slices, maintained in a Krebs (artificial CSF) solution, were treated for 40 minutes with 10 μM of each compound or vehicle (DMSO), as control condition. After treatment, striata were separated from the cortex and homogenized. Rph3A/αsyn interaction was then assessed by co-immunoprecipitation experiments.
Results of the co-immunoprecipitation analyses, shown in Fig.31, indicate that only Compound B is able to decrease in a statistically significant manner the amount of Rph3A bound to αsyn.

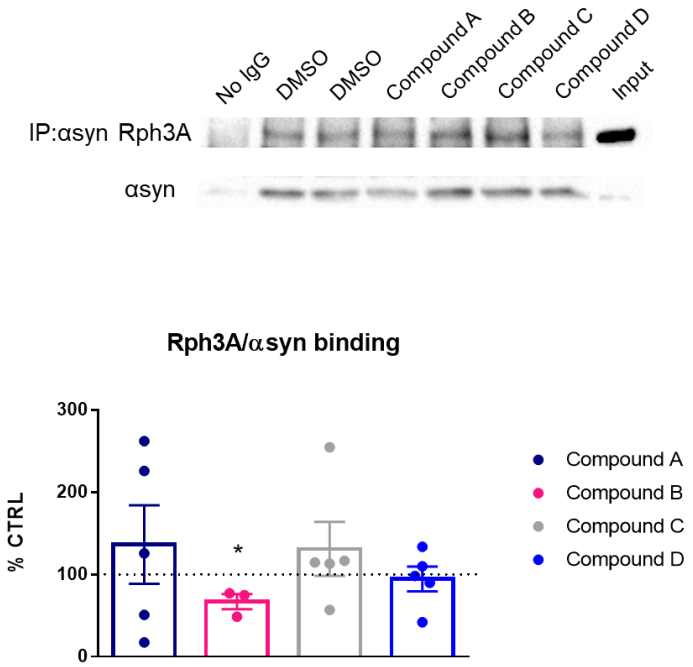

Fig.31. Co-immunoprecipitation analysis of αsyn and Rph3A in corticostriatal slices treated with the 4 selected ASINEX compounds. Rph3A was immunoprecipitated from striatal homogenate samples corresponding to 150 µg of protein and levels of αsyn were evaluated by WB analysis on Rph3A immunoprecipitate (IP). 30 µg of homogenate (corresponding to the 20% of the amount used for co-IP analysis) were loaded as input control. αsyn band was normalized on the corresponding Rph3A band and expressed as OD% of CTRL in the semi-quantitative bar graph.
(n=3-5, unpaired t-test, Compound B vs CTRL *p<0.05)

Co-immunoprecipitation data did not detect significant modulatory activity on Rph3A/αsyn binding in any of the other tested molecules.

To summarize, *in silico* and *ex vivo* data indicate that Rph3A is able to interact with αsyn preferentially through its bottom C2B region and compound B can be used to evaluate the role of Rph3A/αsyn complex in neurons.

3. Characterization of αsyn synaptic toxicity in an early-PD experimental in vivo model

3.1 Characterization of the αsyn-mouse model

Since the discovery of PD patients carrying mutations in *SNCA*, αsyn coding gene, a fundamental role has been attributed to αsyn misfolding and aggregation in the pathophysiology of familiar and sporadic PD (Baba et al., 1998; Polymeropoulos, 1997; Spillantini et al., 1997). In the last years, literature data reported its involvement also in molecular mechanisms behind early stages of the disease, prior to the occurrence of dramatic midbrain neuronal loss. In this context, αsyn was shown to affect neuronal homeostasis and activity even beyond the dopaminergic system. For instance, it was recently demonstrated to impact NMDAR complex activity (Durante et al., 2019; Tozzi et al., 2016). Further supporting this evidence, a fundamental *in vivo* involvement of αsyn in early disease stages was recently reported. Before onset of dramatic neurodegeneration and loss of striatal DA fibres, αsyn fibrils caused alterations of synaptic plasticity within the nigrostriatal circuits together with behavioural abnormalities (Tozzi et al., 2021).

Having confirmed Rph3A as an αsyn interactor at synaptic sites (see above Fig. 21-22-23) and considering the critical role of αsyn in PD pathogenesis, I subsequently moved to investigate Rph3A role and Rph3A/αsyn interplay in an early *in vivo* model of synucleinopathy. Valid tools to reproduce experimentally *in vivo* precocious PD manifestations are represented by rodent model based on injection of pre-formed toxic αsyn species. αsyn, once inoculated in selected brain areas, generates pathology primarily through a prion-like mechanism. Indeed, exogenous αsyn functions as a seed for the formation of new toxic aggregates, fostering phosphorylation and propagation to interconnected brain region of the insoluble inclusions (Luk et al., 2012a; Masuda-Suzukake et al., 2013). In contrast to toxin based or transgenic mouse model, animals develop a slowly progressive disease, allowing to investigate mechanism underlying pathology progression from the very precocious stages (Luk et al., 2012a; Patterson et al., 2019). (See Introduction section).

In order to investigate the impact of pathologic αsyn on the cortico-striatal glutamatergic synapse, I exploited an already highly validated PD model, firstly generated by Luk and coworkers in 2012. Briefly, αsyn is targeted to the dorsal striatum and pathology anterogradely diffuses to the SNpc affecting the nigrostriatal circuitry (Luk et al., 2012a). Two different αsyn species, small oligomers (OLIGO) or pre-formed-fibrils (PFFs) were bilaterally injected by stereotaxic surgery in striatum of 2-months old wild-type C57BL/6J mice. Indeed, the monomeric protein has been already demonstrated incapable of seeding pathology (Masuda-Suzukake et al., 2013) (See Methods section).

According to previous works (Luk et al., 2012a; Tozzi et al., 2021), control mice were injected in the same site with PBS, the vehicle of αsyn preparation.
Literature data on this animal model (Luk et al., 2012), preliminary experiments and a work published very recently together with collaborators contributed to the time points selected (Tozzi et al., 2021). In this regard, significant dopaminergic neurodegeneration in mice is reported to appear after 120 days post injection (dpi 120) (Luk et al, 2012). Therefore, in order to investigate the precocious changes in αsyn-mediated synaptic dysfunction that precedes neuronal death, analyses of the animal model focused on dpi 42 and 84.

3.1.1 Validation of oligomers and PFFs preparation

In the last years, structural biology and biochemistry works helped in the characterization of a large number of αsyn toxic species, that range from small oligomers to large amyloid insoluble fibrils typical of LB inclusions (Bousset et al., 2013b, 2013a; S. W. Chen et al., 2015; Pieri et al., 2016). Recent *in vivo* data on PD model suggests that small species are more prone to induce pathology and start a prion-like progression of the disease (Froula et al., 2019). αsyn PFFs and OLIGO were prepared starting from purified monomeric αsyn, using two already validated protocols. OLIGO were generated by 1h RT incubation of monomeric αsyn, while PFFs aggregation required a 7-day incubation at constant shaking (1000 rpm, 37 °C) (Durante et al., 2019; Polinski et al., 2018). Prior to be inoculated *in vivo*, preparations were always validated to check the successful conversion of the monomeric protein into the desired aggregated species. Specifically, morphology and size of OLIGO (Fig.32a) and PFFs solutions (Fig32b) were analyzed through transmission electron microscopy (TEM), performed at the Unitech NoLimits imaging facility. To note, PFFs preparations usually display an heterogeneous composition due to presence of a wide range of fibrils lengths. Since the amyloid structures contained can be of the order of μM, prior to be used for the *in vivo* inoculations, PFFs solution were subjected to a brief sonication protocol. This step allowed the longest structures to be broken into smaller proto-fibrils of about 50-100 nM in length (Fig.32c), and, therefore, to efficiently originate pathology (Froula et al., 2019).

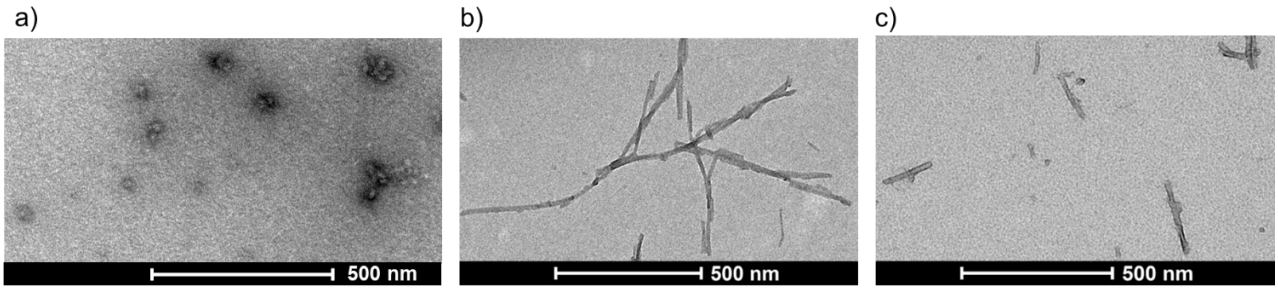

Fig.32. Morphological analysis and validation of aggregated αsyn species (OLIGO and PFFs). Representative images of transmission electron microscopy (TEM) morphological analysis of a) OLIGO, PFFs (b) before the sonication step c) after the sonication protocol. Images were acquired at the Unitech NOLIMITS imaging facility of the University of Milan.

3.2 Biochemical characterization of postsynaptic glutamate receptors and scaffolding proteins at corticostriatal synapses (dpi 42)

Since the discovery of the ability of exogenous αsyn fibrils to mimic a transmissible synucleinopathy *in vivo*, an extensive characterization of αsyn spreading patterns and temporal neuropathology progression in correlation with DA degeneration have been made by several studies (Luk et al., 2012a; Patterson et al., 2019; Stoyka et al., 2020). However, the molecular and postsynaptic mechanisms by which αsyn affects specifically synaptic architecture and activity, finally causing dysfunction to the nigrostriatal and the glutamatergic cortico-striatal circuitry, is still elusive. Therefore, initial analyses performed at dpi 42 were focused on the organization of striatal excitatory post-synaptic compartment. Specifically, brains were dissected to collect the striatum and a subcellular fraction particularly enriched in proteins of the excitatory postsynaptic density (Triton insoluble fraction-TIF) was purified (Gardoni et al 2006). The molecular composition of the postsynaptic compartment in terms of ionotropic glutamate receptor subunits and scaffolding proteins was then evaluated by western blotting on TIF.

Firstly, I measured levels of GluA1, GluA2 and GluA3 subunits of the AMPAR complex. With respect to vehicle injected animals, I found no significant variations in both OLIGO and PFFs mice. Similarly, protein levels of GluN2A, GluN2B and GluN2D of the NMDAR complex were unchanged among striatal TIF fractions from treated and control animals (Fig.33a-b).

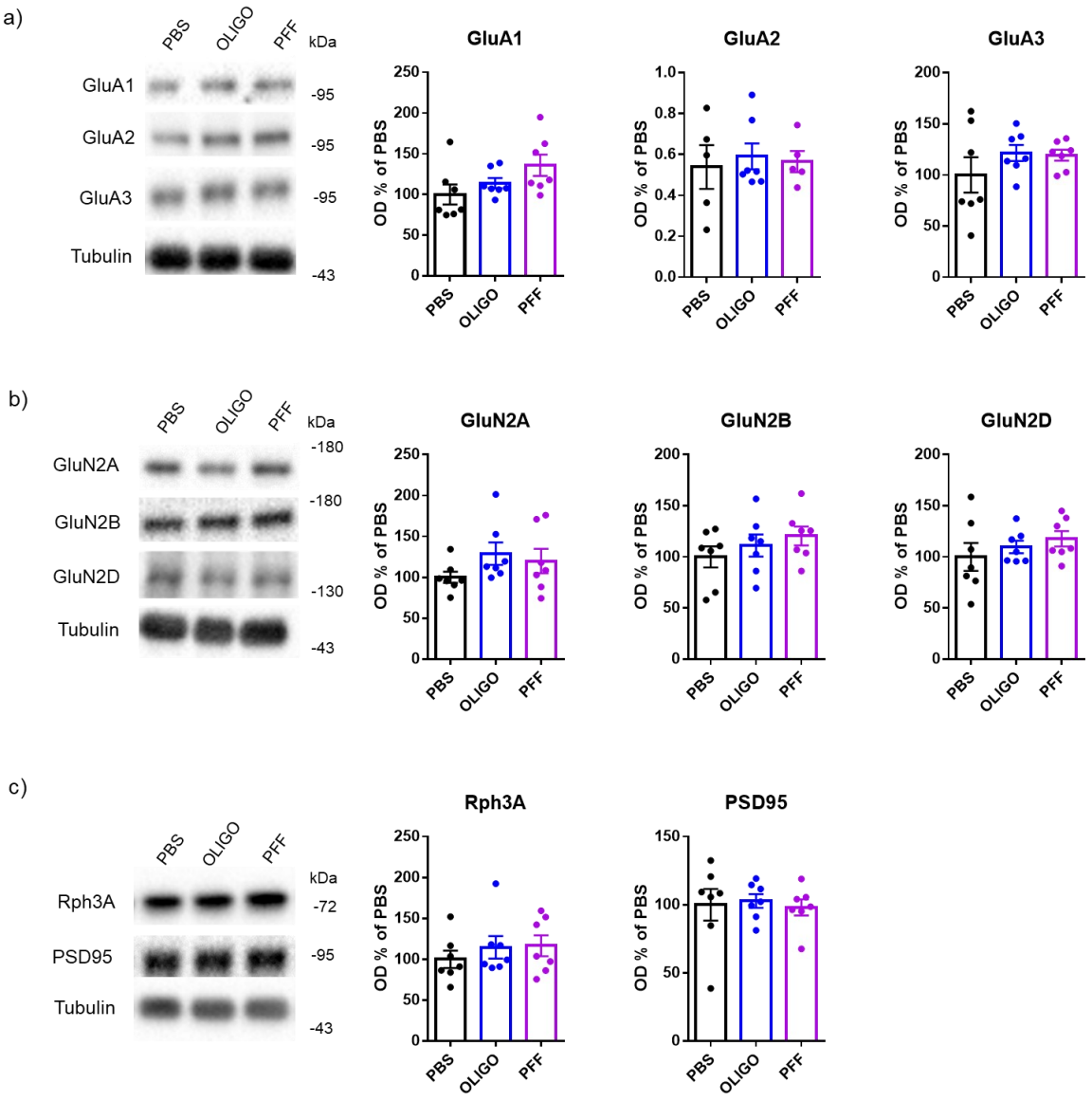

Fig.33. Striatal protein levels on TIF from mice injected with αsyn fibrils (PFF) or oligomers (OLIGO) 42dpi. After homogenization of mice striata and TIF extraction, aliquots of each samples corresponding to 10 µg of TIF proteins were separated by SDS-PAGE and analysed through western blotting (WB). Representative WB images and corresponding semiquantitative graphs of the a) AMPAR (GluA1, GluA2, GluA3), b) NMDAR (GluN2A, GluN2B, GluN2D) subunits and c) scaffolding proteins (Rph3A, PSD95). Protein levels were normalized on tubulin and reported as optical density (OD) % of PBS injected mice. (n=7), unpaired t test vs PBS)

Given the postsynaptic role of Rph3A in synaptic stability of GluN2A-contaning NMDARs (Stanic et al., 2015) and its interplay with αsyn, I next evaluated levels of Rph3A and PSD95, essential scaffolding proteins for a correct postsynaptic architecture. To note, no variations either in Rph3A levels or PSD95 were detected in striata from αsyn OLIGO- and PFF-mice compared to PBS animals, as shown in Fig.33c.

These findings suggest that 42 days after lesion oligomeric and fibrillar αsyn is not yet affecting the molecular structure of the excitatory striatal synapse at the postsynaptic level. Considering these data, the following experimental analyses were conducted only at the second time point considered (dpi 84).

3.3 Characterization of αsyn-mice 84 dpi

Firstly, I assessed if the inoculation of OLIGO and PFFs at this timing already provoked deterioration of dopaminergic (DAergic) striatal fibres, as an sign of neurodegeneration. To this aim, I measured by WB analysis protein levels of the striatal and dopaminergic neuronal marker tyrosine hydroxylase (TH), enzyme catalyzing the rate limiting step in the catecholamine synthesis. As expected, no significant decrease of the protein was found in striatal homogenate in PFFs- and OLIGO-mice with respect to controls, indicating a preserved integrity of the overall DAergic fibres (Fig.34).

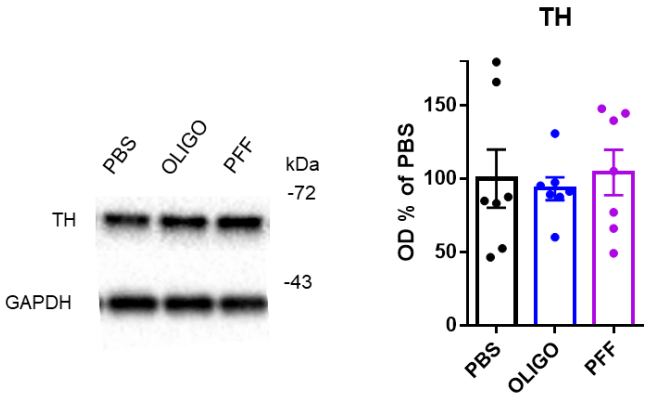

Fig.34 – Striatal tyrosine hydroxylase levels in homogenate fraction of mice injected with αsyn PFF or OLIGO 84 dpi. Representative WB images and respective semiquantitative graphs of and TH reporting protein levels normalized on GAPDH and reported as OD % of PBS-injected mice (n=7).

3.3.1 Biochemical characterization of postsynaptic glutamate receptors and scaffolding proteins at corticostriatal synapses (dpi 84)

In contrast to the findings of the earliest time point, dpi 84 OLIGO- and PFF-mice displayed a profound alteration of the postsynaptic composition of the glutamatergic synapse. Specifically, animals are characterized by a significant reduction of the AMPAR subunit GluA1 upon both OLIGO and PFFs lesion compared to controls. This finding is accompanied by a slight trend in decrease, though not significant, of the AMPAR subunits GluA2, GluA3 and of the serine 845-phosphorylated GluA1 subunit, as shown by Fig. 35a.

Moreover, according to the above-mentioned recent literature findings (Durante et al., 2019; Tozzi et al., 2021, 2016), pathologic αsyn targets the NMDAR complex as well. In particular, PFF- and OLIGO-treated mice show diminished protein levels of postsynaptic GluN2A and GluN2D subunits with respect to controls (Fig. 35b). Although not statistically significant, the GluN2B subunit shows a trend in decrease upon treatment, supporting that these mice have an overall impairment of NMDAR type of glutamate receptors.

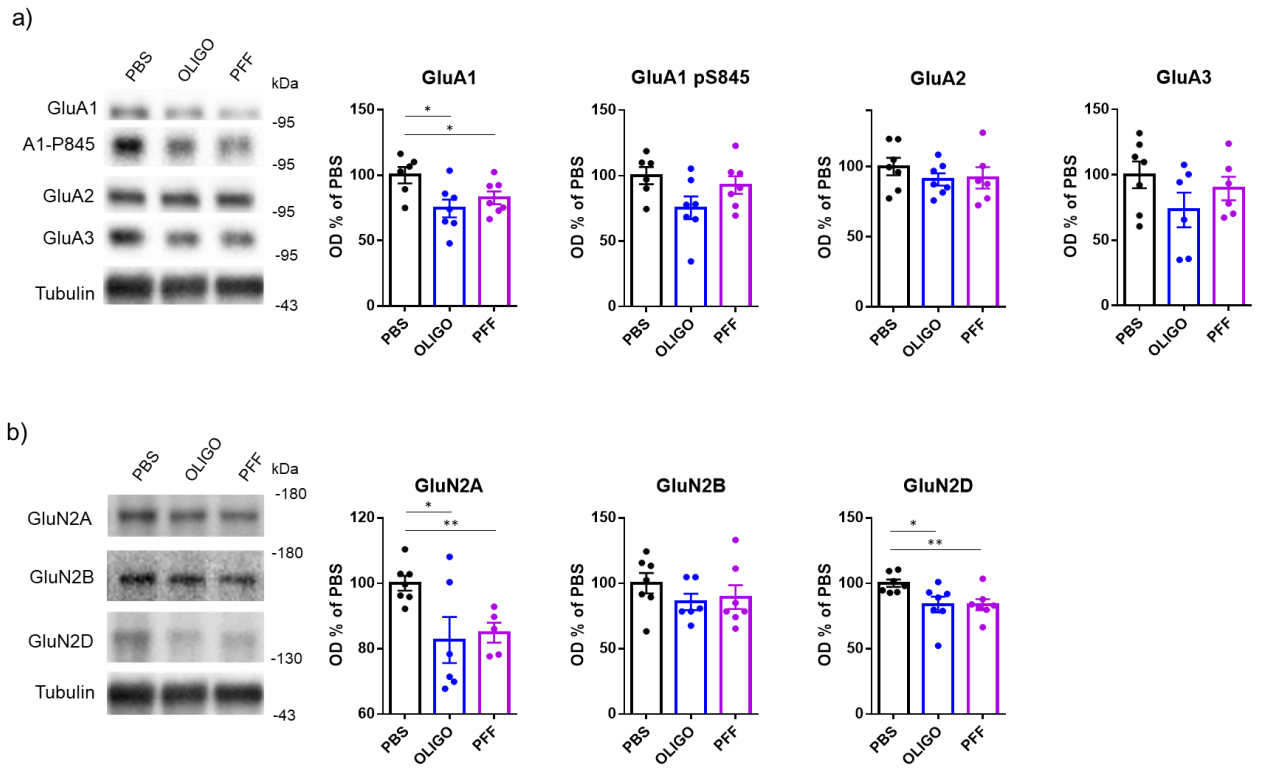

Fig.35. Striatal protein levels on TIF from mice injected with αsyn fibrils (PFF) or oligomers (OLIGO) 84 days after lesion. Representative WB images and corresponding semiquantitative graphs of the a) AMPAR (GluA1, GluA1 pSER845, GluA2, GluA3) and b) NMDAR (GluN2A, GluN2B, GluN2D) subunits reporting protein levels normalized on tubulin and reported as optical density (OD) % of PBS injected mice. (n=7), unpaired t test vs PBS; *p<0.05, **p<0.005)

Interestingly, this significant molecular alteration of the cortico-striatal glutamatergic synapse is in accordance with a very recent work that our laboratory contributed to publish. The group of Prof. Calabresi demonstrated the presence at the same timing of significant electrophysiological alterations in a similar PFFs-based rat model. The described striatal LTP blockade and LTD reduction could be partially interconnected with the molecular modifications found in our murine model (Tozzi et al., 2021).

3.3.2 αsyn impact on striatal spine morphology (dpi 84)

Since αsyn-mice show significant molecular (see above) and functional (Tozzi et al., 2021) impairments of the glutamatergic synapse, I further investigated the impact of αsyn OLIGO and PFF on dendritic spines density of striatal spiny projection neurons (SPNs). Spine morphology analysis (reported in Fig.36a) revealed that PFFs injection significantly affected striatal spine density, causing a 25% reduction with respect to controls.

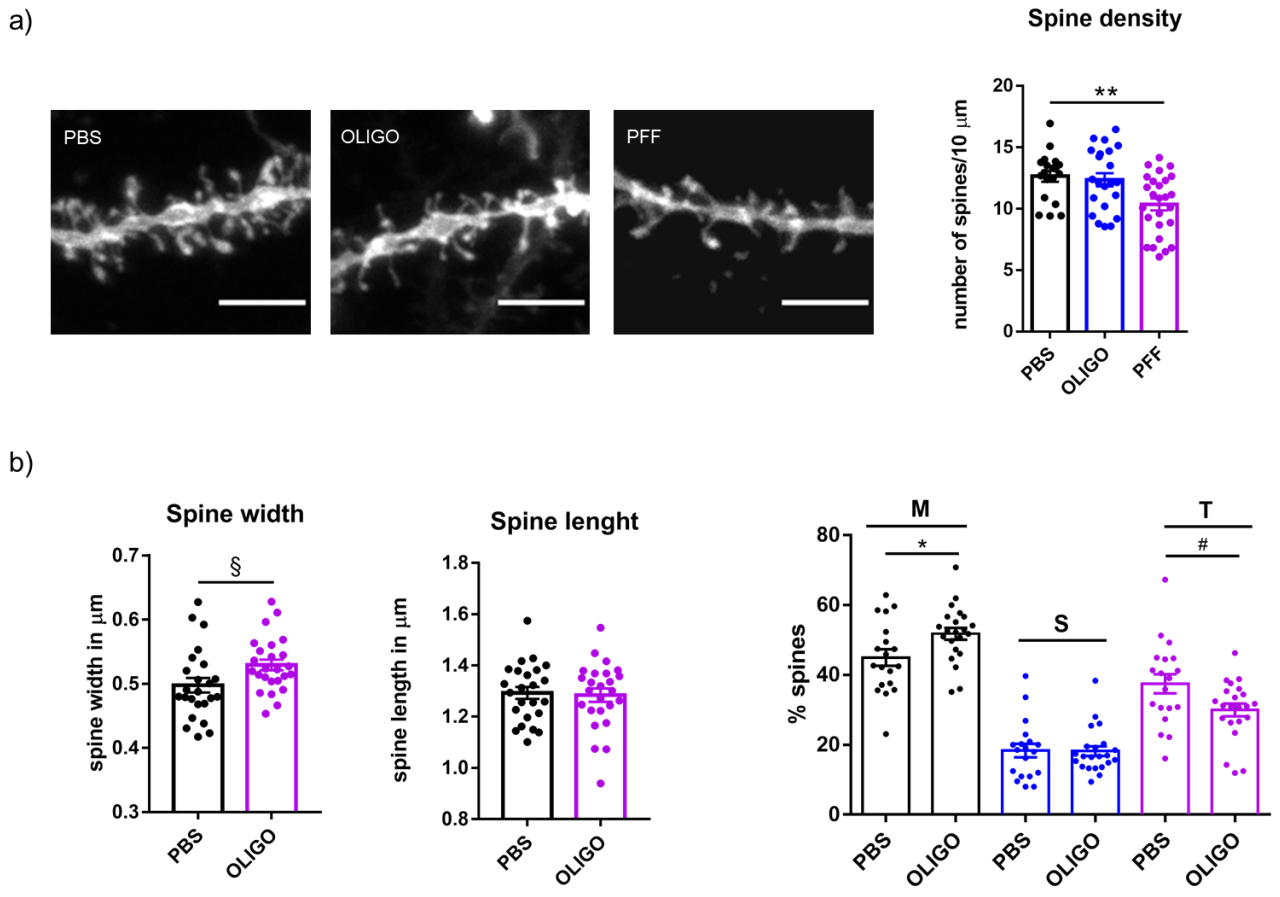

Fig.36. a) Representative confocal images and quantification of spine density of striatal neurons dyed with DiI of PBS, OLIGO and PFF-injected mice and b) spine morphology analysis of OLIGO and PBS-injected mice.
(M=mushroom spines, S=stubby spines, T=thin spines)
Statistical analysis: n=19 (number of neurons, from 3 mice), unpaired t test, **p=0.0017 PBS vs PFF; *p=0.0221 PBS vs OLIGO; #p=0.025 PBS vs OLIGO, §=0.0289 PBS vs OLIGO. Scale bar: 5 µm

OLIGO-mice, instead, did not show a reduction of striatal spine number, but displayed an overall increase in the spine width in presence of a normal spine length (Fig.36b, left). Furthermore, in line with these data, in OLIGO-treated animals the percentage of mushroom-shaped (M) spines, representing stable and mature spines, is significantly increased compared to the control condition. Notably, this event is accompanied by a concomitant decrease of thin (T) spines, more plastic and

immature (Fig.36b-right). Overall, these morphological data could underlie a different type and extent of synaptic toxicity induced by the two diverse αsyn toxic species.

Taking into account that morphological alterations were also accompanied by a modified postsynaptic abundance of ionotropic glutamate receptors, I then evaluated possible downstream signalling defects. Synaptic NMDARs activity, indeed, promote nuclear signalling to cAMP responsive element binding protein (CREB), regulating gene expression of pro-survival factors and anti-apoptotic pathways together with activity of the extracellular signal regulated kinases (ERK) (Hardingham and Bading, 2010). Therefore, I assessed levels of phosphorylated form of ERK (pERK) and CREB (pCREB) by western blot analysis in the striatal homogenate, as shown in Fig.37. Interestingly, no differences in the pCREB/CREB and pERK/ERK ratio were observed comparing PFF and PBS mice. Conversely, upon OLIGO seeding, levels of pERK are significantly diminished with respect to PBS, in absence of CREB phosphorylation changes.

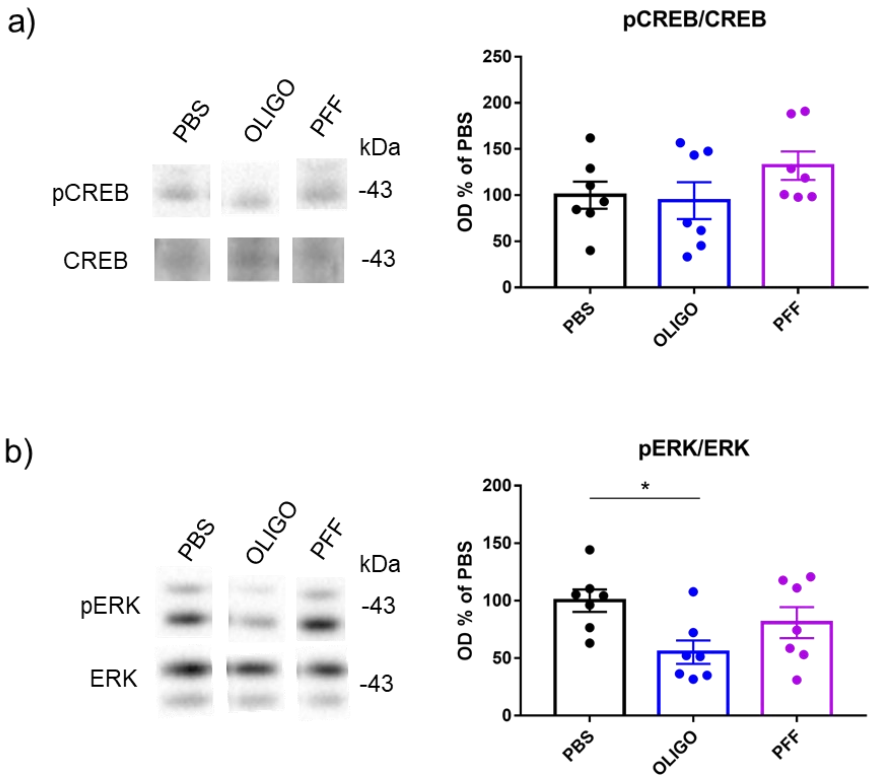

Fig.37. Protein levels of phosphorylated form of ERK (pERK) and CREB (pCREB) in striatal homogenate fraction of mice injected with OLIGO and PFFs 84 dpi. Representative WB images and respective semiquantitative graphs of a) pCREB and CREB and b) pERK, ERK. Levels of pCREB and pERK were normalized, respectively, on CREB and ERK levels and expressed as OD % of PBS in the semi-quantitative bar graph (n=7, Mann-Whitney test *p=0.0175 PBS vs OLIGO).

To summarize, at dpi 84 PFFs cause both a reduction in NMDAR and AMPAR expression and a decrease in spine density. OLIGO, instead, did not decrease spine density but the amount of receptor complexes at the spines, possibly affecting signalling pathways related to ERK activity. Moreover, the increase in spine width and mushroom spines percentage could represent an early compensatory mechanism to overcome the cortico-striatal signalling defects induced by αsyn.

3.3.3 αsyn effects on striatal Rph3A expression 84 dpi

Similarly to analyses conducted on mice 42 dpi, I next assessed striatal Rph3A levels by western blotting on both homogenate fraction (total neuronal level) and TIF. Rph3A levels in the homogenate fraction were found comparable between lesioned and control mice, indicating absence of an αsyn-mediated impact on the overall Rph3A expression (Fig.7a). On the contrary, WB analysis conducted on striatal TIF revealed a significant Rph3A decrease in PFF-mice and a tendency of decrease in OLIGO-injected, although not statistically significant (Fig.7b). These findings indicate a selective toxicity of PFFs towards Rph3A localized at the post-synaptic compartment, effect that was still not apparent at 42 dpi (see Fig.33). To note, levels of PSD95 were not changed even 84 dpi.

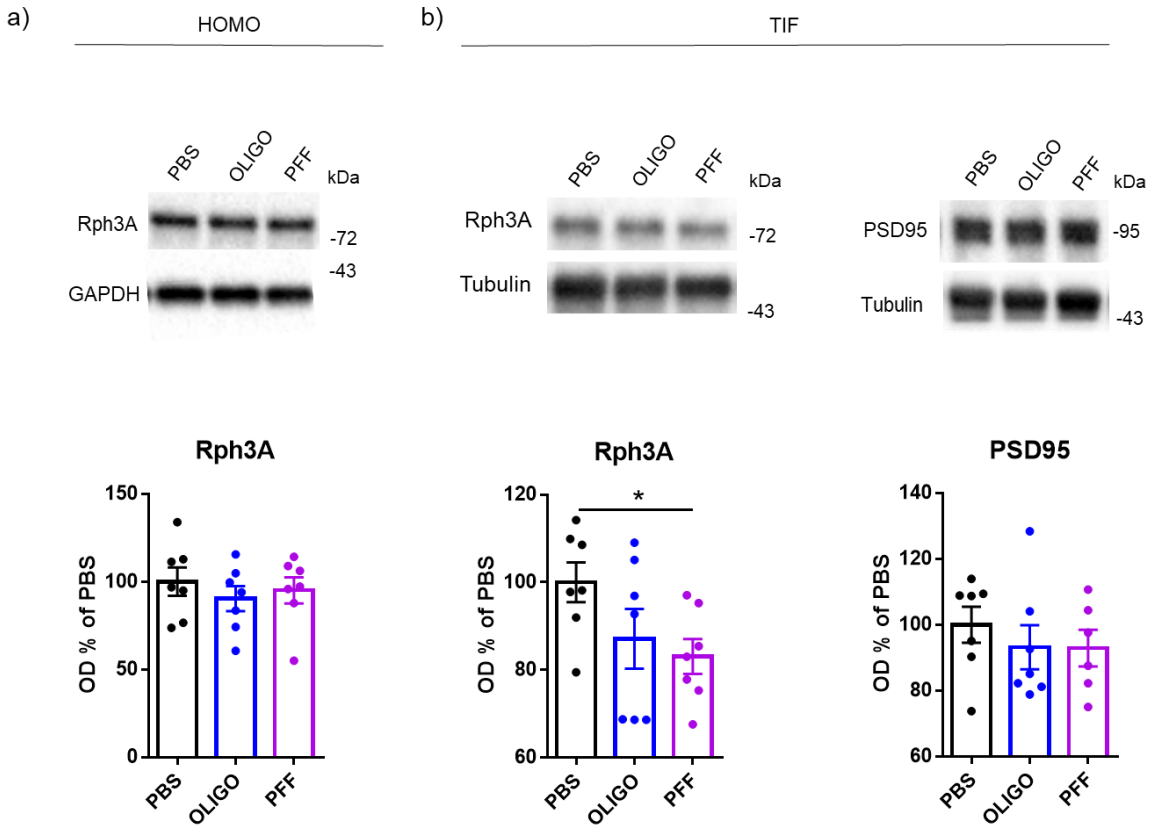

Fig.38. *In vivo* effects of PFF and OLIGO on Rph3A striatal expression and PSD95 expression (84 dpi). Representative WB images and respective semiquantitative graphs of Rph3A evaluated on a) total

stratal homogenate and b) Rph3A and PSD95 evaluated on TIF. Protein levels were normalized on Tubulin as a loading control and then expressed as OD% of PBS in the bar graph. Statistical anlysis: n=7, *p<0.05, PBS vs PFF

Since at the postsynaptic compartment Rph3A has a fundamental role in stabilization and membrane retention of GluN2A-containing NMDARs (Franchini et al., 2019; Stanic et al., 2015), I next assessed its binding to the GluN2A subunit by co-immunoprecipitation experiments, shown in Fig.9. Rph3A was immunoprecipitated from striatal homogenate, levels of GluN2A were assessed by WB analyses and normalized on the amount of Rph3A immunoprecipitated. Interestingly, not only Rph3A is less expressed at the post synaptic compartment, but also its interaction with GluN2A subunit is decreased upon PFF-injection. Similarly to results of Rph3A TIF expression, a statistically not significant tendency of diminished Rph3A/N2A binding in OLIGO-injected mice was found, suggesting either a milder impact of OLIGO with respect to PFFs or a different mechanism of toxicity.

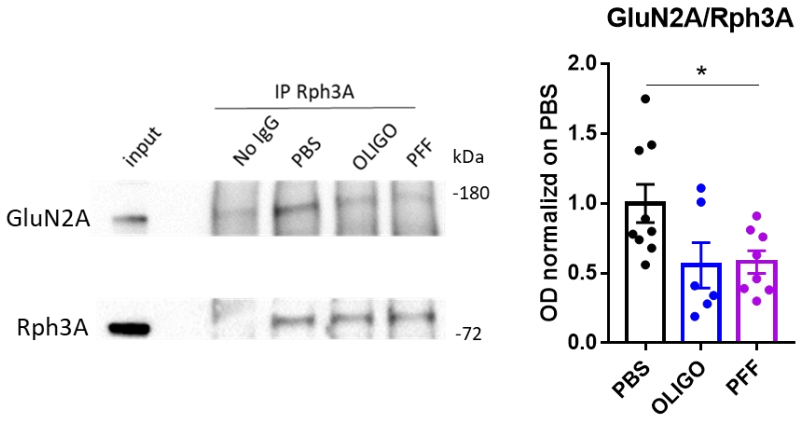

Fig.39. Co-IP analysis of Rph3A and GluN2A subunit in striatal homogenate fraction of PBS, OLIGO or PFF-injected mice 84 dpi. Rph3A was immunoprecipitated from homogenate samples corresponding to 150 µg of protein and levels of GluN2A were evaluated by WB analysis on Rph3A immunoprecipitated (IP). 15 µg of homogenate (corresponding to the 10% of the amount used for co-IP analysis) were loaded as input control. GluN2A band was normalized on the corresponding Rph3A band and expressed as OD% of PBS in the semi-quantitative bar graph. (n=6, unpaired Mann-Whitney test: PBS vs OLIGO ns, p=0,07; * PBS vs PFF p=0.04)

To summarize, data collected on the αsyn *in vivo* model put forward a possible role of Rph3A in mediating αsyn synaptic toxicity. Given the already demonstrated interplay between the two proteins and their link with NMDAR functions, PFFs could directly promote mechanisms able to sequester Rph3A from its physiological synaptic activities.

4. Rph3A modulation in a chronic αsyn PFFs *in vitro* model

On the whole, data collected from the αsyn PFFs *in vivo* model suggest Rph3A as a possible mediator of αsyn-mediated synaptic toxicity in the striatum. Its role as a promising target in synaptopathies is strengthened by its already described involvement in neurodegeneration, movement disorders and its emerging role in synaptic plasticity (Franchini et al., 2019; Smith et al., 2007; Stanic et al., 2017; Tan et al., 2014). Moreover, a large proteomic study associated Rph3A with cognitive resilience in AD patients (Yu et al., 2020).

Based on these considerations, I evaluated the modulation of Rph3A expression levels and Rph3A/αsyn complex as an intriguing approach to ameliorate early synaptic defects induced by αsyn. Specifically, two different strategies were investigated:

a) reducing αsyn/Rph3A interaction by exploiting the Rph3A/αsyn uncoupling compound selected through the bioinformatic screening (see Results - section 2);
b) Rph3A overexpression.

First of all, the two modulation strategies were tested in an *in vitro* setting, to assess their efficacy and possible toxicity.

4.1 Validation an αsyn-induced spine pathology model

I exploited a recently validated *in vitro* neuronal model of αsyn-induced spine pathology, described in a work by Wu and coworkers, with some modifications (Wu et al., 2019). In particular, since mono cultures of primary striatal neurons develop a non-physiologically low number of dendritic spines, primary rat hippocampal neurons were used (Ferrari et al., 2020). Indeed, hippocampal cultures represent a widely validated model to study spine morphology and dynamics *in vitro* (Dailey and Smith, 1996). Hippocampal neurons were chronically treated with αsyn PFFs for 7 days (Wu et al., 2019). In details, 2 different doses of PFFs (1 and 2 μg/ml) were tested by direct treatment in the culture medium at *DIV9*. In order to visualize dendritic spines, cells were transfected at *DIV7* with Green fluorescent protein (GFP). Coherently with the *in vivo* model, control neurons were treated with PBS, the vehicle of PFFs preparation. As already observed in literature (Wu et al., 2019), spine morphology analysis performed at *DIV15* revealed a dose dependent reduction of dendritic spine density (Fig.40a).

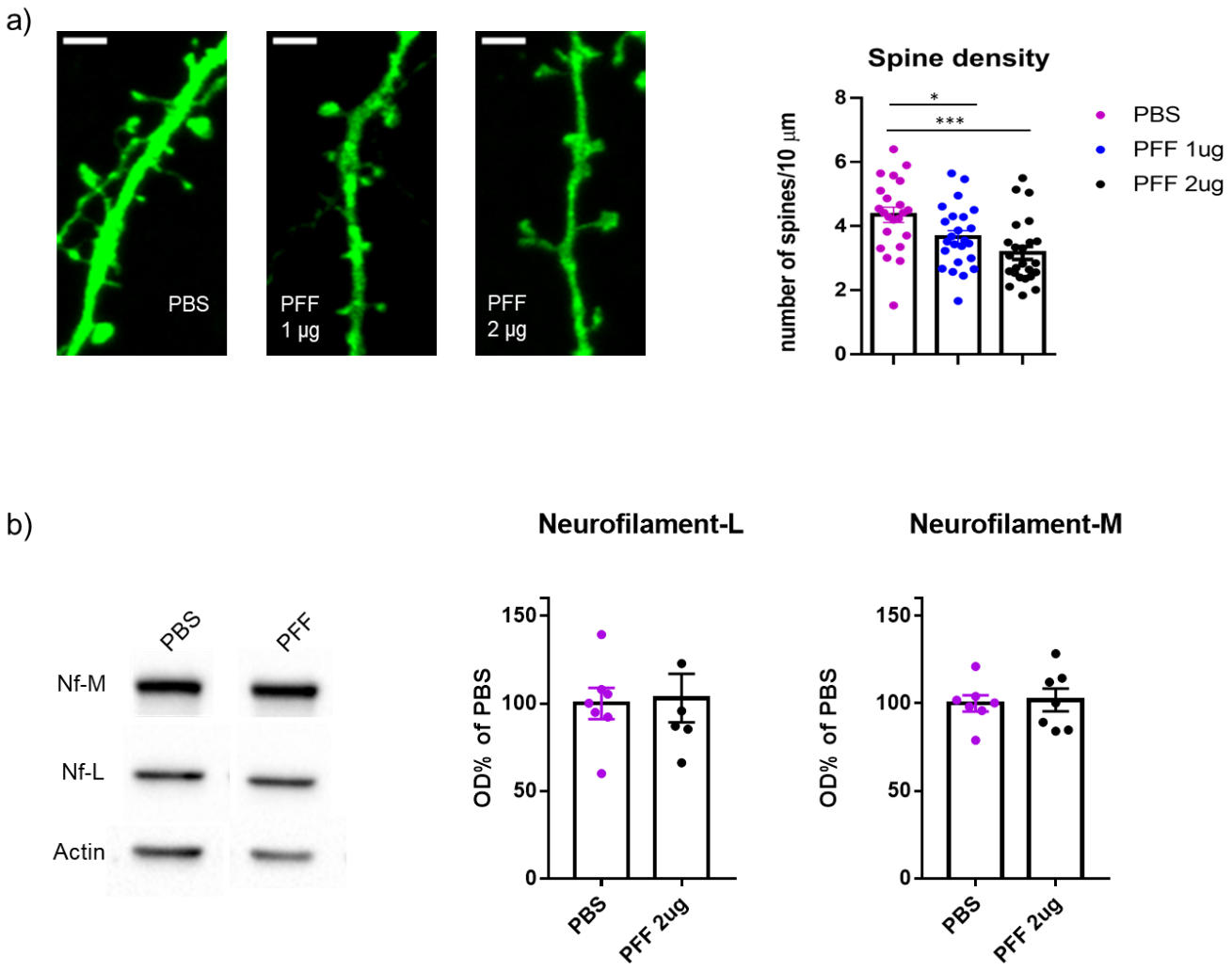

Fig.40. a) Representative confocal images and quantification of spine density of hippocampal primary neurons transfected with GFP (green) upon 7-day treatment with 1, 2 µg PFF or PBS. Statistical analysis: n (number of neurons)=24, Mann-Whitney test, *p=0.0256, PBS vs PFF 1µg; **p=0.0005. Scale bar: 2 µm
b) Protein levels of the main axonal cytoskeletal components Neurofilament-L (Nf-L) and Neurofilament-M (Nf-M) in hippocampal primary neurons transfected with GFP (green) upon 7-day treatment with 1, 2 µg PFFs or PBS. Representative WB images and respective semiquantitative graphs of Neurofilament-L and Neurofilament-M protein levels normalized on Actin and reported as OD % of PBS-treated neurons.

Importantly, concentrations of PFFs in the range of 1-2 µg/ml were described not to affect negatively viability of hippocampal neurons 7 days after seeding; indeed, neuronal death started to appear upon 11-day treatment (Wu et al., 2019). Duration of PFFs treatment, absence of dramatic neurodegeneration and timing of the rescue approaches are indeed crucial aspects of the experimental model in order to allow an early intervention. To note, no decrease in the number of viable neurons was confirmed at *DIV15* (data not shown) in presence of both PFFs doses. As a further control, I subsequently checked if the 7-day treatment with 2 µg of αsyn was able to provoke significant axonal damage. To this purpose, levels of the cytoskeletal proteins Neurofilament-L and M, neuronal specific intermediate filament proteins, were evaluated by western blotting (A. Yuan et al., 2017). As shown

in figure 1b, Neurofilament-L and M, were not altered with respect to PBS condition, suggesting a preserved integrity of axonal compartment. Therefore, the highest PFFs concentration (2 μg/ml) was chosen to perform the following experiments focused on the evaluation of rescue strategies of αsyn-induced synaptic loss.

4.2 *In vitro* modulation of Rph3A interaction and expression

4.2.1 Effects of Rph3A/αsyn uncoupling compound

As a first Rph3A modulatory strategy I assessed the effects of the Rph3A/αsyn uncoupling molecule (compound B) in the chronic PFFs *in vitro* model.

Compound B, the molecule selected with the *in silico* bioinformatic screening (described in section 2 of Results), is predicted to bind the α-helical region in C2B domain of Rph3A and to significantly reduce its binding to αsyn. Due to steric hindrance, the molecule is expected to decrease the amount of Rph3A bound to pathologic αsyn and thus enhance the synaptic availability of the protein.

In details, PFFs seeding started at *DIV9* and the molecule was administered at *DIV12*, concomitant to the beginning of αsyn neuropathology propagation (Wu et al., 2019). Based on pharmacokinetics analyses and *ex-vivo* assays (see Results section 2), a single administration of the compound into the culture medium was used. I firstly evaluated if a 4-day treatment with 10 μm of compound B was able to modify spine density *per se,* regardless of PFFs chronic challenge. Spine density of compound-treated neurons was not significantly different from the one of vehicle-treated neurons, as shown in Fig.41a. Vehicle-treated PBS-neurons and vehicle or compound- treated PFF-neurons were subjected to spine density analyses afterwards. Notably, as shown by Fig.41b, compound B administration fully prevented spine loss found in PFF-neurons.

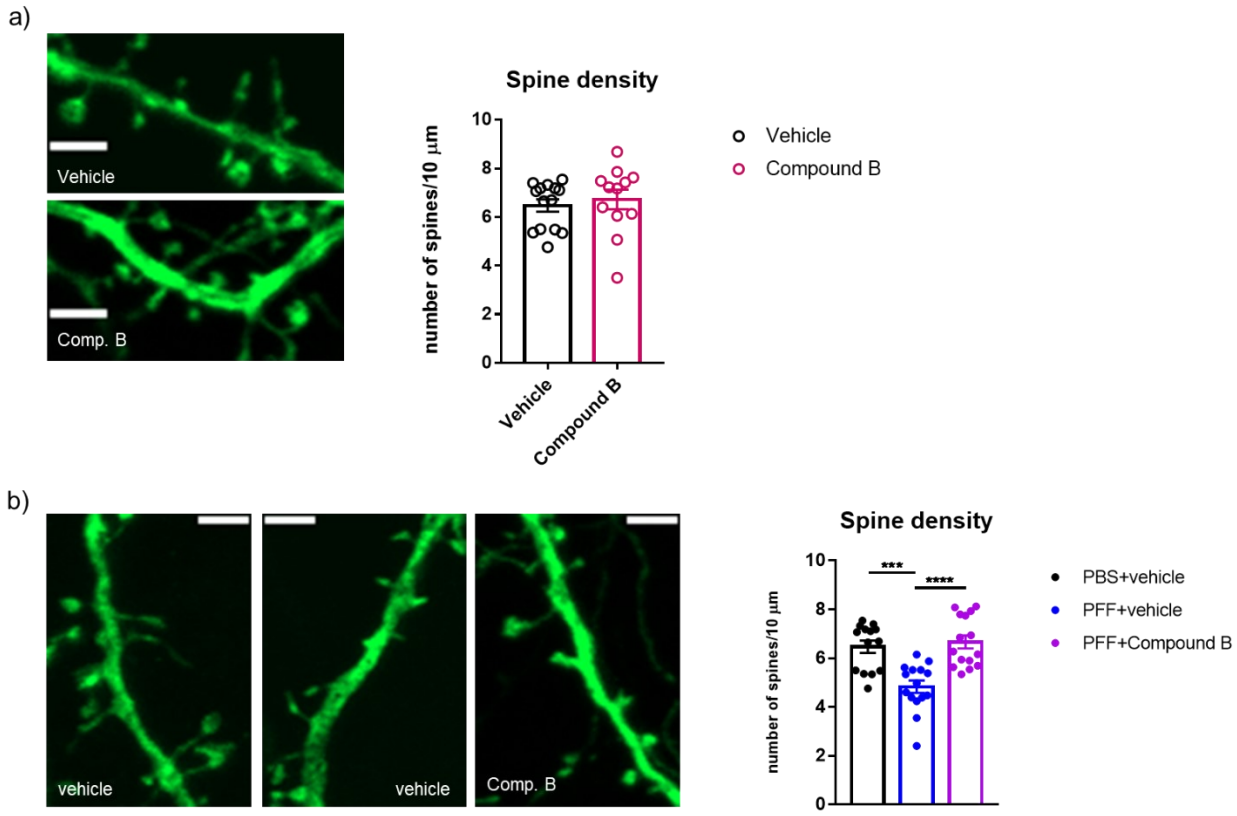

Fig.41. a) Representative confocal images and quantification of spine density of hippocampal primary neurons transfected with GFP (green) and treated with 10 µm compound B (or vehicle) for 4 days. Scale bar: 2µm. Statistical analysis: n (number of neurons)=12, ns, unpaired t-test
b) Representative confocal images and quantification of spine density of hippocampal primary neurons transfected with GFP (green) upon 7-day PFF (or PBS) treatment and co-administration of Rph3A/αsyn uncoupling compound (Compound B) (or vehicle) for the last 4 days. Scale bar: 2µm. Statistical analysis: n=14, one-way ANOVA- Tukey multiple comparison test, ***p=0.0002 PBS+vehicle vs. PFF+vehicle; ****p<0.0001 PFF+vehicle vs PFF+Comp. B

4.2.2 Effects of Rph3A overexpression

As alternative strategy, neurons were treated with αsyn PFFs at *DIV8* and co-transfected at *DIV10* with GFP (to follow dendritic spines) and a plasmid expressing the protein Rph3A fluorescently tagged with a red fluorescent protein (RFP-Rph3A). In this way, full neuronal expression of RFP-Rph3A was achieved at the comparable timing of the compound B administration. As control condition, PBS- and PFF-neurons were co-transfected with the control fluorescent protein TdTomato. Then, spine morphology analyses were conducted at *DIV15*.

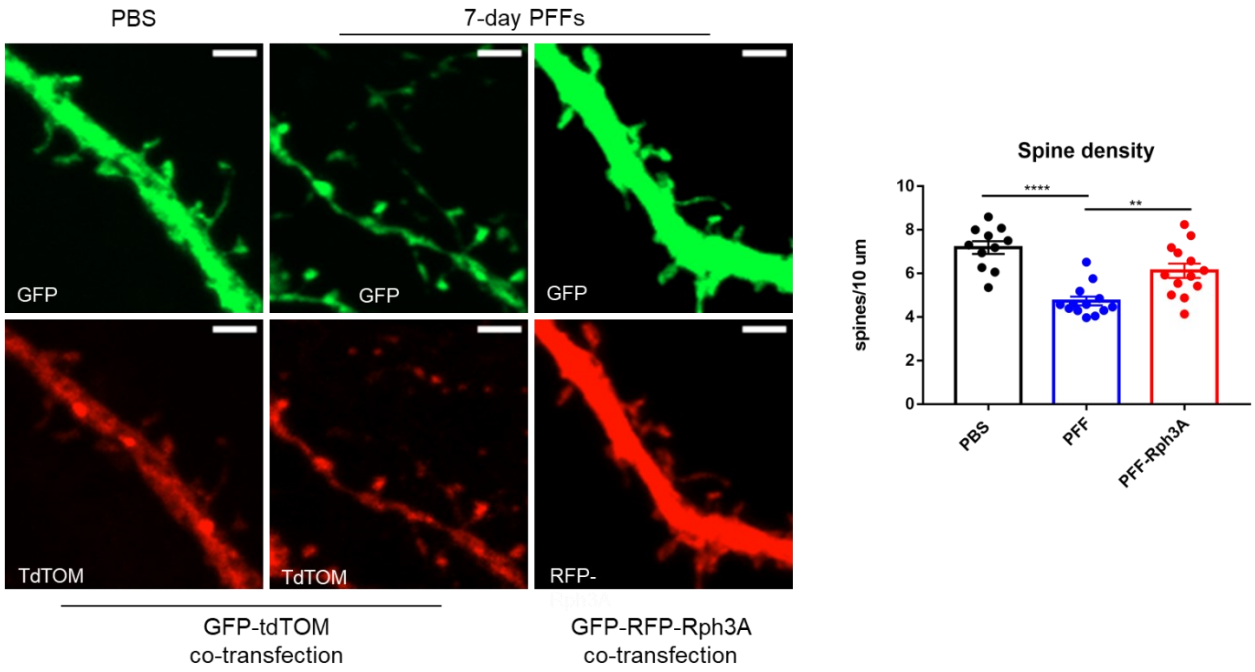

Fig.42. Representative confocal images and quantification of spine density of hippocampal primary neurons upon 7-day PFF (or PBS) treatment and overexpression of RFP-Rph3A (red) or the control red fluorescent protein tdTomato. Hippocampal neurons were treated at DIV8 with PFF 2µg (or PBS) and co-transfected at DIV10 with RFP-Rph3A or tdTomato (TdTOM) and GFP to visualize dendritic spines. Scale bar: 2 µm. Statistical analysis: n=11, one-way ANOVA Tukey multiple comparison test ****p<0.0001 PBS vs PFF; **p=0.0026 PFF vs PFF-Rph3A

Similar to results obtained with the compound B administration, overexpression of RFP-Rph3A resulted successful in preventing spine loss found in neurons treated with PFF and transfected with the control protein tdTomato, as shown by spine density analysis in Fig.42. Interestingly, both approaches revealed to be effective in counteracting the αsyn-induced toxicity towards dendritic spines.

5. *In vivo* strategies to rescue αsyn-induced synaptic toxicity

Both Rph3A modulatory approaches, i.d. Rph3A overexpression and Rph3A/αsyn uncoupling, revealed to be efficacious in blocking αsyn-induced synapse loss *in vitro*. Therefore, I moved to to evaluate the same rescue strategies *in vivo,* exploiting the already characterized αsyn PFF-mouse model. As described above (see Results 3.3.2), the *in vivo* striatal injection of PFF caused stronger consequences with respect to oligomers inoculation, namely a decrease of the density of SPN dendritic spines; therefore, in line with *in vitro* experimental groups, animals were injected with PFFs or PBS.

5.1 *In vivo* assessment of Rph3A/αsyn uncoupling compound

As described above, no toxicity of Compound B has been observed in the *in vitro* experiments at a dose of 10 µm and *in silico* predictions revealed a favourable ADME profile. However, intrinsic physico-chemical properties of the molecule prevent its crossing of the blood-brain barrier. Consequently, the molecule is not suitable for a systemic type of delivery. Accordingly, to reach its chronic availability in the central nervous system, animals were implanted with a guide cannula targeted to the lateral ventricle. As shown in Fig.43, mice were firstly bilaterally injected with PFFs or PBS in the dorsal striatum (see: section 3 of Results) and 65 dpi animals underwent surgery for cannula implant. Compound B has been administered for two weeks every 3 days (5 injections), starting at dpi 70, at a concentration of 1mM. This molarity allowed to reach an estimated concentration of about 85 µM in the cerebrospinal fluid (CSF), considering a total CSF volume of ~35µl in the mice (Rudick et al., 1982). Control PBS and PFF mice were treated with the vehicle of the uncoupling compound; all animals were then sacrificed 24h after the last administration.

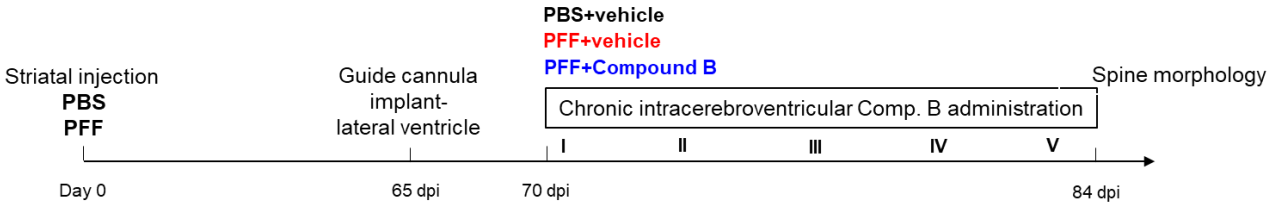

Fig.43. Experimental scheme of the *in vivo* administration of Compound B on the PFF-mouse model.

5.1.2 Effects of Compound B on αsyn-induced spine loss

Compound B revealed to be efficacious in preventing spine loss induced by chronic exposure to PFFs in an *in vitro* neuronal primary model (see Results – Section 4). Therefore, as a first outcome of the effect of the molecule in an *in vivo* setting, I performed spine morphology analysis on the 3

experimental groups of mice: PBS- and PFF-animals receiving the vehicle (PBS+vehicle and PFF+vehicle, respectively) and PFF-animals receiving the compound (PFF+compound B). Spine morphology analysis confirmed PFFs effects on striatal spine density (see Results, section 4, Fig.41). In particular, PFF+vehicle animals displayed a decrease of about 25% in striatal spine number with respect to the PBS+vehicle condition. To note, *in vivo* administration of compound B fully prevented spine loss compared with PFF+vehicle mice (Fig.44).

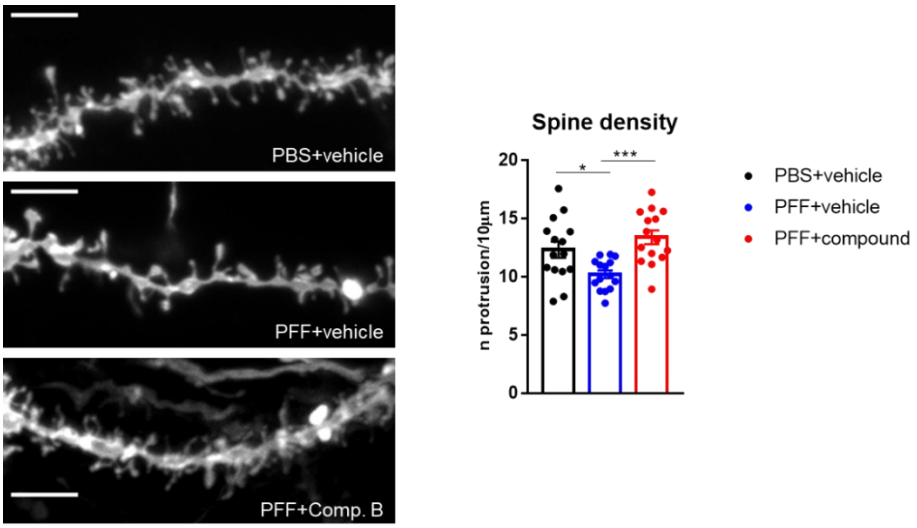

Fig.44. Representative confocal images and quantification of spine density analysis of striatal neurons dyed with DiI of PFF-mice 2-week treated with compound B (or vehicle) and PBS-mice treated with the vehicle.
Scale bar: 5µm. Statistical analyses: n=15 (number of neurons, from 2 mice), *p<0,05, ***p<0,0005, One-way ANOVA Tukey's multiple comparison test)

These promising findings seemed to confirm the efficacy of the molecule in counteracting also *in vivo* the deleterious effect of αsyn-pathology. Furthermore, they corroborate the hypothesis of an involvement of Rph3A/αsyn interaction in the establishment of PD synaptopathy. On the other hand, the physico-chemical structure of the molecule (and the consequent impossible systemic delivery) make this compound a hardly druggable molecule. Therefore, Compound B can be considered a lead compound to be optimized by means of a bioinformatic and chemical improvement of its structure, to go further with the *in vivo* assessment of the efficacy of the Rph3A/αsyn uncoupling strategy.

5.2 In vivo Rph3A striatal overexpression

Rph3A overexpression was achieved by stereotaxic injection in the dorsal striatum, the same site of αsyn seeding, of an adeno-associated viral (AAV) vector expressing RFP-Rph3A. As control of the overexpression experiment, an AAV expressing the control fluorescent protein RFP was used. As schematically represented in Fig.45, animals were firstly injected with αsyn and at 35dpi either with

the AAV-Rph3A (PFF-Rph3A) or the AAV-RFP (PFF-RFP). PBS animals, instead, were injected only with the AAV-RFP vector (PBS-RFP). This timing allowed to reach the peak expression of the protein during progression of early disease stages, thus before the onset of dramatic αsyn toxicity. Most importantly, a sustained striatal expression of the protein would be achieved at the time point of the in vivo evaluation at dpi 70-84. In addition, the striatal delivery of the plasmid allowed to investigate specifically a postsynaptic intervention within the PD pathological nigrostriatal circuitry.

Fig.45. Experimental scheme of the *in vivo* striatal overexpression of RFP-Rph3A on the PFF-mouse model.

5.1.2 Effects on αsyn-induced motor impairments

Studies on experimental rodent models based on transmissible αsyn indicate that PFF-injected animals begin to show motor and behavioral impairments between 3 and 6 months after lesions (Durante et al., 2019; Luk et al., 2012a; Patterson et al., 2019; Tozzi et al., 2021). Among published literature works, discrepancies in entity and type of behavioral alterations can be found, mainly ascribable to differences in the animal model adopted, strain of pathologic αsyn and the presence of a bilateral or unilateral lesion.

Firstly, mice were subjected to the open field test to evaluate the general locomotor ability and assess the presence of possible anxiety-like behavior. Specifically, during the task mice locomotor activity was monitored for a duration of 10 minutes. As shown in Fig.46a, no statistically significant alterations were found comparing PBS-RFP, PFF-RFP and PFF-Rph3A mice in the distance travelled measured in the first and second 5-minute intervals of the task. Comparing the time spent by the animals at the center (Fig.46b) and at the corners (Fig.46c) of the arena, the differences were not statistically significant. These data indicate that at the time point considered, PFF-lesion did not cause an impairment of the general locomotor ability, as already reported in literature (Luk et al., 2012a; Tozzi et al., 2021). Moreover, the treatment seemed not affect the spontaneous explorative and anxiety like behavior of the animals.

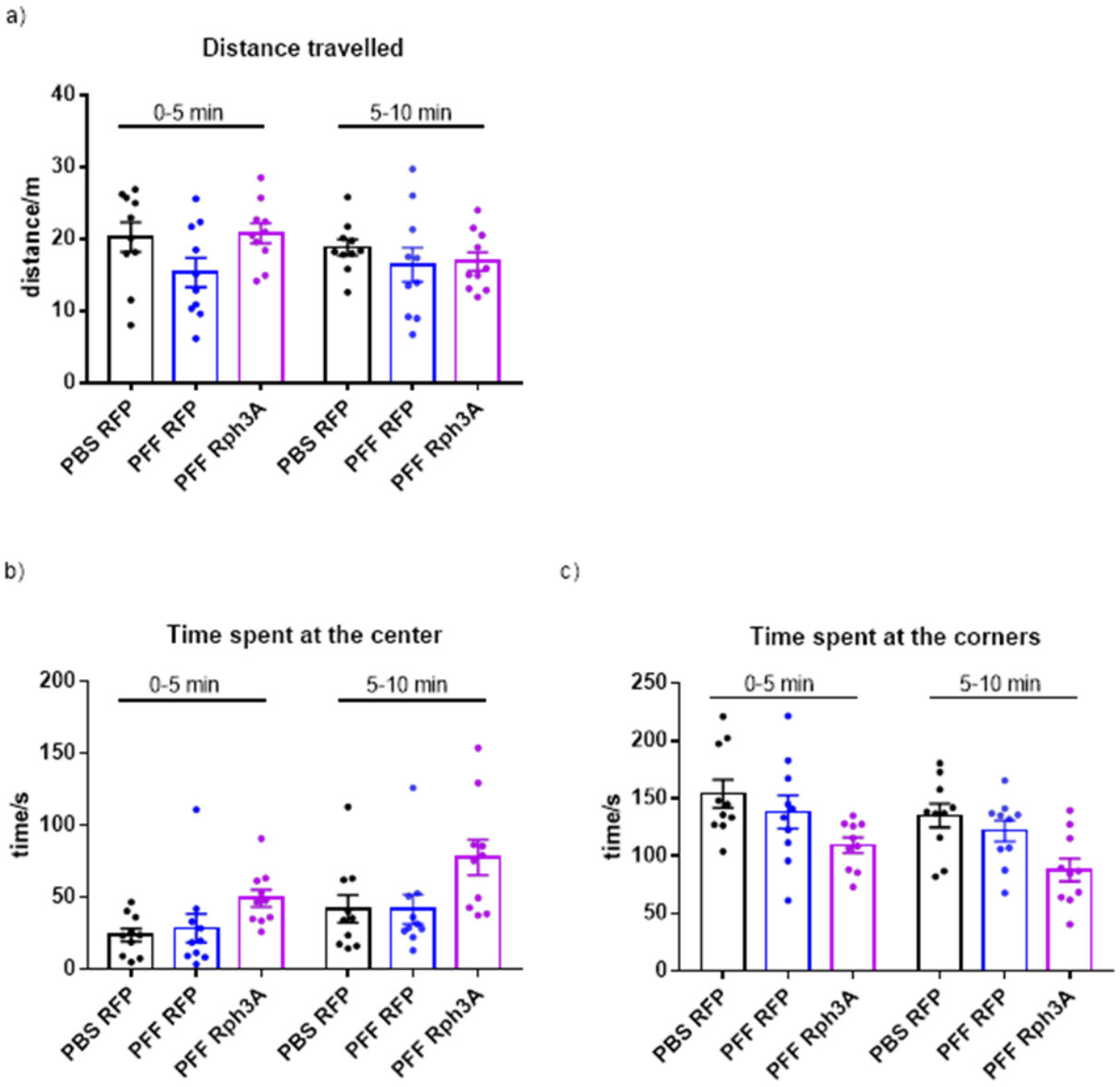

Fig.46. Analyses of the open field test of PBS and PFF mice upon striatal delivery of RFP-Rph3A (or a control RFP protein). Histogram of a) distance travelled b)time spent at the centre and c) time spent at the corners of the arena of PBS-RFP, PFF-RFP and PFF-Rph3A mice, showing no significant differences. (n=10, One-way ANOVA- Tukey's multiple comparisons)

To further evaluate possible motor and coordination impairments in a more targeted way, I performed Rotarod and Grip strength test on the same experimental conditions. In particular, mice were subjected between 75 and 84 dpi to accelerated rotarod (20-40 rpm; 300s), constant speed rotarod (30 rpm) and forelimb grip strength test. These motor behavior tests confirmed a decline in the motor coordination performances, particularly evident in the accelerated rotarod, of PFF-RFP mice with respect with PBS-RFP. To note, upon striatal delivery of AAV-RFP-Rph3A, latency to fall from the rod of PFF-Rph3A mice was comparable to the one of PBS-mice. A statistically significant decrease in forelimb muscle force of αsyn mice with respect to PBS was measured by the grip strength test.

Delivery of AAV-RFP-Rph3A in PFF-animals prevented as well the reduction of forelimb muscle strength of animals injected with αsyn and overexpressing the control protein RFP.

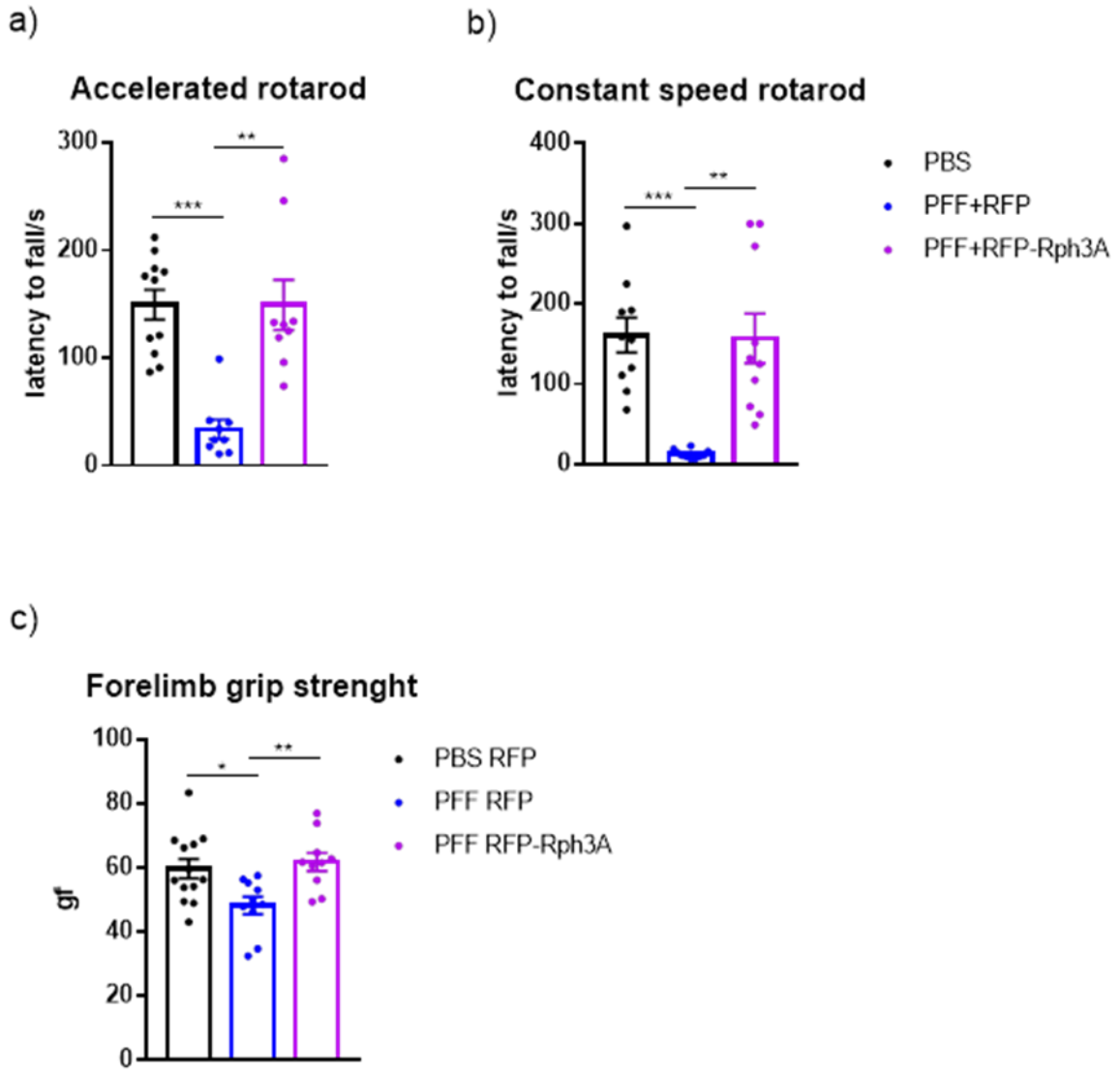

Fig.47. Motor behavioral analysis of PBS and PFF mice upon striatal delivery of RFP-Rph3A (or a control RFP protein). Histograms of a) latency to fall (sec) from the rotating bar evaluated in the accelerated rotarod (starting speed: 20 rpm; final speed 40 rpm in 300s) and b) constant speed rotarod (30 rpm). After the habituation phase, latency to fall has been evaluated as mean of three consecutive trials of the maximum duration of 300s. c) Forelimb muscle strength measured by a grip strength meter. Force (g) of each animal has been evaluated as the mean value of 5 consecutive trials. Statistical analysis: One-way ANOVA, Tukey's multiple comparisons test; n=10, *p<0.05, **p<0.005, ***p<0.0005.

On the whole, behavior data indicate the efficacy of Rph3A striatal overexpression as a strategy to counteract detrimental synaptic effect of αsyn. Increased neuronal expression of Rph3A efficiently compensates toxicity induced by αsyn in the striatum, at least on the motor abilities evaluated. As it

can be deduced by recovery of motor performances, increased Rph3A activity seem to have a positive effect as well on the overall cortico-striatal and nigro-striatal networks.

DISCUSSION

In the last twenty years, several studies investigated the role of the aggregation and toxicity of αsyn in the pathophysiology of familiar and sporadic PD. Although the precise mechanism by which the formation of αsyn aggregates induces neuronal loss is still unclear, aberrant forms and levels of the protein affect multiple cellular pathways and cause synaptic dysfunctions, leading ultimately to neurodegenerative events (Ghiglieri et al., 2018; Wong and Krainc, 2017).

To note, αsyn detrimental effects on the synaptic function was reported even in the early phases of the disease, before the onset of DAergic neuronal loss in the SNpc. Indeed, early PD-related synaptopathy is thought to start with αsyn toxicity on DAergic axons and presynaptic terminal in the striatum, eventually leading to loss of synaptic contacts (Bridi and Hirth, 2018). Besides its effect on the DAergic system, αsyn has been recently reported to affect also the cortico-striatal glutamatergic signalling, (Durante et al., 2019). In particular, fibrillar and oligomeric forms of the protein have been shown to modulate the synaptic levels and activity of NMDA-type of glutamate receptors.

It's known that alterations of NMDA receptors and associated scaffolding proteins play a relevant role in the physiopathology of advanced PD and in the onset of motor complications (Y. Chen et al., 2015; Durante et al., 2019; Mellone and Gardoni, 2018; Tozzi et al., 2021). Scaffolding proteins are essential to modulate the synaptic expression, trafficking and activity of glutamate receptors. Interestingly, Rph3A has been demonstrated by our lab as a fundamental binding partner of the GluN2A subunit of NMDA receptors, stabilizing these receptors at the postsynaptic membrane (Stanic et al., 2015). Rph3A/GluN2A interaction has already been shown to participate to pathophysiology of late stage PD and L-DOPA-induced dyskinesia (Mellone and Gardoni, 2018; Stanic et al., 2017). Moreover, a direct Rph3A/αsyn interaction have been reported, highlighting a putative involvement of Rph3A/αsyn interplay in PD (Dalfó et al., 2004).

Based on these previous findings, the main aims of my PhD project were to dissect the molecular mechanisms underlying the αsyn-induced dysfunction of the glutamatergic synapse in early PD and to investigate possible pharmacological approaches to block this event.

Briefly, this study allowed to demonstrate the presence of a physiological interaction between αsyn and Rph3A, to characterize αsyn-induced early synaptic dysfunction in an *in vivo* PD model, and, ultimately, to prevent the synaptic impairments through modulation of Rph3A expression or Rph3A/αsyn complex.

Firstly, using multiple *in silico, in vitro* and *ex vivo* experimental approaches I confirmed and characterized Rph3A/αsyn interaction. Indeed, in a study on LB disease patients, αsyn/Rph3A complex was already detected only by using a biochemical approach in the entorhinal cortex of healthy individuals (Dalfó et al., 2004). Interestingly, we used a variety of experimental approaches to confirm that this interaction occurs also in primary hippocampal neurons, rat whole brain and striatum, suggesting that Rph3A/αsyn complex could participate in a physiological neuronal synaptic function.

In particular, through an indirect bioinformatic approach we identified the Rph3A domain primarily involved αsyn binding specifically, the C2B bottom surface. This region was already shown to interact with the SNARE-protein SNAP25, key component of synaptic vesicle release machinery (Ferrer-Orta et al., 2017). SNAP25 structural similarity to αsyn and their and preferential pre-synaptic localization suggested a possible comparable mode of interaction with Rph3A. A compound able to target the identified C2B region, selected through a bioinformatic screening, was able to interfere with the formation of Rph3A/αsyn complex, confirming the initial hypothesis. Given Rph3A regulatory role in exocytosis of synaptic vesicles and αsyn presynaptic functions, Rph3A/αsyn interplay possibly participate to modulation of neurotransmitter release (Burré, 2015; Deák et al., 2006a; Tsuboi and Fukuda, 2005).

To investigate the striatal synaptic toxicity of αsyn, I exploited a progressive PD mouse model induced by the striatal injection of pathogenic αsyn species, either oligomeric or fibrillar (PFF). The exogenous aggregated protein raises pathology that progressively engage brain regions directly connected to the injection site, causing DA neurodegeneration by anterograde transfer to the SNpc (Luk et al., 2012a). The PFF-model is a valuable tool to study early disease mechanisms and interventions, being characterized by a slow and progressive onset of neurodegeneration. Moreover, the progression pattern of αsyn inclusions in relation to the onset of DAergic defect and neurodegeneration has already been deeply characterized (Luk et al., 2012a; Patterson et al., 2019). To note, the use of diverse oligomeric and fibrillar αsyn species have been reported to results in different mechanisms and extents of toxicity (Melki, 2015). To replicate early PD, either αsyn PFF or oligomers were used, to highlight possible different pathogenic mechanisms.

In the present study, PFF- and oligomer-injected mice did not show significant alterations of the iGluR receptor levels at the striatal excitatory synapse 42 dpi. This finding is in accordance with previous works showing normal striatal DA levels and limited αsyn pathology at this time point (Luk et al., 2012a; Patterson et al., 2019). Interestingly, 84 dpi αsyn mice showed a significant impairment of the molecular composition of the postsynaptic compartment in the striatum, with significant

decrease of AMPAR-GluA1 and NMDAR-GluN2A and GluN2D subunits, in absence of neurodegeneration. To note, a reduction of GluN2D subunit in striatal cholinergic interneurons was already reported in a rodent model overexpressing αsyn (Tozzi et al., 2016). Moreover, *ex vivo* treatment of cortico-striatal slices with the oligomeric protein was shown to block NMDARs currents and LTP induction in SPNs, selectively targeting the GluN2A subunits (Durante et al., 2019). Most importantly, AMPAR and NMDARs protein reduction is in accordance, and could explain, recent electrophysiological findings published with collaborators (Tozzi et al., 2021). In particular, 84 dpi PFF-lesioned rats displayed impaired striatal LTP, strictly dependent on NMDARs activation, and LTD, plasticity mechanisms finely modulated by DA release. Indeed, impairment of striatal plasticity were paralleled by altered DAergic neuronal firing and striatal DA release, suggesting a complex dysfunction of the nigrostriatal circuitry already at this precocious disease stage (Tozzi et al., 2021).

The above described molecular impairments of the glutamatergic synapse were also reflected in morphological alterations at dendritic spines of striatal SPNs. In particular, PFFs injection significantly reduced striatal spine density, indicating a precocious loss of synaptic contacts. Conversely, even if spine density was unaltered in oligomer-injected mice, we found an overall increase of spine width and percentage of mushroom spines, suggesting a possible early compensatory mechanism to overcome defects of the cortico-striatal signaling. Overall, morphological data together with oligomer-specific alteration of ERK signalling suggest different mechanisms and extent of synaptic toxicity induced by the two types of αsyn aggregates.

The presence of aberrant levels of toxic αsyn was already reported to affect function of different synaptic protein, including Rph3A. For instance, in cortical tissue of patients with LB disease, altered Rab3A/Rph3A interaction, essential for synaptic vesicle cycling, was detected (Dalfó et al., 2004). Altered Rph3A expression was also described in other neurodegenerative conditions as Alzheimer and Huntington disease (Smith et al., 2007; Tan et al., 2014). Although in this study I did not observe changes of total striatal levels of Rph3A, PFF-mice displayed a selective postsynaptic reduction of Rph3A accompanied by diminished GluN2A interaction. Similarly, a trend in decrease of the Rph3A/GluN2A complex was found upon oligomers seeding, indicating a possible milder effect of this αsyn species towards this synaptic complex.

Overall, data on the *in vivo* models suggest that PFFs could promote mechanisms able to sequester Rph3A from physiological synaptic activities. Taking into account the role of Rph3A in the synaptic retention of NMDA receptors (Stanic et al., 2015; Franchini et al., 2019), the sequestering of Rph3A by PFFs could play a key role in the observed decrease of NMDARs postsynaptic abundance. Interestingly, experimental strategies aimed at reducing Rph3A postsynaptic activity were already

demonstrated to decrease not only the synaptic availability of GluN2A-containing NMDA receptors but also the spine density in hippocampal neurons (Stanic et al., 2015). Thereby, decreased Rph3A expression and, consequently, of Rph3A/GluN2A complex could contribute to the *in vivo* spine loss observed in the PFF model.

These data suggest Rph3A as a possible mediator of αsyn-induced synaptic toxicity in the striatum; a modulation of its expression and aberrant interaction with αsyn can thus represent a novel experimental approach to counteract synaptic defects in αsyn models. Rph3A modulatory strategies were firstly tested exploiting a recently validated *in vitro* model of αsyn-induced spine pathology, specifically primary hippocampal neurons chronically treated with αsyn PFFs. As previously reported (Wu et al., 2019), I found a significant decrease of spine density upon 7-day PFFs treatment with a still preserved viability and axonal integrity. Intriguingly, co-administration of the compound B started 4 days post αsyn seeding was sufficient to fully prevent PFFs-induced spine loss. Due to steric hindrance, the molecule is potentially decreasing the amount of Rph3A bound to pathologic αsyn, thus enhancing the synaptic availability of the protein. Furthermore, in the same experimental model, Rph3A overexpression was able as well to rescue the PFF-induced decrease in spine density.

As already described, Rph3A carries out important functions both at the pre-synaptic terminal, taking part to neurotransmitter release cycle, and at the postsynapse, promoting synaptic retention of NMDA receptors (Bourgeois-Jaarsma et al., 2021b; Stanic et al., 2015). Accordingly, it is possible to speculate that Rph3A overexpression acts on both sides of the synapse, resulting sufficient to block PFF detrimental effect on spines.

Proven their efficacy *in vitro*, Rph3A modulatory approaches were then investigated *in vivo,* exploiting the already characterized PFF-mouse model. To note, the compound B-mediated *in vitro* rescue of spine density was confirmed in mice striata as well. In particular, I found that 2-week chronic intracerebroventricle administration, started at 70 dpi, in PFF-mice fully prevented synaptic loss. This *in vivo* finding suggests that the aberrant Rph3A/αsyn interaction can represent a valid pharmacological target to counteract the progression of synaptopathy,

Studies on transmissible αsyn rodent models indicate that motor and behavioral impairments start to appear between three and six months after the lesion, although with some discrepancies of severity among the different studies (Durante et al., 2019; Luk et al., 2012a; Tozzi et al., 2021). In this study, PFF-mice showed impaired rotarod test performances and a mild decrease of the forelimb grip strength. The bilateral PFF-injection can explain the more evident motor coordination impairment found in the present study with respect to the milder dysfunctions previously reported in unilaterally-

lesioned mice (Luk et al., 2012a). Indeed, bilateral lesions were recently described to produce similar early behavioural defects in rats (Tozzi et al., 2021). Since the general locomotor activity, measured in the open field test, of αsyn mice was not altered, it can be supposed that at this time point only more sophisticated motor capabilities are affected (Luk et al., 2012a). Importantly, here I demonstrated that striatal delivery of an AAV-Rph3A in PFF-mice was able to fully rescue the motor impairments observed in PFF-mice. Recovery of motor performances suggest that Rph3A striatal overexpression positively affects the overall nigrostriatal and cortico-striatal network, counteracting detrimental effects of αsyn that leads to precocious motor impairments.

In conclusion, results of this PhD thesis demonstrate that Rph3A and Rph3A/αsyn complex significantly contribute to the pathogenic mechanisms underlying early PD synaptopathy in the striatum, therefore representing novel and promising pharmacological targets.

BIBLIOGRAPHY

Akazawa, C., Shigemoto, R., Bessho, Y., Nakanishi, S., Mizuno, N., 1994. Differential expression of five N-methyl-D-aspartate receptor subunit mRNAs in the cerebellum of developing and adult rats. J. Comp. Neurol. 347, 150–160. https://doi.org/10.1002/cne.903470112

Alam, P., Bousset, L., Melki, R., Otzen, D.E., 2019. α-synuclein oligomers and fibrils: a spectrum of species, a spectrum of toxicities. J. Neurochem. 150, 522–534. https://doi.org/10.1111/jnc.14808

Albert, K., Voutilainen, M., Domanskyi, A., Airavaara, M., 2017. AAV Vector-Mediated Gene Delivery to Substantia Nigra Dopamine Neurons: Implications for Gene Therapy and Disease Models. Genes 8, 63. https://doi.org/10.3390/genes8020063

Albin, R.L., Young, A.B., Penney, J.B., 1989. The functional anatomy of basal ganglia disorders. Trends in Neurosciences 12, 366–375. https://doi.org/10.1016/0166-2236(89)90074-X

AlDakheel, A., Kalia, L.V., Lang, A.E., 2014. Pathogenesis-Targeted, Disease-Modifying Therapies in Parkinson Disease. Neurotherapeutics 11, 6–23. https://doi.org/10.1007/s13311-013-0218-1

Alexander, G.E., Crutcher, M.D., DeLong, M.R., 1990. Basal ganglia-thalamocortical circuits: parallel substrates for motor, oculomotor, "prefrontal" and "limbic" functions. Prog Brain Res 85, 119–146.

Alexander, G.E., DeLong, M.R., Strick, P.L., 1986. Parallel Organization of Functionally Segregated Circuits Linking Basal Ganglia and Cortex. Annu. Rev. Neurosci. 9, 357–381. https://doi.org/10.1146/annurev.ne.09.030186.002041

Alonso Cánovas, A., Luquin Piudo, R., García Ruiz-Espiga, P., Burguera, J.A., Campos Arillo, V., Castro, A., Linazasoro, G., López del Val, J., Vela, L., Martínez Castrillo, J.C., 2014. Agonistas dopaminérgicos en la enfermedad de Parkinson. Neurología 29, 230–241. https://doi.org/10.1016/j.nrl.2011.04.012

Alzheimer's Association, 2014. 2014 Alzheimer's disease facts and figures. Alzheimer's & Dementia 10, e47–e92. https://doi.org/10.1016/j.jalz.2014.02.001

Angot, E., Steiner, J.A., Hansen, C., Li, J.-Y., Brundin, P., 2010. Are synucleinopathies prion-like disorders? The Lancet Neurology 9, 1128–1138. https://doi.org/10.1016/S1474-4422(10)70213-1

Antonini, A., Bravi, D., Sandre, M., Bubacco, L., 2020. Immunization therapies for Parkinson's disease: state of the art and considerations for future clinical trials. Expert Opinion on Investigational Drugs 29, 685–695. https://doi.org/10.1080/13543784.2020.1771693

Aristieta, A., Azkona, G., Sagarduy, A., Miguelez, C., Ruiz-Ortega, J.Á., Sanchez-Pernaute, R., Ugedo, L., 2012. The Role of the Subthalamic Nucleus in L-DOPA Induced Dyskinesia in 6-Hydroxydopamine Lesioned Rats. PLoS ONE 7, e42652. https://doi.org/10.1371/journal.pone.0042652

Arizona Parkinson's Disease Consortium, Beach, T.G., Adler, C.H., Sue, L.I., Vedders, L., Lue, L., White III, C.L., Akiyama, H., Caviness, J.N., Shill, H.A., Sabbagh, M.N., Walker, D.G., 2010.

Multi-organ distribution of phosphorylated α-synuclein histopathology in subjects with Lewy body disorders. Acta Neuropathol 119, 689–702. https://doi.org/10.1007/s00401-010-0664-3

Axelsen, T.M., Woldbye, D.P.D., 2018. Gene Therapy for Parkinson's Disease, An Update. JPD 8, 195–215. https://doi.org/10.3233/JPD-181331

Baba, M., Nakajo, S., Tu, P.H., Tomita, T., Nakaya, K., Lee, V.M., Trojanowski, J.Q., Iwatsubo, T., 1998. Aggregation of alpha-synuclein in Lewy bodies of sporadic Parkinson's disease and dementia with Lewy bodies. Am J Pathol 152, 879–884.

Baldereschi, M., Di Carlo, A., Rocca, W.A., Vanni, P., Maggi, S., Perissinotto, E., Grigoletto, F., Amaducci, L., Inzitari, D., 2000. Parkinson's disease and parkinsonism in a longitudinal study: Two-fold higher incidence in men. Neurology 55, 1358–1363. https://doi.org/10.1212/WNL.55.9.1358

Baltic, S., Perovic, M., Mladenovic, A., Raicevic, N., Ruzdijic, S., Rakic, L., Kanazir, S., 2004. α-Synuclein Is Expressed in Different Tissues During Human Fetal Development. JMN 22, 199–204. https://doi.org/10.1385/JMN:22:3:199

Barker, R.A., Parmar, M., Studer, L., Takahashi, J., 2017. Human Trials of Stem Cell-Derived Dopamine Neurons for Parkinson's Disease: Dawn of a New Era. Cell Stem Cell 21, 569–573. https://doi.org/10.1016/j.stem.2017.09.014

Bartels, T., Choi, J.G., Selkoe, D.J., 2011. α-Synuclein occurs physiologically as a helically folded tetramer that resists aggregation. Nature 477, 107–110. https://doi.org/10.1038/nature10324

Bastide, M.F., Meissner, W.G., Picconi, B., Fasano, S., Fernagut, P.-O., Feyder, M., Francardo, V., Alcacer, C., Ding, Y., Brambilla, R., Fisone, G., Jon Stoessl, A., Bourdenx, M., Engeln, M., Navailles, S., De Deurwaerdère, P., Ko, W.K.D., Simola, N., Morelli, M., Groc, L., Rodriguez, M.-C., Gurevich, E.V., Quik, M., Morari, M., Mellone, M., Gardoni, F., Tronci, E., Guehl, D., Tison, F., Crossman, A.R., Kang, U.J., Steece-Collier, K., Fox, S., Carta, M., Angela Cenci, M., Bézard, E., 2015. Pathophysiology of L-dopa-induced motor and non-motor complications in Parkinson's disease. Progress in Neurobiology 132, 96–168. https://doi.org/10.1016/j.pneurobio.2015.07.002

Bell, K.F., Hardingham, G.E., 2011. The influence of synaptic activity on neuronal health. Current Opinion in Neurobiology 21, 299–305. https://doi.org/10.1016/j.conb.2011.01.002

Berg, D., Schweitzer, K.J., Leitner, P., Zimprich, A., Lichtner, P., Belcredi, P., Brüssel, T., Schulte, C., Maass, S., Nägele, T., Wszolek, Z.K., Gasser, T., 2005. Type and frequency of mutations in the LRRK2 gene in familial and sporadic Parkinson's disease*. Brain 128, 3000–3011. https://doi.org/10.1093/brain/awh666

Birkmayer, W., Hornykiewicz, O., 1961. [The L-3,4-dioxyphenylalanine (DOPA)-effect in Parkinson-akinesia]. Wien Klin Wochenschr 73, 787–788.

Blandini, F., Armentero, M.-T., 2012. Animal models of Parkinson's disease: Animal models of Parkinson's disease. FEBS Journal 279, 1156–1166. https://doi.org/10.1111/j.1742-4658.2012.08491.x

Blandini, F., Armentero, M.-T., Martignoni, E., 2008. The 6-hydroxydopamine model: News from the past. Parkinsonism & Related Disorders 14, S124–S129. https://doi.org/10.1016/j.parkreldis.2008.04.015

Bliss, T.V.P., Collingridge, G.L., 1993. A synaptic model of memory: long-term potentiation in the hippocampus. Nature 361, 31–39. https://doi.org/10.1038/361031a0

Bonifati, V., 2003. Mutations in the DJ-1 Gene Associated with Autosomal Recessive Early-Onset Parkinsonism. Science 299, 256–259. https://doi.org/10.1126/science.1077209

Bose, A., Beal, M.F., 2016. Mitochondrial dysfunction in Parkinson's disease. J. Neurochem. 139, 216–231. https://doi.org/10.1111/jnc.13731

Bourgeois-Jaarsma, Q., Miaja Hernandez, P., Groffen, A.J., 2021a. Ca2+ sensor proteins in spontaneous release and synaptic plasticity: Limited contribution of Doc2c, rabphilin-3a and synaptotagmin 7 in hippocampal glutamatergic neurons. Molecular and Cellular Neuroscience 112, 103613. https://doi.org/10.1016/j.mcn.2021.103613

Bourgeois-Jaarsma, Q., Miaja Hernandez, P., Groffen, A.J., 2021b. Ca2+ sensor proteins in spontaneous release and synaptic plasticity: Limited contribution of Doc2c, rabphilin-3a and synaptotagmin 7 in hippocampal glutamatergic neurons. Molecular and Cellular Neuroscience 112, 103613. https://doi.org/10.1016/j.mcn.2021.103613

Bousset, L., Pieri, L., Ruiz-Arlandis, G., Gath, J., Jensen, P.H., Habenstein, B., Madiona, K., Olieric, V., Böckmann, A., Meier, B.H., Melki, R., 2013a. Structural and functional characterization of two alpha-synuclein strains. Nature Communications 4, 1–13. https://doi.org/10.1038/ncomms3575

Bousset, L., Pieri, L., Ruiz-Arlandis, G., Gath, J., Jensen, P.H., Habenstein, B., Madiona, K., Olieric, V., Böckmann, A., Meier, B.H., Melki, R., 2013b. Structural and functional characterization of two alpha-synuclein strains. Nat Commun 4, 2575. https://doi.org/10.1038/ncomms3575

Braak, H., de Vos, R.A.I., Bohl, J., Del Tredici, K., 2006. Gastric α-synuclein immunoreactive inclusions in Meissner's and Auerbach's plexuses in cases staged for Parkinson's disease-related brain pathology. Neuroscience Letters 396, 67–72. https://doi.org/10.1016/j.neulet.2005.11.012

Braak, H., Del Tredici, K., Rüb, U., de Vos, R.A.I., Jansen Steur, E.N.H., Braak, E., 2003. Staging of brain pathology related to sporadic Parkinson's disease. Neurobiol. Aging 24, 197–211. https://doi.org/10.1016/s0197-4580(02)00065-9

Brehme, M., Voisine, C., Rolland, T., Wachi, S., Soper, J.H., Zhu, Y., Orton, K., Villella, A., Garza, D., Vidal, M., Ge, H., Morimoto, R.I., 2014. A chaperome subnetwork safeguards proteostasis in aging and neurodegenerative disease. Cell Rep 9, 1135–1150. https://doi.org/10.1016/j.celrep.2014.09.042

Bridi, J.C., Hirth, F., 2018. Mechanisms of α-Synuclein Induced Synaptopathy in Parkinson's Disease. Front. Neurosci. 12, 80. https://doi.org/10.3389/fnins.2018.00080

Bronstein, J.M., Tagliati, M., Alterman, R.L., Lozano, A.M., Volkmann, J., Stefani, A., Horak, F.B., Okun, M.S., Foote, K.D., Krack, P., Pahwa, R., Henderson, J.M., Hariz, M.I., Bakay, R.A., Rezai, A., Marks, W.J., Moro, E., Vitek, J.L., Weaver, F.M., Gross, R.E., DeLong, M.R., 2011. Deep Brain Stimulation for Parkinson Disease: An Expert Consensus and Review of Key Issues. Arch Neurol 68. https://doi.org/10.1001/archneurol.2010.260

Brozzi, F., Lajus, S., Diraison, F., Rajatileka, S., Hayward, K., Regazzi, R., Molnár, E., Váradi, A., 2012. MyRIP interaction with MyoVa on secretory granules is controlled by the cAMP-PKA pathway. MBoC 23, 4444–4455. https://doi.org/10.1091/mbc.e12-05-0369

Brundin, P., Dave, K.D., Kordower, J.H., 2017. Therapeutic approaches to target alpha-synuclein pathology. Experimental Neurology 298, 225–235. https://doi.org/10.1016/j.expneurol.2017.10.003

Brundin, P., Melki, R., Kopito, R., 2010. Prion-like transmission of protein aggregates in neurodegenerative diseases. Nat Rev Mol Cell Biol 11, 301–307. https://doi.org/10.1038/nrm2873

Burai, R., Ait-Bouziad, N., Chiki, A., Lashuel, H.A., 2015. Elucidating the Role of Site-Specific Nitration of α-Synuclein in the Pathogenesis of Parkinson's Disease via Protein Semisynthesis and Mutagenesis. J. Am. Chem. Soc. 137, 5041–5052. https://doi.org/10.1021/ja5131726

Burguière, A., De Bundel, D., Valjent, E., Roger, J., Smolders, I., Fagni, L., Perroy, J., 2013. Combination of group I mGlu receptors antagonist with dopaminergic agonists strengthens the synaptic transmission at corticostriatal synapses in culture. Neuropharmacology 66, 151–157. https://doi.org/10.1016/j.neuropharm.2012.03.017

Burns, R.S., LeWitt, P.A., Ebert, M.H., Pakkenberg, H., Kopin, I.J., 1985. The Clinical Syndrome of Striatal Dopamine Deficiency: Parkinsonism Induced by 1-Methyl-4-Phenyl-1,2,3,6-Tetrahydropyridine (MPTP). N Engl J Med 312, 1418–1421. https://doi.org/10.1056/NEJM198505303122203

Burré, J., 2015. The Synaptic Function of α-Synuclein. Journal of Parkinson's Disease 5, 699–713. https://doi.org/10.3233/JPD-150642

Burré, J., Sharma, M., Südhof, T.C., 2018. Cell Biology and Pathophysiology of α-Synuclein. Cold Spring Harb Perspect Med 8, a024091. https://doi.org/10.1101/cshperspect.a024091

Burré, J., Sharma, M., Südhof, T.C., 2014. α-Synuclein assembles into higher-order multimers upon membrane binding to promote SNARE complex formation. Proc Natl Acad Sci USA 111, E4274–E4283. https://doi.org/10.1073/pnas.1416598111

Burre, J., Sharma, M., Tsetsenis, T., Buchman, V., Etherton, M.R., Sudhof, T.C., 2010. -Synuclein Promotes SNARE-Complex Assembly in Vivo and in Vitro. Science 329, 1663–1667. https://doi.org/10.1126/science.1195227

Burré, J., Vivona, S., Diao, J., Sharma, M., Brunger, A.T., Südhof, T.C., 2013. Properties of native brain α-synuclein. Nature 498, E4-6; discussion E6-7. https://doi.org/10.1038/nature12125

Bussell, R., 2005. Helix periodicity, topology, and dynamics of membrane-associated -Synuclein. Protein Science 14, 862–872. https://doi.org/10.1110/ps.041255905

Bussell, R., Eliezer, D., 2003. A Structural and Functional Role for 11-mer Repeats in α-Synuclein and Other Exchangeable Lipid Binding Proteins. Journal of Molecular Biology 329, 763–778. https://doi.org/10.1016/S0022-2836(03)00520-5

Butler, B., Saha, K., Rana, T., Becker, J.P., Sambo, D., Davari, P., Goodwin, J.S., Khoshbouei, H., 2015. Dopamine Transporter Activity Is Modulated by α-Synuclein. J. Biol. Chem. 290, 29542–29554. https://doi.org/10.1074/jbc.M115.691592

Calabresi, P., Picconi, B., Tozzi, A., Di Filippo, M., 2007. Dopamine-mediated regulation of corticostriatal synaptic plasticity. Trends in Neurosciences 30, 211–219. https://doi.org/10.1016/j.tins.2007.03.001

Carta, M., Carlsson, T., Muñoz, A., Kirik, D., Björklund, A., 2010. Role of serotonin neurons in the induction of levodopa- and graft-induced dyskinesias in Parkinson's disease: 5-HT Neurons in Dyskinesia. Mov. Disord. 25, S174–S179. https://doi.org/10.1002/mds.22792

Celej, M.S., Sarroukh, R., Goormaghtigh, E., Fidelio, G.D., Ruysschaert, J.-M., Raussens, V., 2012. Toxic prefibrillar α-synuclein amyloid oligomers adopt a distinctive antiparallel β-sheet structure. Biochem. J. 443, 719–726. https://doi.org/10.1042/BJ20111924

Cenci, M.A., 2014. Presynaptic Mechanisms of l-DOPA-Induced Dyskinesia: The Findings, the Debate, and the Therapeutic Implications. Front Neurol 5, 242. https://doi.org/10.3389/fneur.2014.00242

Challis, C., Hori, A., Sampson, T.R., Yoo, B.B., Challis, R.C., Hamilton, A.M., Mazmanian, S.K., Volpicelli-Daley, L.A., Gradinaru, V., 2020. Gut-seeded α-synuclein fibrils promote gut dysfunction and brain pathology specifically in aged mice. Nature Neuroscience 23, 327–336. https://doi.org/10.1038/s41593-020-0589-7

Chatterjee, D., Kordower, J.H., 2019. Immunotherapy in Parkinson's disease: Current status and future directions. Neurobiology of Disease 132, 104587. https://doi.org/10.1016/j.nbd.2019.104587

Chaudhuri, K.R., Schapira, A.H., 2009. Non-motor symptoms of Parkinson's disease: dopaminergic pathophysiology and treatment. The Lancet Neurology 8, 464–474. https://doi.org/10.1016/S1474-4422(09)70068-7

Chen, R.H.C., Wislet-Gendebien, S., Samuel, F., Visanji, N.P., Zhang, G., Marsilio, D., Langman, T., Fraser, P.E., Tandon, A., 2013. α-Synuclein Membrane Association Is Regulated by the Rab3a Recycling Machinery and Presynaptic Activity*. Journal of Biological Chemistry 288, 7438–7449. https://doi.org/10.1074/jbc.M112.439497

Chen, S.W., Drakulic, S., Deas, E., Ouberai, M., Aprile, F.A., Arranz, R., Ness, S., Roodveldt, C., Guilliams, T., De-Genst, E.J., Klenerman, D., Wood, N.W., Knowles, T.P.J., Alfonso, C., Rivas, G., Abramov, A.Y., Valpuesta, J.M., Dobson, C.M., Cremades, N., 2015. Structural characterization of toxic oligomers that are kinetically trapped during α-synuclein fibril formation. Proc. Natl. Acad. Sci. U.S.A. 112, E1994-2003. https://doi.org/10.1073/pnas.1421204112

Chen, Y., Yang, W., Li, X., Li, X., Yang, H., Xu, Z., Yu, S., 2015. α-Synuclein-induced internalization of NMDA receptors in hippocampal neurons is associated with reduced inward current and Ca2+ influx upon NMDA stimulation. Neuroscience 300, 297–306. https://doi.org/10.1016/j.neuroscience.2015.05.035

Chen-Plotkin, A.S., 2014. Unbiased Approaches to Biomarker Discovery in Neurodegenerative Diseases. Neuron 84, 594–607. https://doi.org/10.1016/j.neuron.2014.10.031

Chiba, K., Trevor, A., Castagnoli, N., 1984. Metabolism of the neurotoxic tertiary amine, MPTP, by brain monoamine oxidase. Biochemical and Biophysical Research Communications 120, 574–578. https://doi.org/10.1016/0006-291X(84)91293-2

Chiti, F., Dobson, C.M., 2006. Protein Misfolding, Functional Amyloid, and Human Disease. Annual Review of Biochemistry 75, 333–366. https://doi.org/10.1146/annurev.biochem.75.101304.123901

Chu, Y., Dodiya, H., Aebischer, P., Olanow, C.W., Kordower, J.H., 2009. Alterations in lysosomal and proteasomal markers in Parkinson's disease: Relationship to alpha-synuclein inclusions. Neurobiology of Disease 35, 385–398. https://doi.org/10.1016/j.nbd.2009.05.023

Chu, Y., Kordower, J.H., 2007. Age-associated increases of α-synuclein in monkeys and humans are associated with nigrostriatal dopamine depletion: Is this the target for Parkinson's disease? Neurobiology of Disease 25, 134–149. https://doi.org/10.1016/j.nbd.2006.08.021

Chu, Y., Muller, S., Tavares, A., Barret, O., Alagille, D., Seibyl, J., Tamagnan, G., Marek, K., Luk, K.C., Trojanowski, J.Q., Lee, V.M.Y., Kordower, J.H., 2019. Intrastriatal alpha-synuclein fibrils in monkeys: spreading, imaging and neuropathological changes. Brain 142, 3565–3579. https://doi.org/10.1093/brain/awz296

Chung, S.-H., Takai, Y., Holz, R.W., 1995. Evidence That the Rab3a-binding Protein, Rabphilin3a, Enhances Regulated Secretion. Journal of Biological Chemistry 270, 16714–16718. https://doi.org/10.1074/jbc.270.28.16714

Citri, A., Malenka, R.C., 2008. Synaptic Plasticity: Multiple Forms, Functions, and Mechanisms. Neuropsychopharmacol 33, 18–41. https://doi.org/10.1038/sj.npp.1301559

Connolly, B., Fox, S.H., 2014. Treatment of Cognitive, Psychiatric, and Affective Disorders Associated with Parkinson's Disease. Neurotherapeutics 11, 78–91. https://doi.org/10.1007/s13311-013-0238-x

Connolly, B.S., Lang, A.E., 2014. Pharmacological treatment of Parkinson disease: a review. JAMA 311, 1670–1683. https://doi.org/10.1001/jama.2014.3654

Corbalan-Garcia, S., Gómez-Fernández, J.C., 2014. Signaling through C2 domains: More than one lipid target. Biochimica et Biophysica Acta (BBA) - Biomembranes 1838, 1536–1547. https://doi.org/10.1016/j.bbamem.2014.01.008

Cremades, N., Cohen, S.I.A., Deas, E., Abramov, A.Y., Chen, A.Y., Orte, A., Sandal, M., Clarke, R.W., Dunne, P., Aprile, F.A., Bertoncini, C.W., Wood, N.W., Knowles, T.P.J., Dobson, C.M., Klenerman, D., 2012. Direct observation of the interconversion of normal and toxic forms of α-synuclein. Cell 149, 1048–1059. https://doi.org/10.1016/j.cell.2012.03.037

Cull-Candy, S., Kelly, L., Farrant, M., 2006. Regulation of Ca2+-permeable AMPA receptors: synaptic plasticity and beyond. Current Opinion in Neurobiology 16, 288–297. https://doi.org/10.1016/j.conb.2006.05.012

Dailey, M.E., Smith, S.J., 1996. The Dynamics of Dendritic Structure in Developing Hippocampal Slices. J. Neurosci. 16, 2983–2994. https://doi.org/10.1523/JNEUROSCI.16-09-02983.1996

Dalfó, E., Barrachina, M., Rosa, J.L., Ambrosio, S., Ferrer, I., 2004. Abnormal α-synuclein interactions with rab3a and rabphilin in diffuse Lewy body disease. Neurobiology of Disease 16, 92–97. https://doi.org/10.1016/j.nbd.2004.01.001

Damier, P., Hirsch, E.C., Agid, Y., Graybiel, A.M., 1999. The substantia nigra of the human brain. Brain 122, 1437–1448. https://doi.org/10.1093/brain/122.8.1437

Davidson, W.S., Jonas, A., Clayton, D.F., George, J.M., 1998. Stabilization of alpha-synuclein secondary structure upon binding to synthetic membranes. J. Biol. Chem. 273, 9443–9449. https://doi.org/10.1074/jbc.273.16.9443

Deák, F., Shin, O.-H., Tang, J., Hanson, P., Ubach, J., Jahn, R., Rizo, J., Kavalali, E.T., Südhof, T.C., 2006a. Rabphilin regulates SNARE-dependent re-priming of synaptic vesicles for fusion. EMBO J 25, 2856–2866. https://doi.org/10.1038/sj.emboj.7601165

Deák, F., Shin, O.-H., Tang, J., Hanson, P., Ubach, J., Jahn, R., Rizo, J., Kavalali, E.T., Südhof, T.C., 2006b. Rabphilin regulates SNARE-dependent re-priming of synaptic vesicles for fusion. EMBO J 25, 2856–2866. https://doi.org/10.1038/sj.emboj.7601165

Decressac, M., Mattsson, B., Lundblad, M., Weikop, P., Björklund, A., 2012. Progressive neurodegenerative and behavioural changes induced by AAV-mediated overexpression of α-synuclein in midbrain dopamine neurons. Neurobiology of Disease 45, 939–953. https://doi.org/10.1016/j.nbd.2011.12.013

Decressac, M., Ulusoy, A., Mattsson, B., Georgievska, B., Romero-Ramos, M., Kirik, D., Bjorklund, A., 2011. GDNF fails to exert neuroprotection in a rat -synuclein model of Parkinson's disease. Brain 134, 2302–2311. https://doi.org/10.1093/brain/awr149

Dehay, B., Bove, J., Rodriguez-Muela, N., Perier, C., Recasens, A., Boya, P., Vila, M., 2010. Pathogenic Lysosomal Depletion in Parkinson's Disease. Journal of Neuroscience 30, 12535–12544. https://doi.org/10.1523/JNEUROSCI.1920-10.2010

Del Tredici, K., Hawkes, C.H., Ghebremedhin, E., Braak, H., 2010. Lewy pathology in the submandibular gland of individuals with incidental Lewy body disease and sporadic Parkinson's disease. Acta Neuropathol 119, 703–713. https://doi.org/10.1007/s00401-010-0665-2

DeLong, M.R., 1990. Primate models of movement disorders of basal ganglia origin. Trends in Neurosciences 13, 281–285. https://doi.org/10.1016/0166-2236(90)90110-V

Deng, Y.-P., Lei, W.-L., Reiner, A., 2006. Differential perikaryal localization in rats of D1 and D2 dopamine receptors on striatal projection neuron types identified by retrograde labeling. Journal of Chemical Neuroanatomy 32, 101–116. https://doi.org/10.1016/j.jchemneu.2006.07.001

Deumens, R., Blokland, A., Prickaerts, J., 2002. Modeling Parkinson's Disease in Rats: An Evaluation of 6-OHDA Lesions of the Nigrostriatal Pathway. Experimental Neurology 175, 303–317. https://doi.org/10.1006/exnr.2002.7891

Deutch, A.Y., Colbran, R.J., Winder, D.J., 2007. Striatal plasticity and medium spiny neuron dendritic remodeling in parkinsonism. Parkinsonism & Related Disorders 13, S251–S258. https://doi.org/10.1016/S1353-8020(08)70012-9

Di Matteo, V., Benigno, A., Pierucci, M., Giuliano, D.A., Crescimanno, G., Esposito, E., Giovanni, G.D., 2006. 7-Nitroindazole Protects Striatal Dopaminergic Neurons against MPP+-Induced Degeneration: An in Vivo Microdialysis Study. Annals of the New York Academy of Sciences 1089, 462–471. https://doi.org/10.1196/annals.1386.015

Diao, J., Burré, J., Vivona, S., Cipriano, D.J., Sharma, M., Kyoung, M., Südhof, T.C., Brunger, A.T., 2013. Native α-synuclein induces clustering of synaptic-vesicle mimics via binding to phospholipids and synaptobrevin-2/VAMP2. eLife 2, e00592. https://doi.org/10.7554/eLife.00592

Dias, V., Junn, E., Mouradian, M.M., 2013. The Role of Oxidative Stress in Parkinson's Disease. Journal of Parkinson's Disease 3, 461–491. https://doi.org/10.3233/JPD-130230

Dickson, D.W., 2018. Neuropathology of Parkinson disease. Parkinsonism & Related Disorders 46, S30–S33. https://doi.org/10.1016/j.parkreldis.2017.07.033

Dickson, D.W., 2012. Parkinson's Disease and Parkinsonism: Neuropathology. Cold Spring Harb Perspect Med 2, a009258. https://doi.org/10.1101/cshperspect.a009258

Dickson, D.W., Braak, H., Duda, J.E., Duyckaerts, C., Gasser, T., Halliday, G.M., Hardy, J., Leverenz, J.B., Del Tredici, K., Wszolek, Z.K., Litvan, I., 2009. Neuropathological assessment of Parkinson's disease: refining the diagnostic criteria. The Lancet Neurology 8, 1150–1157. https://doi.org/10.1016/S1474-4422(09)70238-8

Dijkstra, A.A., Voorn, P., Berendse, H.W., Groenewegen, H.J., Netherlands Brain Bank, Rozemuller, A.J.M., Berg, W.D.J., 2014. Stage-dependent nigral neuronal loss in incidental Lewy body and Parkinson's disease. Mov Disord. 29, 1244–1251. https://doi.org/10.1002/mds.25952

Dingledine, R., Borges, K., Bowie, D., Traynelis, S.F., 1999. The glutamate receptor ion channels. Pharmacol Rev 51, 7–61.

Diogenes, M.J., Dias, R.B., Rombo, D.M., Vicente Miranda, H., Maiolino, F., Guerreiro, P., Nasstrom, T., Franquelim, H.G., Oliveira, L.M.A., Castanho, M.A.R.B., Lannfelt, L., Bergstrom, J., Ingelsson, M., Quintas, A., Sebastiao, A.M., Lopes, L.V., Outeiro, T.F., 2012. Extracellular Alpha-Synuclein Oligomers Modulate Synaptic Transmission and Impair LTP Via NMDA-Receptor Activation. Journal of Neuroscience 32, 11750–11762. https://doi.org/10.1523/JNEUROSCI.0234-12.2012

Dirkx, M.F., den Ouden, H., Aarts, E., Timmer, M., Bloem, B.R., Toni, I., Helmich, R.C., 2016. The Cerebral Network of Parkinson's Tremor: An Effective Connectivity fMRI Study. J. Neurosci. 36, 5362–5372. https://doi.org/10.1523/JNEUROSCI.3634-15.2016

Dorsey, E.R., Constantinescu, R., Thompson, J.P., Biglan, K.M., Holloway, R.G., Kieburtz, K., Marshall, F.J., Ravina, B.M., Schifitto, G., Siderowf, A., Tanner, C.M., 2007. Projected number of people with Parkinson disease in the most populous nations, 2005 through 2030. Neurology 68, 384–386. https://doi.org/10.1212/01.wnl.0000247740.47667.03

Dunah, A.W., Standaert, D.G., 2001. Dopamine D1 Receptor-Dependent Trafficking of Striatal NMDA Glutamate Receptors to the Postsynaptic Membrane. J. Neurosci. 21, 5546–5558. https://doi.org/10.1523/JNEUROSCI.21-15-05546.2001

Dunah, A.W., Wang, Y., Yasuda, R.P., Kameyama, K., Huganir, R.L., Wolfe, B.B., Standaert, D.G., 2000. Alterations in subunit expression, composition, and phosphorylation of striatal N-methyl-D-aspartate glutamate receptors in a rat 6-hydroxydopamine model of Parkinson's disease. Mol Pharmacol 57, 342–352.

Durante, V., de Iure, A., Loffredo, V., Vaikath, N., De Risi, M., Paciotti, S., Quiroga-Varela, A., Chiasserini, D., Mellone, M., Mazzocchetti, P., Calabrese, V., Campanelli, F., Mechelli, A., Di Filippo, M., Ghiglieri, V., Picconi, B., El-Agnaf, O.M., De Leonibus, E., Gardoni, F., Tozzi, A., Calabresi, P., 2019. Alpha-synuclein targets GluN2A NMDA receptor subunit causing striatal synaptic dysfunction and visuospatial memory alteration. Brain 142, 1365–1385. https://doi.org/10.1093/brain/awz065

Eberini, I., Daniele, S., Parravicini, C., Sensi, C., Trincavelli, M.L., Martini, C., Abbracchio, M.P., 2011. In silico identification of new ligands for GPR17: a promising therapeutic target for neurodegenerative diseases. J Comput Aided Mol Des 25, 743–752. https://doi.org/10.1007/s10822-011-9455-8

Emborg, M.E., 2007. Nonhuman Primate Models of Parkinson's Disease. ILAR Journal 48, 339–355. https://doi.org/10.1093/ilar.48.4.339

Emmanouilidou, E., Stefanis, L., Vekrellis, K., 2010. Cell-produced α-synuclein oligomers are targeted to, and impair, the 26S proteasome. Neurobiology of Aging 31, 953–968. https://doi.org/10.1016/j.neurobiolaging.2008.07.008

Fernandes, H.J.R., Hartfield, E.M., Christian, H.C., Emmanoulidou, E., Zheng, Y., Booth, H., Bogetofte, H., Lang, C., Ryan, B.J., Sardi, S.P., Badger, J., Vowles, J., Evetts, S., Tofaris, G.K., Vekrellis, K., Talbot, K., Hu, M.T., James, W., Cowley, S.A., Wade-Martins, R., 2016. ER Stress and Autophagic Perturbations Lead to Elevated Extracellular α-Synuclein in GBA-N370S Parkinson's iPSC-Derived Dopamine Neurons. Stem Cell Reports 6, 342–356. https://doi.org/10.1016/j.stemcr.2016.01.013

Ferrari, E., Cardinale, A., Picconi, B., Gardoni, F., 2020. From cell lines to pluripotent stem cells for modelling Parkinson's Disease. Journal of Neuroscience Methods 340, 108741. https://doi.org/10.1016/j.jneumeth.2020.108741

Ferrer-Orta, C., Pérez-Sánchez, M.D., Coronado-Parra, T., Silva, C., López-Martínez, D., Baltanás-Copado, J., Gómez-Fernández, J.C., Corbalán-García, S., Verdaguer, N., 2017. Structural characterization of the Rabphilin-3A–SNAP25 interaction. Proc Natl Acad Sci USA 114, E5343–E5351. https://doi.org/10.1073/pnas.1702542114

Fox, S.H., Katzenschlager, R., Lim, S.-Y., Ravina, B., Seppi, K., Coelho, M., Poewe, W., Rascol, O., Goetz, C.G., Sampaio, C., 2011. The Movement Disorder Society Evidence-Based Medicine Review Update: Treatments for the motor symptoms of Parkinson's disease. Mov. Disord. 26 Suppl 3, S2-41. https://doi.org/10.1002/mds.23829

Francardo, V., Recchia, A., Popovic, N., Andersson, D., Nissbrandt, H., Cenci, M.A., 2011. Impact of the lesion procedure on the profiles of motor impairment and molecular responsiveness to L-DOPA in the 6-hydroxydopamine mouse model of Parkinson's disease. Neurobiology of Disease 42, 327–340. https://doi.org/10.1016/j.nbd.2011.01.024

Franchini, L., Stanic, J., Ponzoni, L., Mellone, M., Carrano, N., Musardo, S., Zianni, E., Olivero, G., Marcello, E., Pittaluga, A., Sala, M., Bellone, C., Racca, C., Di Luca, M., Gardoni, F., 2019. Linking NMDA Receptor Synaptic Retention to Synaptic Plasticity and Cognition. iScience 19, 927–939. https://doi.org/10.1016/j.isci.2019.08.036

Friesner, R.A., Banks, J.L., Murphy, R.B., Halgren, T.A., Klicic, J.J., Mainz, D.T., Repasky, M.P., Knoll, E.H., Shelley, M., Perry, J.K., Shaw, D.E., Francis, P., Shenkin, P.S., 2004. Glide: A New Approach for Rapid, Accurate Docking and Scoring. 1. Method and Assessment of Docking Accuracy. J. Med. Chem. 47, 1739–1749. https://doi.org/10.1021/jm0306430

Froula, J.M., Castellana-Cruz, M., Anabtawi, N.M., Camino, J.D., Chen, S.W., Thrasher, D.R., Freire, J., Yazdi, A.A., Fleming, S., Dobson, C.M., Kumita, J.R., Cremades, N., Volpicelli-Daley, L.A., 2019. Defining α-synuclein species responsible for Parkinson's disease phenotypes in mice. J. Biol. Chem. 294, 10392–10406. https://doi.org/10.1074/jbc.RA119.007743

Fujiwara, H., Hasegawa, M., Dohmae, N., Kawashima, A., Masliah, E., Goldberg, M.S., Shen, J., Takio, K., Iwatsubo, T., 2002. α-Synuclein is phosphorylated in synucleinopathy lesions. Nature Cell Biology 4, 160–164. https://doi.org/10.1038/ncb748

Fukuda, M., 2003. Distinct Rab Binding Specificity of Rim1, Rim2, Rabphilin, and Noc2. Journal of Biological Chemistry 278, 15373–15380. https://doi.org/10.1074/jbc.M212341200

Fumimura, Y., Ikemura, M., Saito, Y., Sengoku, R., Kanemaru, K., Sawabe, M., Arai, T., Ito, G., Iwatsubo, T., Fukayama, M., Mizusawa, H., Murayama, S., 2007. Analysis of the Adrenal Gland Is Useful for Evaluating Pathology of the Peripheral Autonomic Nervous System in Lewy Body Disease: Journal of Neuropathology and Experimental Neurology 66, 354–362. https://doi.org/10.1097/nen.0b013e3180517454

Fusco, G., Chen, S.W., Williamson, P.T.F., Cascella, R., Perni, M., Jarvis, J.A., Cecchi, C., Vendruscolo, M., Chiti, F., Cremades, N., Ying, L., Dobson, C.M., De Simone, A., 2017. Structural basis of membrane disruption and cellular toxicity by α-synuclein oligomers. Science 358, 1440–1443. https://doi.org/10.1126/science.aan6160

Fusco, G., Pape, T., Stephens, A.D., Mahou, P., Costa, A.R., Kaminski, C.F., Kaminski Schierle, G.S., Vendruscolo, M., Veglia, G., Dobson, C.M., De Simone, A., 2016. Structural basis of synaptic vesicle assembly promoted by α-synuclein. Nat Commun 7, 12563. https://doi.org/10.1038/ncomms12563

Gallegos, S., Pacheco, C., Peters, C., Opazo, C.M., Aguayo, L.G., 2015. Features of alpha-synuclein that could explain the progression and irreversibility of Parkinson's disease. Front. Neurosci. 9. https://doi.org/10.3389/fnins.2015.00059

Galpern, W., 1996. Cell-mediated delivery of brain-derived neurotrophic factor enhances dopamine levels in an MPP+ rat model of substantia nigra degeneration. Cell Transplantation 5, 225–232. https://doi.org/10.1016/0963-6897(95)02030-6

Galvin, J.E., Lee, V.M.-Y., Trojanowski, J.Q., 2001. Synucleinopathies: Clinical and Pathological Implications. Arch Neurol 58, 186. https://doi.org/10.1001/archneur.58.2.186

Games, D., Seubert, P., Rockenstein, E., Patrick, C., Trejo, M., Ubhi, K., Ettle, B., Ghassemiam, M., Barbour, R., Schenk, D., Nuber, S., Masliah, E., 2013. Axonopathy in an α-Synuclein Transgenic Model of Lewy Body Disease Is Associated with Extensive Accumulation of C-Terminal–Truncated α-Synuclein. The American Journal of Pathology 182, 940–953. https://doi.org/10.1016/j.ajpath.2012.11.018

Ganguly, U., Chakrabarti, S.S., Kaur, U., Mukherjee, A., Chakrabarti, S., 2018. Alpha-synuclein, Proteotoxicity and Parkinson's Disease: Search for Neuroprotective Therapy. CN 16, 1086–1097. https://doi.org/10.2174/1570159X15666171129100944

Gao, H.-M., Kotzbauer, P.T., Uryu, K., Leight, S., Trojanowski, J.Q., Lee, V.M.-Y., 2008. Neuroinflammation and Oxidation/Nitration of -Synuclein Linked to Dopaminergic Neurodegeneration. Journal of Neuroscience 28, 7687–7698. https://doi.org/10.1523/JNEUROSCI.0143-07.2008

Gardoni, F., 2006. A Critical Interaction between NR2B and MAGUK in L-DOPA Induced Dyskinesia. Journal of Neuroscience 26, 2914–2922. https://doi.org/10.1523/JNEUROSCI.5326-05.2006

Gardoni, F., Bellone, C., 2015. Modulation of the glutamatergic transmission by Dopamine: a focus on Parkinson, Huntington and Addiction diseases. Front. Cell. Neurosci. 9. https://doi.org/10.3389/fncel.2015.00025

Gardoni, F., Di Luca, M., 2015. Targeting glutamatergic synapses in Parkinson's disease. Current Opinion in Pharmacology 20, 24–28. https://doi.org/10.1016/j.coph.2014.10.011

Gardoni, F., Schrama, L.H., Kamal, A., Gispen, W.H., Cattabeni, F., Di Luca, M., 2001. Hippocampal Synaptic Plasticity Involves Competition between Ca $^{2+}$ /Calmodulin-Dependent Protein Kinase II and Postsynaptic Density 95 for Binding to the NR2A Subunit of the NMDA Receptor. J. Neurosci. 21, 1501–1509. https://doi.org/10.1523/JNEUROSCI.21-05-01501.2001

Gardoni, F., Sgobio, C., Pendolino, V., Calabresi, P., Di Luca, M., Picconi, B., 2012. Targeting NR2A-containing NMDA receptors reduces L-DOPA-induced dyskinesias. Neurobiology of Aging 33, 2138–2144. https://doi.org/10.1016/j.neurobiolaging.2011.06.019

Garitaonandia, I., Gonzalez, R., Christiansen-Weber, T., Abramihina, T., Poustovoitov, M., Noskov, A., Sherman, G., Semechkin, A., Snyder, E., Kern, R., 2016. Neural Stem Cell Tumorigenicity and Biodistribution Assessment for Phase I Clinical Trial in Parkinson's Disease. Sci Rep 6, 34478. https://doi.org/10.1038/srep34478

Garnett, E.S., Firnau, G., Nahmias, C., 1983. Dopamine visualized in the basal ganglia of living man. Nature 305, 137–138. https://doi.org/10.1038/305137a0

George, J.M., Jin, H., Woods, W.S., Clayton, D.F., 1995. Characterization of a novel protein regulated during the critical period for song learning in the zebra finch. Neuron 15, 361–372. https://doi.org/10.1016/0896-6273(95)90040-3

George, S., Brundin, P., 2015. Immunotherapy in Parkinson's Disease: Micromanaging Alpha-Synuclein Aggregation. JPD 5, 413–424. https://doi.org/10.3233/JPD-150630

Geppert, M., Südhof, T.C., 1998. RAB3 AND SYNAPTOTAGMIN: The Yin and Yang of Synaptic Membrane Fusion. Annu. Rev. Neurosci. 21, 75–95. https://doi.org/10.1146/annurev.neuro.21.1.75

Gerfen, C., Engber, T., Mahan, L., Susel, Z., Chase, T., Monsma, F., Sibley, D., 1990. D1 and D2 dopamine receptor-regulated gene expression of striatonigral and striatopallidal neurons. Science 250, 1429–1432. https://doi.org/10.1126/science.2147780

Ghiglieri, V., Calabrese, V., Calabresi, P., 2018. Alpha-Synuclein: From Early Synaptic Dysfunction to Neurodegeneration. Front. Neurol. 9, 295. https://doi.org/10.3389/fneur.2018.00295

Gibb, W.R., Lees, A.J., 1988. The relevance of the Lewy body to the pathogenesis of idiopathic Parkinson's disease. Journal of Neurology, Neurosurgery & Psychiatry 51, 745–752. https://doi.org/10.1136/jnnp.51.6.745

Glinka, Y.Y., Youdim, M.B.H., 1995. Inhibition of mitochondrial complexes I and IV by 6-hydroxydopamine. European Journal of Pharmacology: Environmental Toxicology and Pharmacology 292, 329–332. https://doi.org/10.1016/0926-6917(95)90040-3

Gnanalingham, K.K., Milkowski, N.A., Smith, L.A., Hunter, A.J., Jenner, P., Marsden, C.D., 1995. Short and long-term changes in cerebral [14C]-2-deoxyglucose uptake in the MPTP-treated marmoset: relationship to locomotor activity. J. Neural Transmission 101, 65–82. https://doi.org/10.1007/BF01271546

Goetz, C.G., 2011. The History of Parkinson's Disease: Early Clinical Descriptions and Neurological Therapies. Cold Spring Harbor Perspectives in Medicine 1, a008862–a008862. https://doi.org/10.1101/cshperspect.a008862

Gombash, S.E., Manfredsson, F.P., Kemp, C.J., Kuhn, N.C., Fleming, S.M., Egan, A.E., Grant, L.M., Ciucci, M.R., MacKeigan, J.P., Sortwell, C.E., 2013. Morphological and Behavioral Impact of AAV2/5-Mediated Overexpression of Human Wildtype Alpha-Synuclein in the Rat Nigrostriatal System. PLoS ONE 8, e81426. https://doi.org/10.1371/journal.pone.0081426

Gómez-Benito, M., Granado, N., García-Sanz, P., Michel, A., Dumoulin, M., Moratalla, R., 2020. Modeling Parkinson's Disease With the Alpha-Synuclein Protein. Front. Pharmacol. 11, 356. https://doi.org/10.3389/fphar.2020.00356

Greten-Harrison, B., Polydoro, M., Morimoto-Tomita, M., Diao, L., Williams, A.M., Nie, E.H., Makani, S., Tian, N., Castillo, P.E., Buchman, V.L., Chandra, S.S., 2010. -Synuclein triple knockout mice reveal age-dependent neuronal dysfunction. Proceedings of the National Academy of Sciences 107, 19573–19578. https://doi.org/10.1073/pnas.1005005107

Groc, L., Heine, M., Cousins, S.L., Stephenson, F.A., Lounis, B., Cognet, L., Choquet, D., 2006. NMDA receptor surface mobility depends on NR2A-2B subunits. Proceedings of the National Academy of Sciences 103, 18769–18774. https://doi.org/10.1073/pnas.0605238103

Guardia-Laguarta, C., Area-Gomez, E., Schon, E.A., Przedborski, S., 2015. Novel subcellular localization for α-synuclein: possible functional consequences. Front. Neuroanat. 9. https://doi.org/10.3389/fnana.2015.00017

Guerrero-Ferreira, R., Taylor, N.M., Mona, D., Ringler, P., Lauer, M.E., Riek, R., Britschgi, M., Stahlberg, H., 2018. Cryo-EM structure of alpha-synuclein fibrils. eLife 7, e36402. https://doi.org/10.7554/eLife.36402

Guo, J.T., Chen, A.Q., Kong, Q., Zhu, H., Ma, C.M., Qin, C., 2008. Inhibition of Vesicular Monoamine Transporter-2 Activity in α-Synuclein Stably Transfected SH-SY5Y Cells. Cell Mol Neurobiol 28, 35–47. https://doi.org/10.1007/s10571-007-9227-0

Hagan, J.J., Middlemiss, D.N., Sharpe, P.C., Poste, G.H., 1997. Parkinson's disease: prospects for improved drug therapy. Trends in Pharmacological Sciences 18, 156–163. https://doi.org/10.1016/S0165-6147(97)01050-X

Hallett, P.J., Dunah, A.W., Ravenscroft, P., Zhou, S., Bezard, E., Crossman, A.R., Brotchie, J.M., Standaert, D.G., 2005. Alterations of striatal NMDA receptor subunits associated with the development of dyskinesia in the MPTP-lesioned primate model of Parkinson's disease. Neuropharmacology 48, 503–516. https://doi.org/10.1016/j.neuropharm.2004.11.008

Handley, M.T.W., Burgoyne, R.D., 2008. The Rab27 effector Rabphilin, unlike Granuphilin and Noc2, rapidly exchanges between secretory granules and cytosol in PC12 cells. Biochemical and Biophysical Research Communications 373, 275–281. https://doi.org/10.1016/j.bbrc.2008.06.043

Hansen, K.B., Yi, F., Perszyk, R.E., Furukawa, H., Wollmuth, L.P., Gibb, A.J., Traynelis, S.F., 2018. Structure, function, and allosteric modulation of NMDA receptors. Journal of General Physiology 150, 1081–1105. https://doi.org/10.1085/jgp.201812032

Harder, E., Damm, W., Maple, J., Wu, C., Reboul, M., Xiang, J.Y., Wang, L., Lupyan, D., Dahlgren, M.K., Knight, J.L., Kaus, J.W., Cerutti, D.S., Krilov, G., Jorgensen, W.L., Abel, R.,

Friesner, R.A., 2016. OPLS3: A Force Field Providing Broad Coverage of Drug-like Small Molecules and Proteins. J. Chem. Theory Comput. 12, 281–296. https://doi.org/10.1021/acs.jctc.5b00864

Hardingham, G.E., Bading, H., 2010. Synaptic versus extrasynaptic NMDA receptor signalling: implications for neurodegenerative disorders. Nat Rev Neurosci 11, 682–696. https://doi.org/10.1038/nrn2911

Harris, K.M., 1999. Structure, development, and plasticity of dendritic spines. Current Opinion in Neurobiology 9, 343–348. https://doi.org/10.1016/S0959-4388(99)80050-6

Hawkes, C.H., Del Tredici, K., Braak, H., 2009. Parkinson's Disease: The Dual Hit Theory Revisited. Annals of the New York Academy of Sciences 1170, 615–622. https://doi.org/10.1111/j.1749-6632.2009.04365.x

Hawkes, C.H., Del Tredici, K., Braak, H., 2007. Parkinson's disease: a dual-hit hypothesis. Neuropathol Appl Neurobiol 33, 599–614. https://doi.org/10.1111/j.1365-2990.2007.00874.x

Healy, D.G., Falchi, M., O'Sullivan, S.S., Bonifati, V., Durr, A., Bressman, S., Brice, A., Aasly, J., Zabetian, C.P., Goldwurm, S., Ferreira, J.J., Tolosa, E., Kay, D.M., Klein, C., Williams, D.R., Marras, C., Lang, A.E., Wszolek, Z.K., Berciano, J., Schapira, A.H., Lynch, T., Bhatia, K.P., Gasser, T., Lees, A.J., Wood, N.W., 2008. Phenotype, genotype, and worldwide genetic penetrance of LRRK2-associated Parkinson's disease: a case-control study. The Lancet Neurology 7, 583–590. https://doi.org/10.1016/S1474-4422(08)70117-0

Heise, H., Hoyer, W., Becker, S., Andronesi, O.C., Riedel, D., Baldus, M., 2005. Molecular-level secondary structure, polymorphism, and dynamics of full-length α-synuclein fibrils studied by solid-state NMR. PNAS 102, 15871–15876. https://doi.org/10.1073/pnas.0506109102

Hely, M.A., Morris, J.G.L., Reid, W.G.J., Trafficante, R., 2005. Sydney Multicenter Study of Parkinson's disease: non-L-dopa-responsive problems dominate at 15 years. Mov. Disord. 20, 190–199. https://doi.org/10.1002/mds.20324

Heras-Garvin, A., Stefanova, N., 2020. From Synaptic Protein to Prion: The Long and Controversial Journey of α-Synuclein. Front. Synaptic Neurosci. 12, 584536. https://doi.org/10.3389/fnsyn.2020.584536

Hering, H., Sheng, M., 2001. Dentritic spines : structure, dynamics and regulation. Nat Rev Neurosci 2, 880–888. https://doi.org/10.1038/35104061

Hirsch, E.C., Hunot, S., 2009. Neuroinflammation in Parkinson's disease: a target for neuroprotection? The Lancet Neurology 8, 382–397. https://doi.org/10.1016/S1474-4422(09)70062-6

Hong, Z., Shi, M., Chung, K.A., Quinn, J.F., Peskind, E.R., Galasko, D., Jankovic, J., Zabetian, C.P., Leverenz, J.B., Baird, G., Montine, T.J., Hancock, A.M., Hwang, H., Pan, C., Bradner, J., Kang, U.J., Jensen, P.H., Zhang, J., 2010. DJ-1 and α-synuclein in human cerebrospinal fluid as biomarkers of Parkinson's disease. Brain 133, 713–726. https://doi.org/10.1093/brain/awq008

Hoyer, W., Cherny, D., Subramaniam, V., Jovin, T.M., 2004. Impact of the Acidic C-Terminal Region Comprising Amino Acids 109−140 on α-Synuclein Aggregation in Vitro †. Biochemistry 43, 16233–16242. https://doi.org/10.1021/bi048453u

Hubble, J.P., 2002. Long-term studies of dopamine agonists. Neurology 58, S42–S50. https://doi.org/10.1212/WNL.58.suppl_1.S42

Huganir, R.L., Nicoll, R.A., 2013. AMPARs and Synaptic Plasticity: The Last 25 Years. Neuron 80, 704–717. https://doi.org/10.1016/j.neuron.2013.10.025

Hwang, C.J., Lee, H.P., Choi, D.-Y., Jeong, H.S., Kim, T.H., Lee, T.H., Kim, Y.M., Moon, D.B., Park, S.S., Kim, S.Y., Oh, K.-W., Hwang, D.Y., Han, S.-B., Lee, H.-J., Hong, J.T., 2016. Inhibitory effect of thiacremonone on MPTP-induced dopaminergic neurodegeneration through inhibition of p38 activation. Oncotarget 7, 46943–46958. https://doi.org/10.18632/oncotarget.10504

Iacono, D., Geraci-Erck, M., Rabin, M.L., Adler, C.H., Serrano, G., Beach, T.G., Kurlan, R., 2015. Parkinson disease and incidental Lewy body disease: Just a question of time? Neurology 85, 1670–1679. https://doi.org/10.1212/WNL.0000000000002102

Iljina, M., Garcia, G.A., Horrocks, M.H., Tosatto, L., Choi, M.L., Ganzinger, K.A., Abramov, A.Y., Gandhi, S., Wood, N.W., Cremades, N., Dobson, C.M., Knowles, T.P.J., Klenerman, D., 2016. Kinetic model of the aggregation of alpha-synuclein provides insights into prion-like spreading. PNAS 113, E1206–E1215. https://doi.org/10.1073/pnas.1524128113

International Parkinson's Disease Genomics Consortium (IPDGC), Parkinson's Study Group (PSG) Parkinson's Research: The Organized GENetics Initiative (PROGENI), 23andMe, GenePD, NeuroGenetics Research Consortium (NGRC), Hussman Institute of Human Genomics (HIHG), The Ashkenazi Jewish Dataset Investigator, Cohorts for Health and Aging Research in Genetic Epidemiology (CHARGE), North American Brain Expression Consortium (NABEC), United Kingdom Brain Expression Consortium (UKBEC), Greek Parkinson's Disease Consortium, Alzheimer Genetic Analysis Group, Nalls, M.A., Pankratz, N., Lill, C.M., Do, C.B., Hernandez, D.G., Saad, M., DeStefano, A.L., Kara, E., Bras, J., Sharma, M., Schulte, C., Keller, M.F., Arepalli, S., Letson, C., Edsall, C., Stefansson, H., Liu, X., Pliner, H., Lee, J.H., Cheng, R., Ikram, M.A., Ioannidis, J.P.A., Hadjigeorgiou, G.M., Bis, J.C., Martinez, M., Perlmutter, J.S., Goate, A., Marder, K., Fiske, B., Sutherland, M., Xiromerisiou, G., Myers, R.H., Clark, L.N., Stefansson, K., Hardy, J.A., Heutink, P., Chen, H., Wood, N.W., Houlden, H., Payami, H., Brice, A., Scott, W.K., Gasser, T., Bertram, L., Eriksson, N., Foroud, T., Singleton, A.B., 2014. Large-scale meta-analysis of genome-wide association data identifies six new risk loci for Parkinson's disease. Nat Genet 46, 989–993. https://doi.org/10.1038/ng.3043

Ip, C.W., Klaus, L.-C., Karikari, A.A., Visanji, N.P., Brotchie, J.M., Lang, A.E., Volkmann, J., Koprich, J.B., 2017. AAV1/2-induced overexpression of A53T-α-synuclein in the substantia nigra results in degeneration of the nigrostriatal system with Lewy-like pathology and motor impairment: a new mouse model for Parkinson's disease. acta neuropathol commun 5, 11. https://doi.org/10.1186/s40478-017-0416-x

Irwin, D.J., White, M.T., Toledo, J.B., Xie, S.X., Robinson, J.L., Van Deerlin, V., Lee, V.M.-Y., Leverenz, J.B., Montine, T.J., Duda, J.E., Hurtig, H.I., Trojanowski, J.Q., 2012. Neuropathologic substrates of Parkinson disease dementia. Ann Neurol. 72, 587–598. https://doi.org/10.1002/ana.23659

Iwanaga, K., Wakabayashi, K., Yoshimoto, M., Tomita, I., Satoh, H., Takashima, H., Satoh, A., Seto, M., Tsujihata, M., Takahashi, H., 1999. Lewy body-type degeneration in cardiac plexus in Parkinson's and incidental Lewy body diseases. Neurology 52, 1269–1269. https://doi.org/10.1212/WNL.52.6.1269

Jankovic, J., Poewe, W., 2012. Therapies in Parkinson's disease: Current Opinion in Neurology 25, 433–447. https://doi.org/10.1097/WCO.0b013e3283542fc2

Jenner, P., 1995. The rationale for the use of dopamine agonists in Parkinson's disease. Neurology 45, S6–S12. https://doi.org/10.1212/WNL.45.3_Suppl_3.S6

Jenner, P., Zeng, B.-Y., Smith, L.A., Pearce, R.K.B., Tel, B., Chancharme, L., Moachon, G., 2000. Antiparkinsonian and neuroprotective effects of modafinil in the mptp-treated common marmoset. Experimental Brain Research 133, 178–188. https://doi.org/10.1007/s002210000370

Jo, E., McLaurin, J., Yip, C.M., St. George-Hyslop, P., Fraser, P.E., 2000. α-Synuclein Membrane Interactions and Lipid Specificity. Journal of Biological Chemistry 275, 34328–34334. https://doi.org/10.1074/jbc.M004345200

Johnson, J.W., Ascher, P., 1987. Glycine potentiates the NMDA response in cultured mouse brain neurons. Nature 325, 529–531. https://doi.org/10.1038/325529a0

Kaech, S., Banker, G., 2006. Culturing hippocampal neurons. Nat Protoc 1, 2406–2415. https://doi.org/10.1038/nprot.2006.356

Kalia, L.V., Lang, A.E., 2015. Parkinson's disease. The Lancet 386, 896–912. https://doi.org/10.1016/S0140-6736(14)61393-3

Kato, M., Sasaki, T., Ohya, T., Nakanishi, H., Nishioka, H., Imamura, M., Takai, Y., 1996. Physical and Functional Interaction of Rabphilin-3A with α-Actinin. Journal of Biological Chemistry 271, 31775–31778. https://doi.org/10.1074/jbc.271.50.31775

Kempster, P.A., O'Sullivan, S.S., Holton, J.L., Revesz, T., Lees, A.J., 2010. Relationships between age and late progression of Parkinson's disease: a clinico-pathological study. Brain 133, 1755–1762. https://doi.org/10.1093/brain/awq059

Kilarski, L.L., Pearson, J.P., Newsway, V., Majounie, E., Knipe, M.D.W., Misbahuddin, A., Chinnery, P.F., Burn, D.J., Clarke, C.E., Marion, M.-H., Lewthwaite, A.J., Nicholl, D.J., Wood, N.W., Morrison, K.E., Williams-Gray, C.H., Evans, J.R., Sawcer, S.J., Barker, R.A., Wickremaratchi, M.M., Ben-Shlomo, Y., Williams, N.M., Morris, H.R., 2012. Systematic Review and UK-Based Study of *PARK2 (parkin), PINK1, PARK7 (DJ-1)* and *LRRK2* in early-onset Parkinson's disease: *PARK2, PINK1, PARK7, LRRK2* in EOPD. Mov. Disord. 27, 1522–1529. https://doi.org/10.1002/mds.25132

Kim, B.G., Dai, H.-N., McAtee, M., Vicini, S., Bregman, B.S., 2007. Labeling of dendritic spines with the carbocyanine dye DiI for confocal microscopic imaging in lightly fixed cortical slices. Journal of Neuroscience Methods 162, 237–243. https://doi.org/10.1016/j.jneumeth.2007.01.016

Kim, J., 1997. Evidence that the precursor protein of non-A beta component of Alzheimer's disease amyloid (NACP) has an extended structure primarily composed of random-coil. Mol Cells 7, 78–83.

Kim, S., Kwon, S.-H., Kam, T.-I., Panicker, N., Karuppagounder, S.S., Lee, S., Lee, J.H., Kim, W.R., Kook, M., Foss, C.A., Shen, C., Lee, H., Kulkarni, S., Pasricha, P.J., Lee, G., Pomper, M.G., Dawson, V.L., Dawson, T.M., Ko, H.S., 2019. Transneuronal Propagation of Pathologic α-Synuclein from the Gut to the Brain Models Parkinson's Disease. Neuron 103, 627-641.e7. https://doi.org/10.1016/j.neuron.2019.05.035

Kitada, T., Asakawa, S., Hattori, N., Matsumine, H., Yamamura, Y., Minoshima, S., Yokochi, M., Mizuno, Y., Shimizu, N., 1998. Mutations in the parkin gene cause autosomal recessive juvenile parkinsonism. Nature 392, 605–608. https://doi.org/10.1038/33416

Klein, C., Westenberger, A., 2012. Genetics of Parkinson's Disease. Cold Spring Harb Perspect Med 2, a008888. https://doi.org/10.1101/cshperspect.a008888

Komuro, R., Sasaki, T., Orita, S., Maeda, M., Takai, Y., 1996. Involvement of Rabphilin-3A in Ca2+-Dependent Exocytosis from PC12 Cells. Biochemical and Biophysical Research Communications 219, 435–440. https://doi.org/10.1006/bbrc.1996.0251

Kopec, C.D., 2006. Glutamate Receptor Exocytosis and Spine Enlargement during Chemically Induced Long-Term Potentiation. Journal of Neuroscience 26, 2000–2009. https://doi.org/10.1523/JNEUROSCI.3918-05.2006

Koprich, J.B., Johnston, T.H., Huot, P., Reyes, M.G., Espinosa, M., Brotchie, J.M., 2011. Progressive Neurodegeneration or Endogenous Compensation in an Animal Model of Parkinson's Disease Produced by Decreasing Doses of Alpha-Synuclein. PLoS ONE 6, e17698. https://doi.org/10.1371/journal.pone.0017698

Koprich, J.B., Johnston, T.H., Reyes, M.G., Sun, X., Brotchie, J.M., 2010. Expression of human A53T alpha-synuclein in the rat substantia nigra using a novel AAV1/2 vector produces a rapidly evolving pathology with protein aggregation, dystrophic neurite architecture and nigrostriatal degeneration with potential to model the pathology of Parkinson's disease. Mol Neurodegeneration 5, 43. https://doi.org/10.1186/1750-1326-5-43

Kordower, J.H., Dodiya, H.B., Kordower, A.M., Terpstra, B., Paumier, K., Madhavan, L., Sortwell, C., Steece-Collier, K., Collier, T.J., 2011. Transfer of host-derived alpha synuclein to grafted dopaminergic neurons in rat. Neurobiology of Disease 43, 552–557. https://doi.org/10.1016/j.nbd.2011.05.001

Krüger, R., Kuhn, W., Müller, T., Woitalla, D., Graeber, M., Kösel, S., Przuntek, H., Epplen, J.T., Schols, L., Riess, O., 1998. AlaSOPro mutation in the gene encoding α-synuclein in Parkinson's disease. Nat Genet 18, 106–108. https://doi.org/10.1038/ng0298-106

Kuan, W.-L., Stott, K., He, X., Wood, T.C., Yang, S., Kwok, J.C.F., Hall, K., Zhao, Y., Tietz, O., Aigbirhio, F.I., Vernon, A.C., Barker, R.A., 2019. Systemic α-synuclein injection triggers selective neuronal pathology as seen in patients with Parkinson's disease. Molecular Psychiatry 1–12. https://doi.org/10.1038/s41380-019-0608-9

Kusumi, M., Nakashima, K., Harada, H., Nakayama, H., Takahashi, K., 1996. Epidemiology of Parkinson's Disease in Yonago City, Japan: Comparison with a Study Carried Out 12 Years Ago. Neuroepidemiology 15, 201–207. https://doi.org/10.1159/000109908

Langston, J.W., 2017. The MPTP Story. JPD 7, S11–S19. https://doi.org/10.3233/JPD-179006

Langston, J.W., Langston, E.B., Irwin, I., 1984. MPTP-induced parkinsonism in human and non-human primates--clinical and experimental aspects. Acta Neurol Scand Suppl 100, 49–54.

Lesage, S., Anheim, M., Letournel, F., Bousset, L., Honoré, A., Rozas, N., Pieri, L., Madiona, K., Dürr, A., Melki, R., Verny, C., Brice, A., for the French Parkinson's Disease Genetics Study Group, 2013. G51D α-synuclein mutation causes a novel Parkinsonian-pyramidal syndrome: SNCA G51D in Parkinsonism. Ann Neurol. 73, 459–471. https://doi.org/10.1002/ana.23894

Lester, J., Fink, S., Aronin, N., DiFiglia, M., 1993. Colocalization of D1 and D2 dopamine receptor mRNAs in striatal neurons. Brain Research 621, 106–110. https://doi.org/10.1016/0006-8993(93)90303-5

LeWitt, P.A., Fahn, S., 2016. Levodopa therapy for Parkinson disease: A look backward and forward. Neurology 86, S3-12. https://doi.org/10.1212/WNL.0000000000002509

Li, C., Takei, K., Geppert, M., Daniell, L., Stenius, K., Chapman, E.R., Jahn, R., De Camilli, P., Südhof, T.C., 1994. Synaptic targeting of rabphilin-3A, a synaptic vesicle Ca2+/phospholipid-binding protein, depends on rab3A/3C. Neuron 13, 885–898. https://doi.org/10.1016/0896-6273(94)90254-2

Li, J.-Y., Englund, E., Holton, J.L., Soulet, D., Hagell, P., Lees, A.J., Lashley, T., Quinn, N.P., Rehncrona, S., Björklund, A., Widner, H., Revesz, T., Lindvall, O., Brundin, P., 2008. Lewy bodies in grafted neurons in subjects with Parkinson's disease suggest host-to-graft disease propagation. Nature Medicine 14, 501–503. https://doi.org/10.1038/nm1746

Li, Y., Zhao, C., Luo, F., Liu, Z., Gui, X., Luo, Z., Zhang, X., Li, D., Liu, C., Li, X., 2018. Amyloid fibril structure of α-synuclein determined by cryo-electron microscopy. Cell Research 28, 897–903. https://doi.org/10.1038/s41422-018-0075-x

Lin, X., Parisiadou, L., Sgobio, C., Liu, G., Yu, J., Sun, L., Shim, H., Gu, X.-L., Luo, J., Long, C.-X., Ding, J., Mateo, Y., Sullivan, P.H., Wu, L.-G., Goldstein, D.S., Lovinger, D., Cai, H., 2012. Conditional Expression of Parkinson's Disease-Related Mutant -Synuclein in the Midbrain Dopaminergic Neurons Causes Progressive Neurodegeneration and Degradation of Transcription Factor Nuclear Receptor Related 1. Journal of Neuroscience 32, 9248–9264. https://doi.org/10.1523/JNEUROSCI.1731-12.2012

Liu, S.J., Zukin, R.S., 2007. Ca2+-permeable AMPA receptors in synaptic plasticity and neuronal death. Trends in Neurosciences 30, 126–134. https://doi.org/10.1016/j.tins.2007.01.006

Longhena, F., Faustini, G., Spillantini, M.G., Bellucci, A., 2019. Living in Promiscuity: The Multiple Partners of Alpha-Synuclein at the Synapse in Physiology and Pathology. IJMS 20, 141. https://doi.org/10.3390/ijms20010141

Lopes, F.M., Bristot, I.J., da Motta, L.L., Parsons, R.B., Klamt, F., 2017. Mimicking Parkinson's Disease in a Dish: Merits and Pitfalls of the Most Commonly used Dopaminergic In Vitro Models. Neuromol Med 19, 241–255. https://doi.org/10.1007/s12017-017-8454-x

Lotharius, J., Brundin, P., 2002. Pathogenesis of parkinson's disease: dopamine, vesicles and α-synuclein. Nat Rev Neurosci 3, 932–942. https://doi.org/10.1038/nrn983

Lu, J., Sun, F., Ma, H., Qing, H., Deng, Y., 2015. Comparison between α-synuclein wild-type and A53T mutation in a progressive Parkinson's disease model. Biochemical and Biophysical Research Communications 464, 988–993. https://doi.org/10.1016/j.bbrc.2015.07.007

Luk, K.C., Kehm, V., Carroll, J., Zhang, B., O'Brien, P., Trojanowski, J.Q., Lee, V.M.-Y., 2012a. Pathological α-Synuclein Transmission Initiates Parkinson-like Neurodegeneration in Nontransgenic Mice. Science 338, 949–953. https://doi.org/10.1126/science.1227157

Luk, K.C., Kehm, V.M., Zhang, B., O'Brien, P., Trojanowski, J.Q., Lee, V.M.Y., 2012b. Intracerebral inoculation of pathological α-synuclein initiates a rapidly progressive

neurodegenerative α-synucleinopathy in mice. Journal of Experimental Medicine 209, 975–986. https://doi.org/10.1084/jem.20112457

Luk, K.C., Song, C., O'Brien, P., Stieber, A., Branch, J.R., Brunden, K.R., Trojanowski, J.Q., Lee, V.M.-Y., 2009. Exogenous α-synuclein fibrils seed the formation of Lewy body-like intracellular inclusions in cultured cells. PNAS 106, 20051–20056. https://doi.org/10.1073/pnas.0908005106

Mahlknecht, P., Hotter, A., Hussl, A., Esterhammer, R., Schocke, M., Seppi, K., 2010. Significance of MRI in diagnosis and differential diagnosis of Parkinson's disease. Neurodegener Dis 7, 300–318. https://doi.org/10.1159/000314495

Mahlknecht, P., Seppi, K., Poewe, W., 2015. The Concept of Prodromal Parkinson's Disease. JPD 5, 681–697. https://doi.org/10.3233/JPD-150685

Maroteaux, L., Campanelli, J.T., Scheller, R.H., 1988. Synuclein: a neuron-specific protein localized to the nucleus and presynaptic nerve terminal. J. Neurosci. 8, 2804–2815.

Martel, M.-A., Ryan, T.J., Bell, K.F.S., Fowler, J.H., McMahon, A., Al-Mubarak, B., Komiyama, N.H., Horsburgh, K., Kind, P.C., Grant, S.G.N., Wyllie, D.J.A., Hardingham, G.E., 2012. The Subtype of GluN2 C-terminal Domain Determines the Response to Excitotoxic Insults. Neuron 74, 543–556. https://doi.org/10.1016/j.neuron.2012.03.021

Martens, S., 2010. Role of C2 domain proteins during synaptic vesicle exocytosis. Biochemical Society Transactions 38, 213–216. https://doi.org/10.1042/BST0380213

Martinez-Martin, P., Rodriguez-Blazquez, C., Kurtis, M.M., Chaudhuri, K.R., NMSS Validation Group, 2011. The impact of non-motor symptoms on health-related quality of life of patients with Parkinson's disease. Mov. Disord. 26, 399–406. https://doi.org/10.1002/mds.23462

Masuda-Suzukake, M., Nonaka, T., Hosokawa, M., Kubo, M., Shimozawa, A., Akiyama, H., Hasegawa, M., 2014. Pathological alpha-synuclein propagates through neural networks. Acta Neuropathol Commun 2, 88. https://doi.org/10.1186/s40478-014-0088-8

Masuda-Suzukake, M., Nonaka, T., Hosokawa, M., Oikawa, T., Arai, T., Akiyama, H., Mann, D.M.A., Hasegawa, M., 2013. Prion-like spreading of pathological α-synuclein in brain. Brain 136, 1128–1138. https://doi.org/10.1093/brain/awt037

McGregor, M.M., Nelson, A.B., 2019. Circuit Mechanisms of Parkinson's Disease. Neuron 101, 1042–1056. https://doi.org/10.1016/j.neuron.2019.03.004

McKiernan, C.J., Stabila, P.F., Macara, I.G., 1996. Role of the Rab3A-binding domain in targeting of rabphilin-3A to vesicle membranes of PC12 cells. Mol Cell Biol 16, 4985–4995. https://doi.org/10.1128/MCB.16.9.4985

Melamed, E., Hefti, F., Wurtman, R.J., 1980. Nonaminergic striatal neurons convert exogenous l-dopa to dopamine in parkinsonism. Ann Neurol. 8, 558–563. https://doi.org/10.1002/ana.410080603

Melki, R., 2015. Role of Different Alpha-Synuclein Strains in Synucleinopathies, Similarities with other Neurodegenerative Diseases. Journal of Parkinson's Disease 5, 217–227. https://doi.org/10.3233/JPD-150543

Mellone, M., Gardoni, F., 2018. Glutamatergic mechanisms in l-DOPA-induced dyskinesia and therapeutic implications. J Neural Transm 125, 1225–1236. https://doi.org/10.1007/s00702-018-1846-8

Mellone, M., Gardoni, F., 2013. Modulation of NMDA receptor at the synapse: Promising therapeutic interventions in disorders of the nervous system. European Journal of Pharmacology 719, 75–83. https://doi.org/10.1016/j.ejphar.2013.04.054

Mellone, M., Stanic, J., Hernandez, L.F., Iglesias, E., Zianni, E., Longhi, A., Prigent, A., Picconi, B., Calabresi, P., Hirsch, E.C., Obeso, J.A., Di Luca, M., Gardoni, F., 2015. NMDA receptor GluN2A/GluN2B subunit ratio as synaptic trait of levodopa-induced dyskinesias: from experimental models to patients. Front. Cell. Neurosci. 9. https://doi.org/10.3389/fncel.2015.00245

Mendes-Pinheiro, B., Anjo, S.I., Manadas, B., Da Silva, J.D., Marote, A., Behie, L.A., Teixeira, F.G., Salgado, A.J., 2019. Bone Marrow Mesenchymal Stem Cells' Secretome Exerts Neuroprotective Effects in a Parkinson's Disease Rat Model. Front. Bioeng. Biotechnol. 7, 294. https://doi.org/10.3389/fbioe.2019.00294

Meredith, G.E., Rademacher, D.J., 2011. MPTP Mouse Models of Parkinson's Disease: An Update. Journal of Parkinson's Disease 1, 19–33. https://doi.org/10.3233/JPD-2011-11023

Michel, P.P., Hirsch, E.C., Hunot, S., 2016. Understanding Dopaminergic Cell Death Pathways in Parkinson Disease. Neuron 90, 675–691. https://doi.org/10.1016/j.neuron.2016.03.038

Middleton, E.R., Rhoades, E., 2010. Effects of Curvature and Composition on α-Synuclein Binding to Lipid Vesicles. Biophysical Journal 99, 2279–2288. https://doi.org/10.1016/j.bpj.2010.07.056

Mizoguchi, A., Yano, Y., Hamaguchi, H., Yanagida, H., Ide, C., Zahraoui, A., Shirataki, H., Sasaki, T., Takai, Y., 1994. Localization of Rabphilin-3A on the Synaptic Vesicle. Biochemical and Biophysical Research Communications 202, 1235–1243. https://doi.org/10.1006/bbrc.1994.2063

Moehle, M.S., West, A.B., 2015. M1 and M2 immune activation in Parkinson's Disease: Foe and ally? Neuroscience 302, 59–73. https://doi.org/10.1016/j.neuroscience.2014.11.018

Montaville, P., Coudevylle, N., Radhakrishnan, A., Leonov, A., Zweckstetter, M., Becker, S., 2008. The PIP2 binding mode of the C2 domains of rabphilin-3A. Protein Sci. 17, 1025–1034. https://doi.org/10.1110/ps.073326608

Monyer, H., Burnashev, N., Laurie, D.J., Sakmann, B., Seeburg, P.H., 1994. Developmental and regional expression in the rat brain and functional properties of four NMDA receptors. Neuron 12, 529–540. https://doi.org/10.1016/0896-6273(94)90210-0

Morimoto, R.I., 2011. The Heat Shock Response: Systems Biology of Proteotoxic Stress in Aging and Disease. Cold Spring Harb Symp Quant Biol 76, 91–99. https://doi.org/10.1101/sqb.2012.76.010637

Muenter, M.D., Tyce, G.M., 1971. L-dopa therapy of Parkinson's disease: plasma L-dopa concentration, therapeutic response, and side effects. Mayo Clin Proc 46, 231–239.

Müller, T., 2015. Catechol-O-Methyltransferase Inhibitors in Parkinson's Disease. Drugs 75, 157–174. https://doi.org/10.1007/s40265-014-0343-0

Nägerl, U.V., Eberhorn, N., Cambridge, S.B., Bonhoeffer, T., 2004. Bidirectional Activity-Dependent Morphological Plasticity in Hippocampal Neurons. Neuron 44, 759–767. https://doi.org/10.1016/j.neuron.2004.11.016

Nakai, M., Fujita, M., Waragai, M., Sugama, S., Wei, J., Akatsu, H., Ohtaka-Maruyama, C., Okado, H., Hashimoto, M., 2007. Expression of α-synuclein, a presynaptic protein implicated in Parkinson's disease, in erythropoietic lineage. Biochemical and Biophysical Research Communications 358, 104–110. https://doi.org/10.1016/j.bbrc.2007.04.108

Nambu, A., Tokuno, H., Hamada, I., Kita, H., Imanishi, M., Akazawa, T., Ikeuchi, Y., Hasegawa, N., 2000. Excitatory Cortical Inputs to Pallidal Neurons Via the Subthalamic Nucleus in the Monkey. Journal of Neurophysiology 84, 289–300. https://doi.org/10.1152/jn.2000.84.1.289

Nash, J.E., Johnston, T.H., Collingridge, G.L., Garner, C.C., Brotchie, J.M., 2005. Subcellular redistribution of the synapse-associated proteins PSD-95 and SAP97 in animal models of Parkinson&s disease and L-DOPA-induced dyskinesia. FASEB j. 19, 1–25. https://doi.org/10.1096/fj.04-1854fje

Navarria, L., Zaltieri, M., Longhena, F., Spillantini, M.G., Missale, C., Spano, P., Bellucci, A., 2015. Alpha-synuclein modulates NR2B-containing NMDA receptors and decreases their levels after rotenone exposure. Neurochemistry International 85–86, 14–23. https://doi.org/10.1016/j.neuint.2015.03.008

Newpher, T.M., Ehlers, M.D., 2008. Glutamate Receptor Dynamics in Dendritic Microdomains. Neuron 58, 472–497. https://doi.org/10.1016/j.neuron.2008.04.030

Nielsen, M.S., Vorum, H., Lindersson, E., Jensen, P.H., 2001. Ca2+ Binding to α-Synuclein Regulates Ligand Binding and Oligomerization. J. Biol. Chem. 276, 22680–22684. https://doi.org/10.1074/jbc.M101181200

Noyce, A.J., Bestwick, J.P., Silveira-Moriyama, L., Hawkes, C.H., Giovannoni, G., Lees, A.J., Schrag, A., 2012. Meta-analysis of early nonmotor features and risk factors for Parkinson disease. Ann. Neurol. 72, 893–901. https://doi.org/10.1002/ana.23687

Nutt, J.G., 2000. Effect of COMT inhibition on the pharmacokinetics and pharmacodynamics of levodopa in parkinsonian patients. Neurology 55, S33-37; discussion S38-41.

Nutt, J.G., Woodward, W.R., Beckner, R.M., Stone, C.K., Berggren, K., Carter, J.H., Gancher, S.T., Hammerstad, J.P., Gordin, A., 1994. Effect of peripheral catechol-O-methyltransferase inhibition on the pharmacokinetics and pharmacodynamics of levodopa in parkinsonian patients. Neurology 44, 913–913. https://doi.org/10.1212/WNL.44.5.913

Obeso, J.A., Rodriguez, M.C., DeLong, M.R., 1997. Basal ganglia pathophysiology. A critical review. Adv Neurol 74, 3–18.

Obeso, J.A., Rodriguez-Oroz, M.C., Rodriguez, M., Lanciego, J.L., Artieda, J., Gonzalo, N., Olanow, C.W., 2000. Pathophysiology of the basal ganglia in Parkinson's disease. Trends in Neurosciences 23, S8–S19. https://doi.org/10.1016/S1471-1931(00)00028-8

Obrenovitch, T.P., Urenjak, J., Zilkha, E., Jay, T.M., 2000. Excitotoxicity in neurological disorders — the glutamate paradox. Int. j. dev. neurosci. 18, 281–287. https://doi.org/10.1016/S0736-5748(99)00096-9

Oishi, H., Sasaki, T., Takai, Y., 1996. Interaction of Both the C2A and C2B Domains of Rabphilin3 with Ca2+and Phospholipid. Biochemical and Biophysical Research Communications 229, 498–503. https://doi.org/10.1006/bbrc.1996.1833

Olanow, C.W., Obeso, J.A., Stocchi, F., 2006. Continuous dopamine-receptor treatment of Parkinson's disease: scientific rationale and clinical implications. Lancet Neurol 5, 677–687. https://doi.org/10.1016/S1474-4422(06)70521-X

Olanow, C.W., Stern, M.B., Sethi, K., 2009. The scientific and clinical basis for the treatment of Parkinson disease (2009). Neurology 72, S1–S136. https://doi.org/10.1212/WNL.0b013e3181a1d44c

Oliveras-Salvá, M., Van der Perren, A., Casadei, N., Stroobants, S., Nuber, S., D'Hooge, R., Van den Haute, C., Baekelandt, V., 2013. rAAV2/7 vector-mediated overexpression of alpha-synuclein in mouse substantia nigra induces protein aggregation and progressive dose-dependent neurodegeneration. Mol Neurodegeneration 8, 44. https://doi.org/10.1186/1750-1326-8-44

Opazo, P., Choquet, D., 2011. A three-step model for the synaptic recruitment of AMPA receptors. Molecular and Cellular Neuroscience 46, 1–8. https://doi.org/10.1016/j.mcn.2010.08.014

Ostrerova, N., Petrucelli, L., Farrer, M., Mehta, N., Choi, P., Hardy, J., Wolozin, B., 1999. α-Synuclein Shares Physical and Functional Homology with 14-3-3 Proteins. J Neurosci 19, 5782–5791. https://doi.org/10.1523/JNEUROSCI.19-14-05782.1999

Oueslati, A., Fournier, M., Lashuel, H.A., 2010. Role of post-translational modifications in modulating the structure, function and toxicity of α-synuclein, in: Progress in Brain Research. Elsevier, pp. 115–145. https://doi.org/10.1016/S0079-6123(10)83007-9

Paille, V., Picconi, B., Bagetta, V., Ghiglieri, V., Sgobio, C., Di Filippo, M., Viscomi, M.T., Giampa, C., Fusco, F.R., Gardoni, F., Bernardi, G., Greengard, P., Di Luca, M., Calabresi, P., 2010. Distinct Levels of Dopamine Denervation Differentially Alter Striatal Synaptic Plasticity and NMDA Receptor Subunit Composition. Journal of Neuroscience 30, 14182–14193. https://doi.org/10.1523/JNEUROSCI.2149-10.2010

Paisán-Ruíz, C., Jain, S., Evans, E.W., Gilks, W.P., Simón, J., van der Brug, M., de Munain, A.L., Aparicio, S., Gil, A.M., Khan, N., Johnson, J., Martinez, J.R., Nicholl, D., Carrera, I.M., Peňa, A.S., de Silva, R., Lees, A., Martí-Massó, J.F., Pérez-Tur, J., Wood, N.W., Singleton, A.B., 2004. Cloning of the Gene Containing Mutations that Cause PARK8-Linked Parkinson's Disease. Neuron 44, 595–600. https://doi.org/10.1016/j.neuron.2004.10.023

Paoletti, P., Bellone, C., Zhou, Q., 2013. NMDA receptor subunit diversity: impact on receptor properties, synaptic plasticity and disease. Nat Rev Neurosci 14, 383–400. https://doi.org/10.1038/nrn3504

Park, S.E., Song, K.-I., Kim, H., Chung, S., Youn, I., 2018. Graded 6-OHDA-induced dopamine depletion in the nigrostriatal pathway evokes progressive pathological neuronal activities in the subthalamic nucleus of a hemi-parkinsonian mouse. Behavioural Brain Research 344, 42–47. https://doi.org/10.1016/j.bbr.2018.02.014

Parkinson, J., 2002. An Essay on the Shaking Palsy. JNP 14, 223–236. https://doi.org/10.1176/jnp.14.2.223

Patterson, J.R., Duffy, M.F., Kemp, C.J., Howe, J.W., Collier, T.J., Stoll, A.C., Miller, K.M., Patel, P., Levine, N., Moore, D.J., Luk, K.C., Fleming, S.M., Kanaan, N.M., Paumier, K.L., El-Agnaf, O.M.A., Sortwell, C.E., 2019. Time course and magnitude of alpha-synuclein inclusion formation and nigrostriatal degeneration in the rat model of synucleinopathy triggered by intrastriatal α-synuclein preformed fibrils. Neurobiology of Disease 130, 104525. https://doi.org/10.1016/j.nbd.2019.104525

Paumier, K.L., Luk, K.C., Manfredsson, F.P., Kanaan, N.M., Lipton, J.W., Collier, T.J., Steece-Collier, K., Kemp, C.J., Celano, S., Schulz, E., Sandoval, I.M., Fleming, S., Dirr, E., Polinski, N.K., Trojanowski, J.Q., Lee, V.M., Sortwell, C.E., 2015. Intrastriatal injection of pre-formed mouse α-synuclein fibrils into rats triggers α-synuclein pathology and bilateral nigrostriatal degeneration. Neurobiol. Dis. 82, 185–199. https://doi.org/10.1016/j.nbd.2015.06.003

PD MED Collaborative Group, 2014. Long-term effectiveness of dopamine agonists and monoamine oxidase B inhibitors compared with levodopa as initial treatment for Parkinson's disease (PD MED): a large, open-label, pragmatic randomised trial. The Lancet 384, 1196–1205. https://doi.org/10.1016/S0140-6736(14)60683-8

Peelaerts, W., Bousset, L., Van der Perren, A., Moskalyuk, A., Pulizzi, R., Giugliano, M., Van den Haute, C., Melki, R., Baekelandt, V., 2015. α-Synuclein strains cause distinct synucleinopathies after local and systemic administration. Nature 522, 340–344. https://doi.org/10.1038/nature14547

Penzes, P., Cahill, M.E., Jones, K.A., VanLeeuwen, J.-E., Woolfrey, K.M., 2011. Dendritic spine pathology in neuropsychiatric disorders. Nat Neurosci 14, 285–293. https://doi.org/10.1038/nn.2741

Perez, R.G., Waymire, J.C., Lin, E., Liu, J.J., Guo, F., Zigmond, M.J., 2002. A role for alpha-synuclein in the regulation of dopamine biosynthesis. J. Neurosci. 22, 3090–3099. https://doi.org/20026307

Perez-Lloret, S., Rascol, O., 2018. Efficacy and safety of amantadine for the treatment of l-DOPA-induced dyskinesia. J Neural Transm 125, 1237–1250. https://doi.org/10.1007/s00702-018-1869-1

Perez-Lloret, S., Rey, M.V., Pavy-Le Traon, A., Rascol, O., 2013. Emerging drugs for autonomic dysfunction in Parkinson's disease. Expert Opin Emerg Drugs 18, 39–53. https://doi.org/10.1517/14728214.2013.766168

Perez-Pardo, P., Kliest, T., Dodiya, H.B., Broersen, L.M., Garssen, J., Keshavarzian, A., Kraneveld, A.D., 2017. The gut-brain axis in Parkinson's disease: Possibilities for food-based therapies. European Journal of Pharmacology 817, 86–95. https://doi.org/10.1016/j.ejphar.2017.05.042

Peters, A., Kaiserman-Abramof, I.R., 1970. The small pyramidal neuron of the rat cerebral cortex. The perikaryon, dendrites and spines. Am. J. Anat. 127, 321–355. https://doi.org/10.1002/aja.1001270402

Picconi, B., Pisani, A., Barone, I., Bonsi, P., Centonze, D., Bernardi, G., Calabresi, P., 2005. Pathological Synaptic Plasticity in the Striatum: Implications for Parkinson's Disease. NeuroToxicology 26, 779–783. https://doi.org/10.1016/j.neuro.2005.02.002

Pickrell, A.M., Youle, R.J., 2015. The Roles of PINK1, Parkin, and Mitochondrial Fidelity in Parkinson's Disease. Neuron 85, 257–273. https://doi.org/10.1016/j.neuron.2014.12.007

Pieri, L., Madiona, K., Melki, R., 2016. Structural and functional properties of prefibrillar α-synuclein oligomers. Scientific Reports 6, 1–15. https://doi.org/10.1038/srep24526

Pignataro, D., Sucunza, D., Rico, A.J., Dopeso-Reyes, I.G., Roda, E., Rodríguez-Perez, A.I., Labandeira-Garcia, J.L., Broccoli, V., Kato, S., Kobayashi, K., Lanciego, J.L., 2018. Gene therapy approaches in the non-human primate model of Parkinson's disease. J Neural Transm 125, 575–589. https://doi.org/10.1007/s00702-017-1681-3

Pinter, B., Diem-Zangerl, A., Wenning, G.K., Scherfler, C., Oberaigner, W., Seppi, K., Poewe, W., 2015. Mortality in Parkinson's disease: A 38-year follow-up study: Mortality in Parkinson's Disease. Mov Disord. 30, 266–269. https://doi.org/10.1002/mds.26060

Pissadaki, E.K., Bolam, J.P., 2013. The energy cost of action potential propagation in dopamine neurons: clues to susceptibility in Parkinson's disease. Front. Comput. Neurosci. 7. https://doi.org/10.3389/fncom.2013.00013

Poewe, W., Antonini, A., 2015. Novel formulations and modes of delivery of levodopa: Novel Formulations and Delivery of Levodopa. Mov Disord. 30, 114–120. https://doi.org/10.1002/mds.26078

Poewe, W., Seppi, K., Tanner, C.M., Halliday, G.M., Brundin, P., Volkmann, J., Schrag, A.-E., Lang, A.E., 2017. Parkinson disease. Nat Rev Dis Primers 3, 17013. https://doi.org/10.1038/nrdp.2017.13

Polinski, N.K., Volpicelli-Daley, L.A., Sortwell, C.E., Luk, K.C., Cremades, N., Gottler, L.M., Froula, J., Duffy, M.F., Lee, V.M.Y., Martinez, T.N., Dave, K.D., 2018. Best Practices for Generating and Using Alpha-Synuclein Pre-Formed Fibrils to Model Parkinson's Disease in Rodents. JPD 8, 303–322. https://doi.org/10.3233/JPD-171248

Politis, M., 2014. Neuroimaging in Parkinson disease: from research setting to clinical practice. Nat Rev Neurol 10, 708–722. https://doi.org/10.1038/nrneurol.2014.205

Polymeropoulos, M.H., 1997. Mutation in the -Synuclein Gene Identified in Families with Parkinson's Disease. Science 276, 2045–2047. https://doi.org/10.1126/science.276.5321.2045

Postuma, R.B., Aarsland, D., Barone, P., Burn, D.J., Hawkes, C.H., Oertel, W., Ziemssen, T., 2012. Identifying prodromal Parkinson's disease: pre-motor disorders in Parkinson's disease. Mov. Disord. 27, 617–626. https://doi.org/10.1002/mds.24996

Postuma, R.B., Berg, D., Stern, M., Poewe, W., Olanow, C.W., Oertel, W., Obeso, J., Marek, K., Litvan, I., Lang, A.E., Halliday, G., Goetz, C.G., Gasser, T., Dubois, B., Chan, P., Bloem, B.R., Adler, C.H., Deuschl, G., 2015. MDS clinical diagnostic criteria for Parkinson's disease: MDS-PD Clinical Diagnostic Criteria. Mov Disord. 30, 1591–1601. https://doi.org/10.1002/mds.26424

Pringsheim, T., Jette, N., Frolkis, A., Steeves, T.D.L., 2014. The prevalence of Parkinson's disease: A systematic review and meta-analysis: PD PREVALENCE. Mov Disord. 29, 1583–1590. https://doi.org/10.1002/mds.25945

Priyadarshi, A., Khuder, S.A., Schaub, E.A., Shrivastava, S., 2000. A meta-analysis of Parkinson's disease and exposure to pesticides. Neurotoxicology 21, 435–440.

Proukakis, C., Dudzik, C.G., Brier, T., MacKay, D.S., Cooper, J.M., Millhauser, G.L., Houlden, H., Schapira, A.H., 2013. A novel -synuclein missense mutation in Parkinson disease. Neurology 80, 1062–1064. https://doi.org/10.1212/WNL.0b013e31828727ba

Przedborski, S., Tieu, K., Perier, C., Vila, M., 2004. MPTP as a Mitochondrial Neurotoxic Model of Parkinson's Disease. J Bioenerg Biomembr 36, 375–379. https://doi.org/10.1023/B:JOBB.0000041771.66775.d5

Pylypenko, O., Hammich, H., Yu, I.-M., Houdusse, A., 2018. Rab GTPases and their interacting protein partners: Structural insights into Rab functional diversity. Small GTPases 9, 22–48. https://doi.org/10.1080/21541248.2017.1336191

Ramonet, D., Daher, J.P.L., Lin, B.M., Stafa, K., Kim, J., Banerjee, R., Westerlund, M., Pletnikova, O., Glauser, L., Yang, L., Liu, Y., Swing, D.A., Beal, M.F., Troncoso, J.C., McCaffery, J.M., Jenkins, N.A., Copeland, N.G., Galter, D., Thomas, B., Lee, M.K., Dawson, T.M., Dawson, V.L., Moore, D.J., 2011. Dopaminergic Neuronal Loss, Reduced Neurite Complexity and Autophagic Abnormalities in Transgenic Mice Expressing G2019S Mutant LRRK2. PLoS ONE 6, e18568. https://doi.org/10.1371/journal.pone.0018568

Ramsay, R.R., Krueger, M.J., Youngster, S.K., Gluck, M.R., Casida, J.E., Singer, T.P., 1991. Interaction of 1-Methyl-4-Phenylpyridinium Ion (MPP^+) and Its Analogs with the Rotenone/Piericidin Binding Site of NADH Dehydrogenase. J Neurochem 56, 1184–1190. https://doi.org/10.1111/j.1471-4159.1991.tb11409.x

Rastaldi, M.P., Armelloni, S., Berra, S., Li, M., Pesaresi, M., Poczewski, H., Langer, B., Kerjaschki, D., Henger, A., Blattner, S.M., Kretzler, M., Wanke, R., D'Amico, G., 2003. Glomerular Podocytes Possess the Synaptic Vesicle Molecule Rab3A and Its Specific Effector Rabphilin-3a. The American Journal of Pathology 163, 889–899. https://doi.org/10.1016/S0002-9440(10)63449-9

Rautio, J., Kumpulainen, H., Heimbach, T., Oliyai, R., Oh, D., Järvinen, T., Savolainen, J., 2008. Prodrugs: design and clinical applications. Nat Rev Drug Discov 7, 255–270. https://doi.org/10.1038/nrd2468

Rey, N.L., Steiner, J.A., Maroof, N., Luk, K.C., Madaj, Z., Trojanowski, J.Q., Lee, V.M.-Y., Brundin, P., 2016. Widespread transneuronal propagation of α-synucleinopathy triggered in olfactory bulb mimics prodromal Parkinson's disease. Journal of Experimental Medicine 213, 1759–1778. https://doi.org/10.1084/jem.20160368

Rideout, H.J., Stefanis, L., 2014. The Neurobiology of LRRK2 and its Role in the Pathogenesis of Parkinson's Disease. Neurochem Res 39, 576–592. https://doi.org/10.1007/s11064-013-1073-5

Rizzo, G., Copetti, M., Arcuti, S., Martino, D., Fontana, A., Logroscino, G., 2016. Accuracy of clinical diagnosis of Parkinson disease: A systematic review and meta-analysis. Neurology 86, 566–576. https://doi.org/10.1212/WNL.0000000000002350

Rocha, E.M., Smith, G.A., Park, E., Cao, H., Brown, E., Hallett, P., Isacson, O., 2015. Progressive decline of glucocerebrosidase in aging and P arkinson's disease. Ann Clin Transl Neurol 2, 433–438. https://doi.org/10.1002/acn3.177

Rudick, R.A., Zirretta, D.K., Herndon, R.M., 1982. Clearance of albumin from mouse subarachnoid space: a measure of CSF bulk flow. Journal of Neuroscience Methods 6, 253–259. https://doi.org/10.1016/0165-0270(82)90088-7

Schapira, A.H.V., 2011. Monoamine Oxidase B Inhibitors for the Treatment of Parkinson's Disease: A Review of Symptomatic and Potential Disease-Modifying Effects. CNS Drugs 25, 1061–1071. https://doi.org/10.2165/11596310-000000000-00000

Schapira, A.H.V., 2007. Mitochondrial dysfunction in Parkinson's disease. Cell Death Differ 14, 1261–1266. https://doi.org/10.1038/sj.cdd.4402160

Schinelli, S., Zuddas, A., Kopin, I.J., Barker, J.L., Porzio, U., 1988. 1-Methyl-4-Phenyl-1,2,3,6-Tetrahydropyridine Metabolism and l-Methyl-4-Phenylpyridinium Uptake in Dissociated Cell Cultures from the Embryonic Mesencephalon. J Neurochem 50, 1900–1907. https://doi.org/10.1111/j.1471-4159.1988.tb02495.x

Schluter, O.M., 2004. A Complete Genetic Analysis of Neuronal Rab3 Function. Journal of Neuroscience 24, 6629–6637. https://doi.org/10.1523/JNEUROSCI.1610-04.2004

Schlüter, O.M., Schnell, E., Verhage, M., Tzonopoulos, T., Nicoll, R.A., Janz, R., Malenka, R.C., Geppert, M., Südhof, T.C., 1999. Rabphilin Knock-Out Mice Reveal That Rabphilin Is Not Required for Rab3 Function in Regulating Neurotransmitter Release. J. Neurosci. 19, 5834–5846. https://doi.org/10.1523/JNEUROSCI.19-14-05834.1999

Schober, A., 2004. Classic toxin-induced animal models of Parkinson's disease: 6-OHDA and MPTP. Cell Tissue Res. 318, 215–224. https://doi.org/10.1007/s00441-004-0938-y

Seeburg, P.H., Hartner, J., 2003. Regulation of ion channel/neurotransmitter receptor function by RNA editing. Current Opinion in Neurobiology 13, 279–283. https://doi.org/10.1016/S0959-4388(03)00062-X

Segal, M., Greenberger, V., Korkotian, E., 2003. Formation of dendritic spines in cultured striatal neurons depends on excitatory afferent activity: Afferents determine dendritic spine formation. European Journal of Neuroscience 17, 2573–2585. https://doi.org/10.1046/j.1460-9568.2003.02696.x

Selikhova, M., Williams, D.R., Kempster, P.A., Holton, J.L., Revesz, T., Lees, A.J., 2009. A clinico-pathological study of subtypes in Parkinson's disease. Brain 132, 2947–2957. https://doi.org/10.1093/brain/awp234

Seppi, K., Weintraub, D., Coelho, M., Perez-Lloret, S., Fox, S.H., Katzenschlager, R., Hametner, E.-M., Poewe, W., Rascol, O., Goetz, C.G., Sampaio, C., 2011. The Movement Disorder Society Evidence-Based Medicine Review Update: Treatments for the non-motor symptoms of Parkinson's disease. Mov. Disord. 26, S42–S80. https://doi.org/10.1002/mds.23884

Sgambato-Faure, V., Cenci, M.A., 2012. Glutamatergic mechanisms in the dyskinesias induced by pharmacological dopamine replacement and deep brain stimulation for the treatment of Parkinson's disease. Progress in Neurobiology 96, 69–86. https://doi.org/10.1016/j.pneurobio.2011.10.005

Sheng, M., 2002. Postsynaptic Signaling and Plasticity Mechanisms. Science 298, 776–780. https://doi.org/10.1126/science.1075333

Sheng, M., Cummings, J., Roldan, L.A., Jan, Y.N., Jan, L.Y., 1994. Changing subunit composition of heteromeric NMDA receptors during development of rat cortex. Nature 368, 144–147. https://doi.org/10.1038/368144a0

Shepherd, J.D., Huganir, R.L., 2007. The Cell Biology of Synaptic Plasticity: AMPA Receptor Trafficking. Annu. Rev. Cell Dev. Biol. 23, 613–643. https://doi.org/10.1146/annurev.cellbio.23.090506.123516

Shi, M., Bradner, J., Hancock, A.M., Chung, K.A., Quinn, J.F., Peskind, E.R., Galasko, D., Jankovic, J., Zabetian, C.P., Kim, H.M., Leverenz, J.B., Montine, T.J., Ginghina, C., Kang, U.J., Cain, K.C., Wang, Y., Aasly, J., Goldstein, D., Zhang, J., 2011. Cerebrospinal fluid biomarkers for Parkinson disease diagnosis and progression. Ann Neurol. 69, 570–580. https://doi.org/10.1002/ana.22311

Shimoji, M., Zhang, L., Mandir, A.S., Dawson, V.L., Dawson, T.M., 2005. Absence of inclusion body formation in the MPTP mouse model of Parkinson's disease. Molecular Brain Research 134, 103–108. https://doi.org/10.1016/j.molbrainres.2005.01.012

Shirataki, H., Kaibuchi, K., Sakoda, T., Kishida, S., Yamaguchi, T., Wada, K., Miyazaki, M., Takai, Y., 1993. Rabphilin-3A, a putative target protein for smg p25A/rab3A p25 small GTP-binding protein related to synaptotagmin. Mol. Cell. Biol. 13, 2061–2068. https://doi.org/10.1128/MCB.13.4.2061

Sidransky, E., Nalls, M.A., Aasly, J.O., Aharon-Peretz, J., Annesi, G., Barbosa, E.R., Bar-Shira, A., Berg, D., Bras, J., Brice, A., Chen, C.-M., Clark, L.N., Condroyer, C., De Marco, E.V., Dürr, A., Eblan, M.J., Fahn, S., Farrer, M.J., Fung, H.-C., Gan-Or, Z., Gasser, T., Gershoni-Baruch, R., Giladi, N., Griffith, A., Gurevich, T., Januario, C., Kropp, P., Lang, A.E., Lee-Chen, G.-J., Lesage, S., Marder, K., Mata, I.F., Mirelman, A., Mitsui, J., Mizuta, I., Nicoletti, G., Oliveira, C., Ottman, R., Orr-Urtreger, A., Pereira, L.V., Quattrone, A., Rogaeva, E., Rolfs, A., Rosenbaum, H., Rozenberg, R., Samii, A., Samaddar, T., Schulte, C., Sharma, M., Singleton, A., Spitz, M., Tan, E.-K., Tayebi, N., Toda, T., Troiano, A.R., Tsuji, S., Wittstock, M., Wolfsberg, T.G., Wu, Y.-R., Zabetian, C.P., Zhao, Y., Ziegler, S.G., 2009. Multicenter Analysis of Glucocerebrosidase Mutations in Parkinson's Disease. N Engl J Med 361, 1651–1661. https://doi.org/10.1056/NEJMoa0901281

Singleton, A.B., Farrer, M.J., Bonifati, V., 2013. The genetics of Parkinson's disease: Progress and therapeutic implications: The Genetics of PD. Mov Disord 28, 14–23. https://doi.org/10.1002/mds.25249

Smith, R., Klein, P., Koc-Schmitz, Y., Waldvogel, H.J., Faull, R.L.M., Brundin, P., Plomann, M., Li, J.-Y., 2007. Loss of SNAP-25 and rabphilin 3a in sensory-motor cortex in Huntington?s disease. J Neurochem 0, 070630082917008-??? https://doi.org/10.1111/j.1471-4159.2007.04703.x

Sorra, K.E., Harris, K.M., 2000. Overview on the structure, composition, function, development, and plasticity of hippocampal dendritic spines. Hippocampus 10, 501–511. https://doi.org/10.1002/1098-1063(2000)10:5<501::AID-HIPO1>3.0.CO;2-T

Souza, J.M., Giasson, B.I., Chen, Q., Lee, V.M.-Y., Ischiropoulos, H., 2000. Dityrosine Cross-linking Promotes Formation of Stable α-Synuclein Polymers IMPLICATION OF NITRATIVE AND OXIDATIVE STRESS IN THE PATHOGENESIS OF NEURODEGENERATIVE SYNUCLEINOPATHIES. J. Biol. Chem. 275, 18344–18349. https://doi.org/10.1074/jbc.M000206200

Spillantini, M.G., Crowther, R.A., Jakes, R., Hasegawa, M., Goedert, M., 1998. alpha-Synuclein in filamentous inclusions of Lewy bodies from Parkinson's disease and dementia with lewy bodies. Proc. Natl. Acad. Sci. U.S.A. 95, 6469–6473. https://doi.org/10.1073/pnas.95.11.6469

Spillantini, M.G., Schmidt, M.L., Lee, V.M.-Y., Trojanowski, J.Q., Jakes, R., Goedert, M., 1997. α-Synuclein in Lewy bodies. Nature 388, 839–840. https://doi.org/10.1038/42166

Stanic, J., Carta, M., Eberini, I., Pelucchi, S., Marcello, E., Genazzani, A.A., Racca, C., Mulle, C., Di Luca, M., Gardoni, F., 2015. Rabphilin 3A retains NMDA receptors at synaptic sites through interaction with GluN2A/PSD-95 complex. Nat Commun 6, 10181. https://doi.org/10.1038/ncomms10181

Stanic, J., Mellone, M., Napolitano, F., Racca, C., Zianni, E., Minocci, D., Ghiglieri, V., Thiolat, M.-L., Li, Q., Longhi, A., De Rosa, A., Picconi, B., Bezard, E., Calabresi, P., Di Luca, M., Usiello, A., Gardoni, F., 2017. Rabphilin 3A: A novel target for the treatment of levodopa-induced dyskinesias. Neurobiology of Disease 108, 54–64. https://doi.org/10.1016/j.nbd.2017.08.001

Steele, J.W., Ju, S., Lachenmayer, M.L., Liken, J., Stock, A., Kim, S.H., Delgado, L.M., Alfaro, I.E., Bernales, S., Verdile, G., Bharadwaj, P., Gupta, V., Barr, R., Friss, A., Dolios, G., Wang, R., Ringe, D., Protter, A.A., Martins, R.N., Ehrlich, M.E., Yue, Z., Petsko, G.A., Gandy, S., 2013. Latrepirdine stimulates autophagy and reduces accumulation of α-synuclein in cells and in mouse brain. Mol Psychiatry 18, 882–888. https://doi.org/10.1038/mp.2012.115

Stephenson, D.T., Meglasson, M.D., Connell, M.A., Childs, M.A., Hajos-Korcsok, E., Emborg, M.E., 2005. The Effects of a Selective Dopamine D $_2$ Receptor Agonist on Behavioral and Pathological Outcome in 1-Methyl-4-phenyl-1,2,3,6-tetrahydropyridine-Treated Squirrel Monkeys. J Pharmacol Exp Ther 314, 1257–1266. https://doi.org/10.1124/jpet.105.087379

Stoessl, A.J., Lehericy, S., Strafella, A.P., 2014. Imaging insights into basal ganglia function, Parkinson's disease, and dystonia. Lancet 384, 532–544. https://doi.org/10.1016/S0140-6736(14)60041-6

Stoyka, L.E., Arrant, A.E., Thrasher, D.R., Russell, D.L., Freire, J., Mahoney, C.L., Narayanan, A., Dib, A.G., Standaert, D.G., Volpicelli-Daley, L.A., 2020. Behavioral defects associated with amygdala and cortical dysfunction in mice with seeded α-synuclein inclusions. Neurobiology of Disease 134, 104708. https://doi.org/10.1016/j.nbd.2019.104708

Studer, L., 1997. Culture of Substantia Nigra Neurons. Current Protocols in Neuroscience 00. https://doi.org/10.1002/0471142301.ns0303s00

Surmeier, D.J., Guzman, J.N., Sanchez-Padilla, J., Schumacker, P.T., 2011. The role of calcium and mitochondrial oxidant stress in the loss of substantia nigra pars compacta dopaminergic neurons in Parkinson's disease. Neuroscience 198, 221–231. https://doi.org/10.1016/j.neuroscience.2011.08.045

Swant, J., Goodwin, J.S., North, A., Ali, A.A., Gamble-George, J., Chirwa, S., Khoshbouei, H., 2011. α-Synuclein Stimulates a Dopamine Transporter-dependent Chloride Current and Modulates the Activity of the Transporter. Journal of Biological Chemistry 286, 43933–43943. https://doi.org/10.1074/jbc.M111.241232

Takahashi, K., Yamanaka, S., 2006. Induction of Pluripotent Stem Cells from Mouse Embryonic and Adult Fibroblast Cultures by Defined Factors. Cell 126, 663–676. https://doi.org/10.1016/j.cell.2006.07.024

Tan, M.G.K., Lee, C., Lee, J.H., Francis, P.T., Williams, R.J., Ramírez, M.J., Chen, C.P., Wong, P.T.-H., Lai, M.K.P., 2014. Decreased rabphilin 3A immunoreactivity in Alzheimer's disease is associated with Aβ burden. Neurochemistry International 64, 29–36. https://doi.org/10.1016/j.neuint.2013.10.013

Taylor, K.S.M., Cook, J.A., Counsell, C.E., 2007. Heterogeneity in male to female risk for Parkinson's disease. Journal of Neurology, Neurosurgery & Psychiatry 78, 905–906. https://doi.org/10.1136/jnnp.2006.104695

Tolosa, E., Wenning, G., Poewe, W., 2006. The diagnosis of Parkinson's disease. The Lancet Neurology 5, 75–86. https://doi.org/10.1016/S1474-4422(05)70285-4

Tovar, K.R., Westbrook, G.L., 2002. Mobile NMDA Receptors at Hippocampal Synapses. Neuron 34, 255–264. https://doi.org/10.1016/S0896-6273(02)00658-X

Tovar, K.R., Westbrook, G.L., 1999. The Incorporation of NMDA Receptors with a Distinct Subunit Composition at Nascent Hippocampal Synapses *In Vitro*. J. Neurosci. 19, 4180–4188. https://doi.org/10.1523/JNEUROSCI.19-10-04180.1999

Tozzi, A., de Iure, A., Bagetta, V., Tantucci, M., Durante, V., Quiroga-Varela, A., Costa, C., Di Filippo, M., Ghiglieri, V., Latagliata, E.C., Wegrzynowicz, M., Decressac, M., Giampà, C., Dalley, J.W., Xia, J., Gardoni, F., Mellone, M., El-Agnaf, O.M., Ardah, M.T., Puglisi-Allegra, S., Björklund, A., Spillantini, M.G., Picconi, B., Calabresi, P., 2016. Alpha-Synuclein Produces Early Behavioral Alterations via Striatal Cholinergic Synaptic Dysfunction by Interacting With GluN2D N -Methyl-D-Aspartate Receptor Subunit. Biological Psychiatry 79, 402–414. https://doi.org/10.1016/j.biopsych.2015.08.013

Tozzi, A., Sciaccaluga, M., Loffredo, V., Megaro, A., Ledonne, A., Cardinale, A., Federici, M., Bellingacci, L., Paciotti, S., Ferrari, E., La Rocca, A., Martini, A., Mercuri, N.B., Gardoni, F., Picconi, B., Ghiglieri, V., De Leonibus, E., Calabresi, P., 2021. Dopamine-dependent early synaptic and motor dysfunctions induced by α-synuclein in the nigrostriatal circuit. Brain awab242. https://doi.org/10.1093/brain/awab242

Traynelis, S.F., Wollmuth, L.P., McBain, C.J., Menniti, F.S., Vance, K.M., Ogden, K.K., Hansen, K.B., Yuan, H., Myers, S.J., Dingledine, R., 2010. Glutamate Receptor Ion Channels: Structure, Regulation, and Function. Pharmacol Rev 62, 405–496. https://doi.org/10.1124/pr.109.002451

Trinh, J., Farrer, M., 2013. Advances in the genetics of Parkinson disease. Nat Rev Neurol 9, 445–454. https://doi.org/10.1038/nrneurol.2013.132

Tronci, E., Francardo, V., 2018. Animal models of l-DOPA-induced dyskinesia: the 6-OHDA-lesioned rat and mouse. J Neural Transm 125, 1137–1144. https://doi.org/10.1007/s00702-017-1825-5

Tsuboi, T., Fukuda, M., 2005. The C2B Domain of Rabphilin Directly Interacts with SNAP-25 and Regulates the Docking Step of Dense Core Vesicle Exocytosis in PC12 Cells. Journal of Biological Chemistry 280, 39253–39259. https://doi.org/10.1074/jbc.M507173200

Tuttle, M.D., Comellas, G., Nieuwkoop, A.J., Covell, D.J., Berthold, D.A., Kloepper, K.D., Courtney, J.M., Kim, J.K., Barclay, A.M., Kendall, A., Wan, W., Stubbs, G., Schwieters, C.D., Lee, V.M.Y., George, J.M., Rienstra, C.M., 2016. Solid-state NMR structure of a pathogenic fibril of full-length human α-synuclein. Nature Structural & Molecular Biology 23, 409–415. https://doi.org/10.1038/nsmb.3194

Twelves, D., Perkins, K.S.M., Counsell, C., 2003. Systematic review of incidence studies of Parkinson's disease. Mov. Disord. 18, 19–31. https://doi.org/10.1002/mds.10305

Ubach, J., García, J., Nittler, M.P., Südhof, T.C., Rizo, J., 1999. Structure of the Janus-faced C2B domain of rabphilin. Nat Cell Biol 1, 106–112. https://doi.org/10.1038/10076

Ulmer, T.S., Bax, A., Cole, N.B., Nussbaum, R.L., 2005. Structure and dynamics of micelle-bound human alpha-synuclein. J. Biol. Chem. 280, 9595–9603. https://doi.org/10.1074/jbc.M411805200

Ungerstedt, U., Ljungberg, T., Steg, G., 1974. Behavioral, physiological, and neurochemical changes after 6-hydroxydopamine-induced degeneration of the nigro-striatal dopamine neurons. Adv Neurol 5, 421–426.

Valente, E.M., 2004. Hereditary Early-Onset Parkinson's Disease Caused by Mutations in PINK1. Science 304, 1158–1160. https://doi.org/10.1126/science.1096284

Valera, E., Masliah, E., 2013. Immunotherapy for neurodegenerative diseases: Focus on α-synucleinopathies. Pharmacology & Therapeutics 138, 311–322. https://doi.org/10.1016/j.pharmthera.2013.01.013

Van Den Eeden, S.K., 2003. Incidence of Parkinson's Disease: Variation by Age, Gender, and Race/Ethnicity. American Journal of Epidemiology 157, 1015–1022. https://doi.org/10.1093/aje/kwg068

Vandenberg, R.J., Ryan, R.M., 2013. Mechanisms of Glutamate Transport. Physiological Reviews 93, 1621–1657. https://doi.org/10.1152/physrev.00007.2013

Vargas, J.Y., Grudina, C., Zurzolo, C., 2019. The prion-like spreading of α-synuclein: From in vitro to in vivo models of Parkinson's disease. Ageing Research Reviews 50, 89–101. https://doi.org/10.1016/j.arr.2019.01.012

Verasdonck, J., Bousset, L., Gath, J., Melki, R., Böckmann, A., Meier, B.H., 2016. Further exploration of the conformational space of α-synuclein fibrils: solid-state NMR assignment of a high-pH polymorph. Biomol NMR Assign 10, 5–12. https://doi.org/10.1007/s12104-015-9628-9

Vilariño-Güell, C., Wider, C., Ross, O.A., Dachsel, J.C., Kachergus, J.M., Lincoln, S.J., Soto-Ortolaza, A.I., Cobb, S.A., Wilhoite, G.J., Bacon, J.A., Behrouz, B., Melrose, H.L., Hentati, E., Puschmann, A., Evans, D.M., Conibear, E., Wasserman, W.W., Aasly, J.O., Burkhard, P.R., Djaldetti, R., Ghika, J., Hentati, F., Krygowska-Wajs, A., Lynch, T., Melamed, E., Rajput, A., Rajput, A.H., Solida, A., Wu, R.-M., Uitti, R.J., Wszolek, Z.K., Vingerhoets, F., Farrer, M.J., 2011. VPS35 Mutations in Parkinson Disease. The American Journal of Human Genetics 89, 162–167. https://doi.org/10.1016/j.ajhg.2011.06.001

Villalba, R.M., Smith, Y., 2010. Striatal Spine Plasticity in Parkinson's Disease. Front. Neuroanat. 4. https://doi.org/10.3389/fnana.2010.00133

Voges, J., Hilker, R., Bötzel, K., Kiening, K.L., Kloss, M., Kupsch, A., Schnitzler, A., Schneider, G., Steude, U., Deuschl, G., Pinsker, M.O., 2007. Thirty days complication rate following surgery performed for deep-brain-stimulation. Mov. Disord. 22, 1486–1489. https://doi.org/10.1002/mds.21481

Volc, D., Poewe, W., Kutzelnigg, A., Lührs, P., Thun-Hohenstein, C., Schneeberger, A., Galabova, G., Majbour, N., Vaikath, N., El-Agnaf, O., Winter, D., Mihailovska, E., Mairhofer, A., Schwenke, C., Staffler, G., Medori, R., 2020. Safety and immunogenicity of the α-synuclein active immunotherapeutic PD01A in patients with Parkinson's disease: a randomised, single-blinded, phase 1 trial. The Lancet Neurology 19, 591–600. https://doi.org/10.1016/S1474-4422(20)30136-8

Volkmann, J., Daniels, C., Witt, K., 2010. Neuropsychiatric effects of subthalamic neurostimulation in Parkinson disease. Nat Rev Neurol 6, 487–498. https://doi.org/10.1038/nrneurol.2010.111

Volpicelli-Daley, L.A., Luk, K.C., Patel, T.P., Tanik, S.A., Riddle, D.M., Stieber, A., Meaney, D.F., Trojanowski, J.Q., Lee, V.M.-Y., 2011. Exogenous α-Synuclein Fibrils Induce Lewy Body Pathology Leading to Synaptic Dysfunction and Neuron Death. Neuron 72, 57–71. https://doi.org/10.1016/j.neuron.2011.08.033

Voon, V., Mehta, A.R., Hallett, M., 2011. Impulse control disorders in Parkinson's disease: recent advances. Curr Opin Neurol 24, 324–330. https://doi.org/10.1097/WCO.0b013e3283489687

Wakabayashi, K., Tanji, K., Odagiri, S., Miki, Y., Mori, F., Takahashi, H., 2013. The Lewy Body in Parkinson's Disease and Related Neurodegenerative Disorders. Mol Neurobiol 47, 495–508. https://doi.org/10.1007/s12035-012-8280-y

Wang, L., Das, U., Scott, D.A., Tang, Y., McLean, P.J., Roy, S., 2014. α-Synuclein Multimers Cluster Synaptic Vesicles and Attenuate Recycling. Current Biology 24, 2319–2326. https://doi.org/10.1016/j.cub.2014.08.027

Wang, Y.-K., Zhu, W.-W., Wu, M.-H., Wu, Y.-H., Liu, Z.-X., Liang, L.-M., Sheng, C., Hao, J., Wang, L., Li, W., Zhou, Q., Hu, B.-Y., 2018. Human Clinical-Grade Parthenogenetic ESC-Derived Dopaminergic Neurons Recover Locomotive Defects of Nonhuman Primate Models of Parkinson's Disease. Stem Cell Reports 11, 171–182. https://doi.org/10.1016/j.stemcr.2018.05.010

Weinert, M., Selvakumar, T., Tierney, T.S., Alavian, K.N., 2015. Isolation, Culture and Long-Term Maintenance of Primary Mesencephalic Dopaminergic Neurons From Embryonic Rodent Brains. JoVE 52475. https://doi.org/10.3791/52475

Weinreb, P.H., Zhen, W., Poon, A.W., Conway, K.A., Lansbury, P.T., 1996. NACP, A Protein Implicated in Alzheimer's Disease and Learning, Is Natively Unfolded. Biochemistry 35, 13709–13715. https://doi.org/10.1021/bi961799n

Winkler, C., Kirik, D., Björklund, A., Cenci, M.A., 2002. l-DOPA-Induced Dyskinesia in the Intrastriatal 6-Hydroxydopamine Model of Parkinson's Disease: Relation to Motor and Cellular Parameters of Nigrostriatal Function. Neurobiology of Disease 10, 165–186. https://doi.org/10.1006/nbdi.2002.0499

Winner, B., Jappelli, R., Maji, S.K., Desplats, P.A., Boyer, L., Aigner, S., Hetzer, C., Loher, T., Vilar, M., Campioni, S., Tzitzilonis, C., Soragni, A., Jessberger, S., Mira, H., Consiglio, A., Pham, E., Masliah, E., Gage, F.H., Riek, R., 2011. In vivo demonstration that alpha-synuclein oligomers are toxic. Proc. Natl. Acad. Sci. U.S.A. 108, 4194–4199. https://doi.org/10.1073/pnas.1100976108

Withers, G.S., George, J.M., Banker, G.A., Clayton, D.F., 1997. Delayed localization of synelfin (synuclein, NACP) to presynaptic terminals in cultured rat hippocampal neurons. Developmental Brain Research 99, 87–94. https://doi.org/10.1016/S0165-3806(96)00210-6

Wong, Y.C., Krainc, D., 2017. α-synuclein toxicity in neurodegeneration: mechanism and therapeutic strategies. Nat Med 23, 1–13. https://doi.org/10.1038/nm.4269

Wu, Q., Takano, H., Riddle, D.M., Trojanowski, J.Q., Coulter, D.A., Lee, V.M.-Y., 2019. α-Synuclein (αSyn) Preformed Fibrils Induce Endogenous αSyn Aggregation, Compromise Synaptic Activity and Enhance Synapse Loss in Cultured Excitatory Hippocampal Neurons. J. Neurosci. 39, 5080–5094. https://doi.org/10.1523/JNEUROSCI.0060-19.2019

Xu, L., Nussinov, R., Ma, B., 2016. Coupling of the non-amyloid-component (NAC) domain and the KTK(E/Q)GV repeats stabilize the α-synuclein fibrils. European Journal of Medicinal Chemistry 121, 841–850. https://doi.org/10.1016/j.ejmech.2016.01.044

Xu, Q., Langley, M., Kanthasamy, A.G., Reddy, M.B., 2017. Epigallocatechin Gallate Has a Neurorescue Effect in a Mouse Model of Parkinson Disease. J. Nutr. 147, 1926–1931. https://doi.org/10.3945/jn.117.255034

Yamaguchi, T., Shirataki, H., Kishida, S., Miyazaki, M., Nishikawa, J., Wada, K., Numata, S., Kaibuchi, K., Takai, Y., 1993. Two functionally different domains of rabphilin-3A, Rab3A p25/smg p25A-binding and phospholipid- and Ca(2+)-binding domains. J Biol Chem 268, 27164–27170.

Yu, L., Tasaki, S., Schneider, J.A., Arfanakis, K., Duong, D.M., Wingo, A.P., Wingo, T.S., Kearns, N., Thatcher, G.R.J., Seyfried, N.T., Levey, A.I., De Jager, P.L., Bennett, D.A., 2020. Cortical Proteins Associated With Cognitive Resilience in Community-Dwelling Older Persons. JAMA Psychiatry 77, 1172. https://doi.org/10.1001/jamapsychiatry.2020.1807

Yuan, A., Rao, M.V., Veeranna, Nixon, R.A., 2017. Neurofilaments and Neurofilament Proteins in Health and Disease. Cold Spring Harb Perspect Biol 9, a018309. https://doi.org/10.1101/cshperspect.a018309

Yuan, J., Zhao, Y., 2013. Evolutionary aspects of the synuclein super-family and sub-families based on large-scale phylogenetic and group-discrimination analysis. Biochemical and Biophysical Research Communications 441, 308–317. https://doi.org/10.1016/j.bbrc.2013.09.132

Yuan, Q., Ren, C., Xu, W., Petri, B., Zhang, J., Zhang, Y., Kubes, P., Wu, D., Tang, W., 2017. PKN1 Directs Polarized RAB21 Vesicle Trafficking via RPH3A and Is Important for Neutrophil Adhesion and Ischemia-Reperfusion Injury. Cell Reports 19, 2586–2597. https://doi.org/10.1016/j.celrep.2017.05.080

Zaja-Milatovic, S., Milatovic, D., Schantz, A.M., Zhang, J., Montine, K.S., Samii, A., Deutch, A.Y., Montine, T.J., 2005. Dendritic degeneration in neostriatal medium spiny neurons in Parkinson disease. Neurology 64, 545–547. https://doi.org/10.1212/01.WNL.0000150591.33787.A4

Zaltieri, M., Grigoletto, J., Longhena, F., Navarria, L., Favero, G., Castrezzati, S., Colivicchi, M.A., Della Corte, L., Rezzani, R., Pizzi, M., Benfenati, F., Spillantini, M.G., Missale, C., Spano, P., Bellucci, A., 2015. α-synuclein and synapsin III cooperatively regulate synaptic function in dopamine neurons. Journal of Cell Science 128, 2231–2243. https://doi.org/10.1242/jcs.157867

Zarranz, J.J., Alegre, J., Gómez-Esteban, J.C., Lezcano, E., Ros, R., Ampuero, I., Vidal, L., Hoenicka, J., Rodriguez, O., Atarés, B., Llorens, V., Tortosa, E.G., del Ser, T., Muñoz, D.G., de Yebenes, J.G., 2004. The new mutation, E46K, of α-synuclein causes parkinson and Lewy body dementia: New α-Synuclein Gene Mutation. Ann Neurol. 55, 164–173. https://doi.org/10.1002/ana.10795

Zheng, B., Liao, Z., Locascio, J.J., Lesniak, K.A., Roderick, S.S., Watt, M.L., Eklund, A.C., Zhang-James, Y., Kim, P.D., Hauser, M.A., Grunblatt, E., Moran, L.B., Mandel, S.A., Riederer, P., Miller, R.M., Federoff, H.J., Wullner, U., Papapetropoulos, S., Youdim, M.B., Cantuti-Castelvetri, I., Young, A.B., Vance, J.M., Davis, R.L., Hedreen, J.C., Adler, C.H., Beach, T.G., Graeber, M.B., Middleton, F.A., Rochet, J.-C., Scherzer, C.R., the Global PD Gene Expression (GPEX) Consortium, 2010. PGC-1 , A Potential Therapeutic Target for Early Intervention in Parkinson's Disease. Science Translational Medicine 2, 52ra73-52ra73. https://doi.org/10.1126/scitranslmed.3001059

Zhou, Q., Homma, K.J., Poo, M., 2004. Shrinkage of Dendritic Spines Associated with Long-Term Depression of Hippocampal Synapses. Neuron 44, 749–757. https://doi.org/10.1016/j.neuron.2004.11.011

Zhou, Q., Lai, Y., Bacaj, T., Zhao, M., Lyubimov, A.Y., Uervirojnangkoorn, M., Zeldin, O.B., Brewster, A.S., Sauter, N.K., Cohen, A.E., Soltis, S.M., Alonso-Mori, R., Chollet, M., Lemke, H.T., Pfuetzner, R.A., Choi, U.B., Weis, W.I., Diao, J., Südhof, T.C., Brunger, A.T., 2015. Architecture of the synaptotagmin–SNARE machinery for neuronal exocytosis. Nature 525, 62–67. https://doi.org/10.1038/nature14975